

11.0 Performance Evaluation of Partial Depth Repair Materials (Task 11)

11.1 Introduction

Corrosion induced deterioration has been identified through field investigations as the major cause of beam end distress for I-beams in Michigan bridges. The resulting forms of distress include concrete spalling, delamination, cracking, and corrosion of reinforcement. The loss of concrete permits accelerated deterioration of reinforcing and prestressing steels, allows detensioning of prestressing steel, and increases the stress demand (bearing, shear, flexural) on the remaining section (see Photo 11-1).

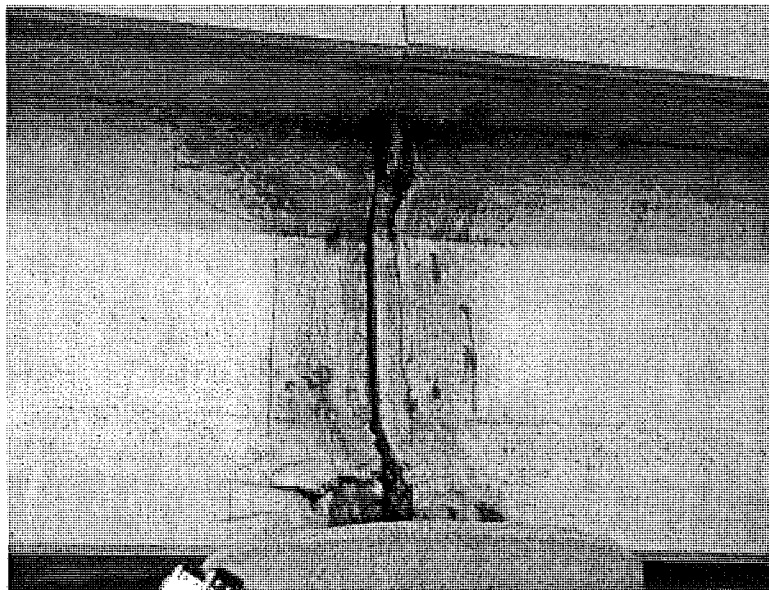


Photo 11-1. Typical beam-end deterioration

While complete replacement of the superstructure beam is an option, it is costly. If certain conditions are met, a more attractive alternative is to repair the deteriorated beam-end. At a minimum, a properly functioning repair can restore cover to reinforcing and prestressing steels and re-establish the original intended cross section of the concrete.

Briefly summarizing Chapter 2, several techniques exist for preventative maintenance and repair of concrete. These techniques may be subjectively categorized for low, moderate and high

severity distress levels. Some of these techniques include those listed in Table 11-1. Additional techniques are included in Appendix J.

Table 11-1. Preventive Maintenance and Repair Options for Deteriorated Beam-Ends

Low Severity Distress	Moderate Severity Distress	High Severity Distress
Sealers	Partial Depth Repair	Partial Depth Repair
Coatings	Cathodic Protection	Replacement
Do Nothing	Combined Sealers and Coatings	---

A partial depth repair procedure exists to perform prestressed concrete I-beam end repairs (Needham, 1999). This “chip and overcast” procedure could be applied to all levels of beam end distress, but is perhaps most effective for high and moderate severity conditions. It may therefore be a conservative approach if say less than 50-percent of the beam end surface area was damaged behind the diaphragm. For these situations, a less aggressive approach such as patching may be warranted. Other options such as sealers and coatings are specified by the MDOT and are useful for low distress levels. Current research through MDOT is underway regarding cathodic protection.

In addition to the specifications of Section 712 in the 1996 *MDOT Standard Specifications for Construction*, at least one MDOT special provision exists for “Vertical and Overhead Structure Repairs” (Staton, 2001; MDOT, 1996; MDOT, 2000). From a review of the 2001 MDOT Materials Source Guide, there are no products for vertical or overhead prepackaged patching materials listed on the MDOT Qualified Products List (MDOT, 2001c). According to MDOT, the three vertical and overhead patching materials listed as approved materials in the MDOT special provision were selected based on the manufacturers technical product literature (Staton, 2001). The three repair materials are Sika’s Sika Top 126 Plus, ThoRoc’s HB2, and Master Builder Technologies’ Emaco R350-CI. These materials were chosen because of manufacturer tested bond strength and inclusion of corrosion inhibitors (Staton, 2001). However, at the project interim meeting of October 25, 2001, some MDOT personnel stated concerns with patching of I-beam ends, including adhesion problems, and the potential for a shrinkage differential between the patch material and the substrate that could allow future degradation of the materials through water infiltration.

From the above discussion, there is value to be gained in performing concrete repairs on prestressed concrete I-beam ends. However, the procedures and materials specified in the MDOT special provision for “Vertical and Overhead Structure Repairs” have not been subjected to substantial examination for their use in repair of deteriorated I-beam ends. Patches are typically referred to as ‘shallow’ for depths less than 1-in. and ‘deep’ for 1 to 3-in. Patch depths greater than 3-in are not recommended for the products listed in the special provision.

For a concrete repair to perform successfully in a relatively corrosive and high stress environment (such as a beam end when exposed to de-icing salts through leaking expansion joints and high bearing stresses) it must have several qualities. At a minimum the repair must:

- protect the reinforcing and prestressing steels. It cannot crack or shrink and allow rapid contaminant ingress at the patch edges, and it must
- develop sufficient bond / adhesion and compressive strength to assist the parent member in carrying loads. At a minimum it cannot debond from the substrate.

11.2 Experimental Program

11.2.1 Objective and Approach

The objective of the experimental testing was to verify that the repair materials referenced in the MDOT special provision perform at a minimum acceptable level of performance through the following assessments:

1. Evaluate the shrinkage and cracking of that materials with various repair depths compared to the surrounding concrete substrate.
2. Experimentally verify that repairs of various depths can develop sufficient tensile bond to the concrete substrate without mechanical anchorage when subjected to two environmental (thermal-cycle) scenarios.
3. Experimentally verify that each repair material can develop sufficient compressive strength to assist the substrate in carrying compressive loads.

In addition, a fourth objective could be assessed:

4. Determine whether or not performing vertical and overhead partial depth repairs is feasible.

11.2.2 Substrate specimens

An illustration of a typical specimen repaired in the vertical position is shown in Figure 11-1. In order to provide a host material for the repair materials, it was necessary to cast blank concrete specimens. Considerations and details on the construction of the substrate specimens follow.

11.2.2.1 Formwork

Individual single-use wood forms were constructed for fabrication of the substrate specimens. Pine boards having a 1-in nominal thickness were cut to 6-in width for the ends and bottom of the forms. The sides of the forms were constructed using 7/16-in OSB sheathing. Formwork pieces were cut such that the finished inside dimensions of the form were 6-in deep by 6-in wide by 21-in long. For ease of stripping, a release agent was applied to the inside of the forms approximately one-hour prior to the placement of concrete.

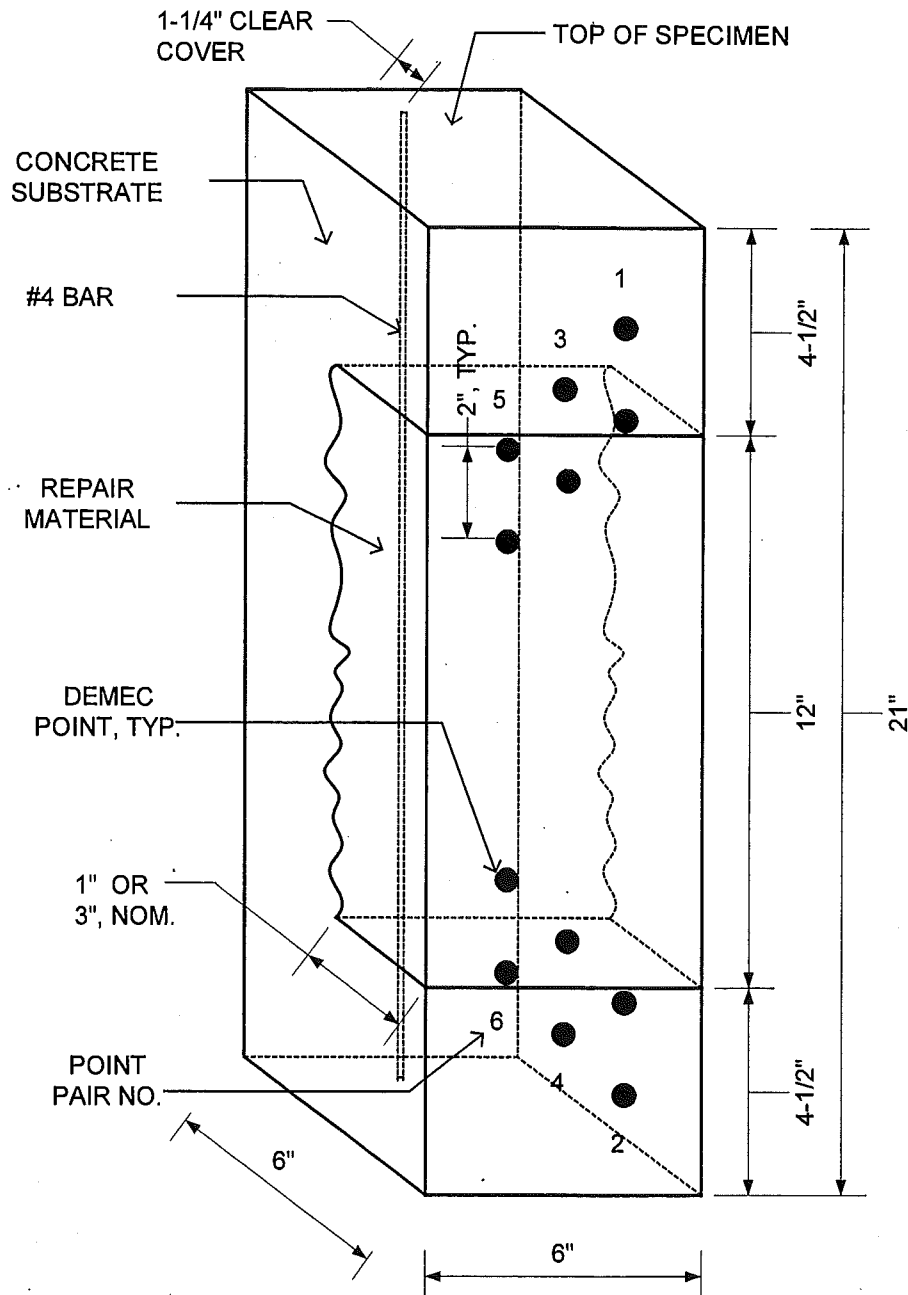


Figure 11-1. Typical Repair Specimen in Vertical Position

11.2.2.2 Reinforcement

Reinforcing bars were included in the fabrication of the substrate specimens for added ductility and strength. A single No. 4 bar 20-in long was selected for this purpose. After the forms had been oiled, the bars were set inside the formwork, supported on each end by polystyrene blocks. Once seated into the blocks, roughly 1 1/4-in of concrete cover was beneath the bars. Photo 11-2 shows a pallet of forms with bars in place.

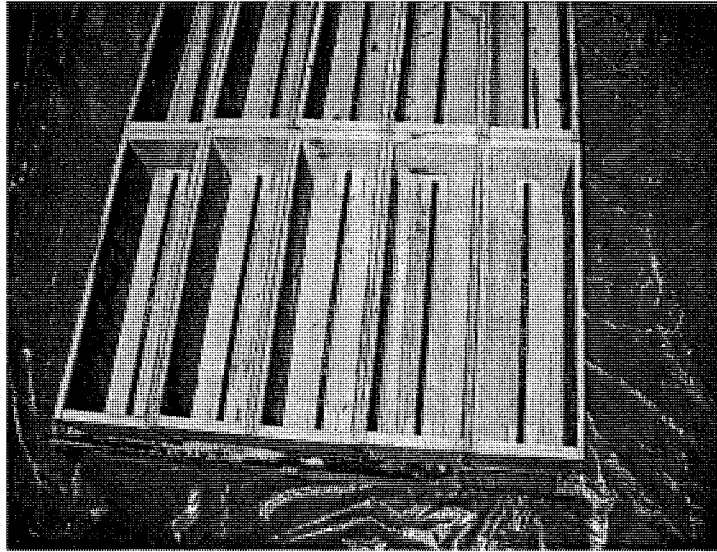


Photo 11-2. Formwork coated with release agent and reinforcing bars in place

11.2.2.3 *Portland Cement Concrete*

It was desirable that the substrate specimens be as nearly identical as possible to that of concrete being used by Michigan I-beam precasters. Additionally, because bridges built in the 1960's are more likely to be susceptible to beam end deterioration (Ahlborn et al, 2001), a specimen having properties of this era would likely represent the type of substrate to which a repair material would be applied.

To this end, MDOT was able to provide a copy of the 1961 MDOT Specification and minutes from a 1957 plant trip to a Detroit precaster (Till, 2001c). It was decided to follow the guidance of the specification in setting the proportions for this project. A summary of the specification is shown in Table 11-2. The mix ordered for the project was the most representative mix relative to the 1961 mix based on aggregate classes, compressive strength, slump and air content that the local ready-mix supplier provided.

Table 11-2. Summary of Specified, Ordered, and As-Delivered Concrete Proportions and Properties

Mix	1961 Specification	Ordered for Project	As-Delivered
Cement	max. 705 lb/cy, Type I	658 lb/cy, Type I	657 lb/cy, Type I
Coarse Aggregate	see note, class 10B	1738 lb/cy, class 6A	1760 lb/cy, class 6A
Fine Aggregate	see note, class 2NS	1262 lb/cy, class 2NS	1413 lb/cy, class 2NS
Water	see note	28 - 29 gal/cy	12.7 gal/cy
Water Reducer	see note	26 oz/cy	26 oz/cy
Air Entrainment	see note	< 4 oz/cy	2.67 oz/cy
Compressive Strength (ASTM C39)	5000-psi at 28 days	5000-psi at 28 days	5070-psi at 24 days
Slump (ASTM C143)	3-inches, max.	3-inches, max.	5-inches
Total Air Content (ASTM C231)	5.5 ± 1.5 percent	5.5 ± 1.5 percent	4.0 percent

Note: Proportion per manufacturer

11.2.2.4 Substrate Fabrication

Specimens were cast on January 8, 2002 on the heated Dillman Hall loading dock on the campus of Michigan Tech (see Photo 11-3). The concrete, supplied by Moyle Concrete of Houghton, MI, was batched in a mobile mixer with the proportions and properties noted in Table 11-2 under “As- Delivered”.



Photo 11-3. Placing concrete on the Dillman Hall loading dock

Tasks used in casting specimens included positioning forms, placing concrete, consolidating concrete, screeding specimens, inserting polystyrene blanks (top side), and performing field tests. The batch to final unload time was approximately one hour. Concrete consolidation was performed using a normal construction type hand-held concrete vibrator. The vibrator was inserted twice at roughly the third points of each specimen until the surface of the concrete was relatively smooth. Insertion points were offset from the specimen center to avoid contact with the substrate specimen reinforcement. Screeding of the specimens was accomplished with a wood straightedge. Multiple passes with the straightedge were performed to result in finished specimens with a consistent height.

Twenty-two of the thirty-nine specimens were fitted with 2-in polystyrene blanks over the middle 10-in of the specimen top (see Photo 11-4). The blanks served to reduce, but not eliminate, the need for concrete cutting during selective demolition of specimens to receive the 3-in deep patches. Blanks were inserted after screeding. The concrete was then finished around the blanks in the forms using the same floats.

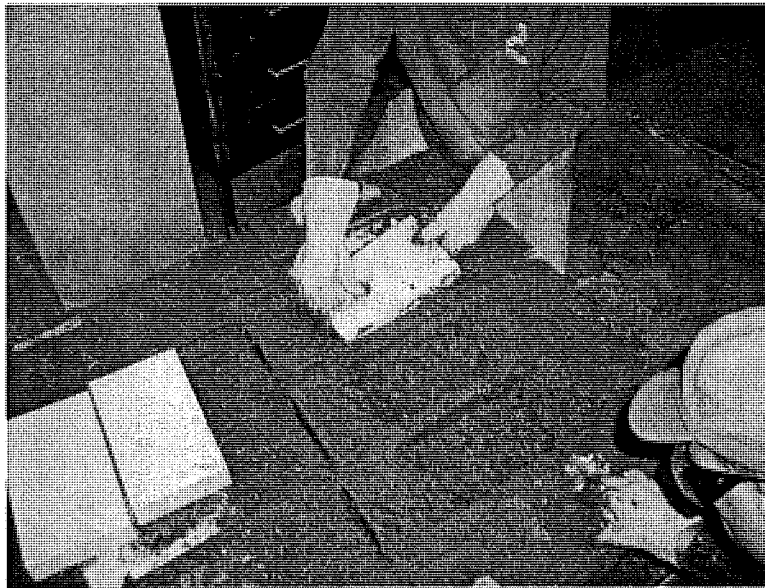


Photo 11-4. Inserting polystyrene blocks in deep repair specimens

11.2.2.5 *Laboratory Tests*

Properties of the freshly mixed concrete were determined at the time of concrete placement. Tests were performed under the direction of an ACI Field Testing Technician – Grade I. Consistency and air entrainment tests were performed in accordance with ASTM C143/C143M-00 and C231-97e1 respectively (ASTM, 2000, 1997). Slump and air content results of the “as-delivered” mix were listed previously in Table 11-2.

11.2.2.6 *Curing*

After casting, the specimens were immediately covered with multiple layers of polyethylene sheeting as shown in Photo 11-5. The sheeting was weighted with dimension lumber at the edges to trap moisture in the specimens. The sheeting remained in place for 22 hours before being transported from the loading dock to the curing laboratory with a pallet truck. Forms were stripped with hand tools and the specimens placed vertically in a pair of cure tanks (see Photo

11-6). Cure tank water was conditioned with Type S lime in accordance with ASTM C511-98 to prevent leaching of lime from the specimens (ASTM, 1998; Kosmatka et al 2002). Form removal and specimen placement in the tanks were completed in 4 hours with a 3-person team.

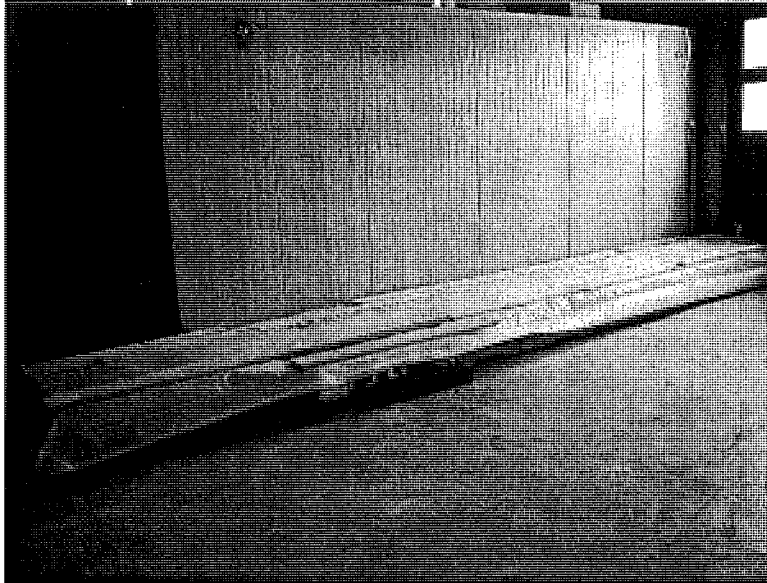


Photo 11-5. Short-term curing on the Dillman Hall loading dock

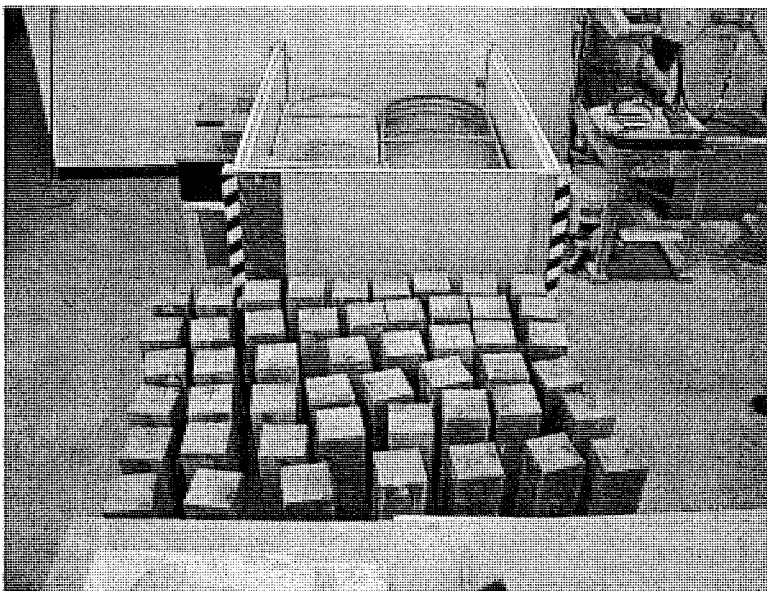


Photo 11-6. Substrate specimens stripped from forms and ready to be placed in cure tanks

The bath temperatures were maintained between 138 and 144 degrees Fahrenheit. The relatively high curing temperature and wet curing methods were selected to increase the degree of hydration within a short time period (Mindess and Young, 1981).

Tank water was heated and circulated in each tank with a Neslab Instruments, Inc. Model RTE-4 circulating bath. A temporary enclosure was constructed around the tanks using 2-inch

polystyrene insulation panels to assist the heaters in maintaining the desired tank temperatures and retain tank water. Cure tank temperatures and water depths were monitored daily using a Testo Model 925 digital thermometer and wooden yardstick. A completed temperature and depth log is located in Appendix D of Kasper's report (Kasper, 2002).

The specimens remained in the tanks for 7 days whereupon they were removed for selective demolition operations. The duration of room temperature/humidity curing prior to repair placement ranged from 7 days (January 16, 2002 to January 23, 2002) to 21 days (January 16, 2002 to February 5, 2002) depending on the specific specimen.

11.2.2.7 *Selective Demolition*

Concrete was removed from the top face (not confined by formwork) of the test substrate specimens using a concrete saw and rotary hammer. The saw selected for removal was a Champion Manufacturing Co. 20-inch stationary Blok Saw equipped with an 18-inch diamond tipped blade (shown in Photo 11-7). Due to the operational characteristics of this saw, it was necessary to cut the substrate specimens in the horizontal position. The dates that sawing was performed and the operator performing the work were documented and are included in Appendix E of Kasper's report (Kasper, 2002).

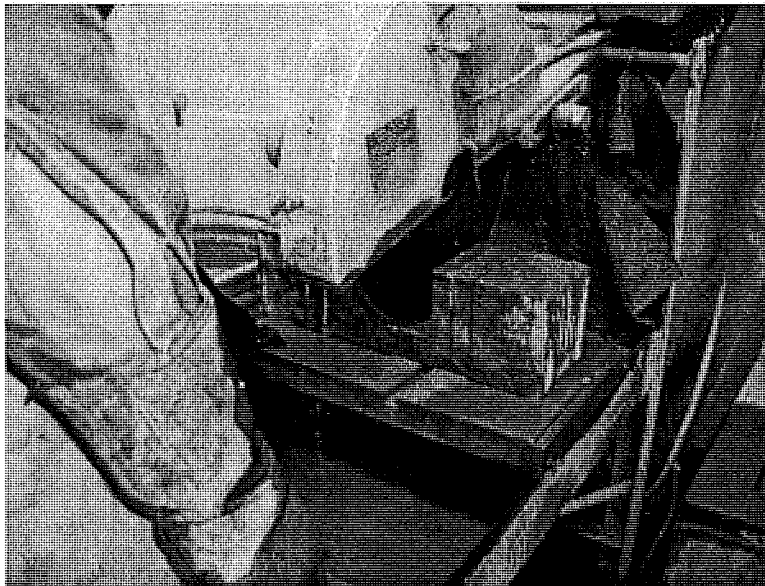


Photo 11-7. Passing the substrate specimen through the saw blade.

Saw cuts were spaced roughly one-inch apart across the face of the specimen by positioning the substrate specimens on the saw cart and passing the specimen through the blade. Saw depths of either 1-in or 3-in were made, based on whether or not the specimen was selected for a shallow or deep repair, respectively. For cuts made on the deep repair specimens, no effort was made to remove the polystyrene block prior to cutting. The above photo shows the saw at a depth of 3-in. An example of a fully sawn specimen is shown in Photo 11-8.

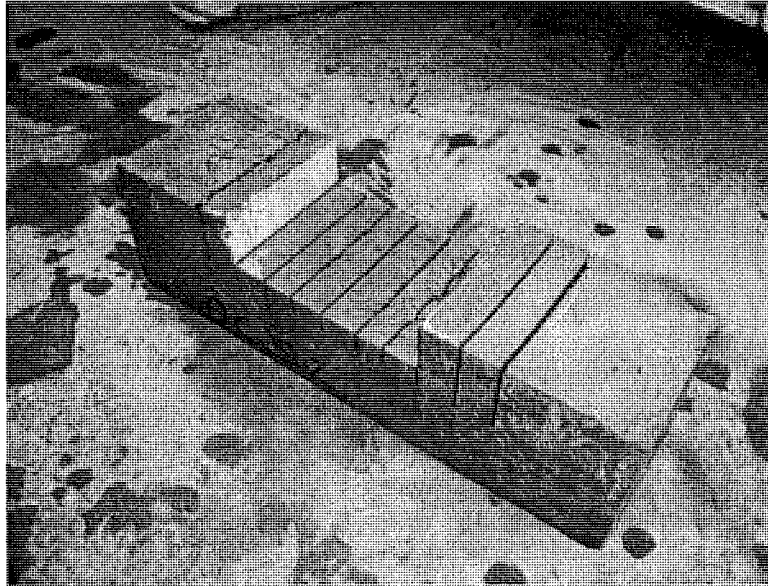


Photo 11-8. Fully cut substrate specimen. Polystyrene block has partially dislodged from void.

A Bosch 11219EVS rotary hammer fitted with a scaling chisel was used to break out sections of the concrete between the saw-cuts. As shown in Photo 11-9, break out was performed in the horizontal position on the laboratory floor. Typically the second section of concrete in from the outer edge of concrete to remain was removed first. With this section dislodged, removal efforts were directed to additional sections of scored concrete toward the center and eventually the opposite end of the specimen. Removal of an individual section was relatively easy when the chisel was oriented as close to parallel of the removal surface as possible.

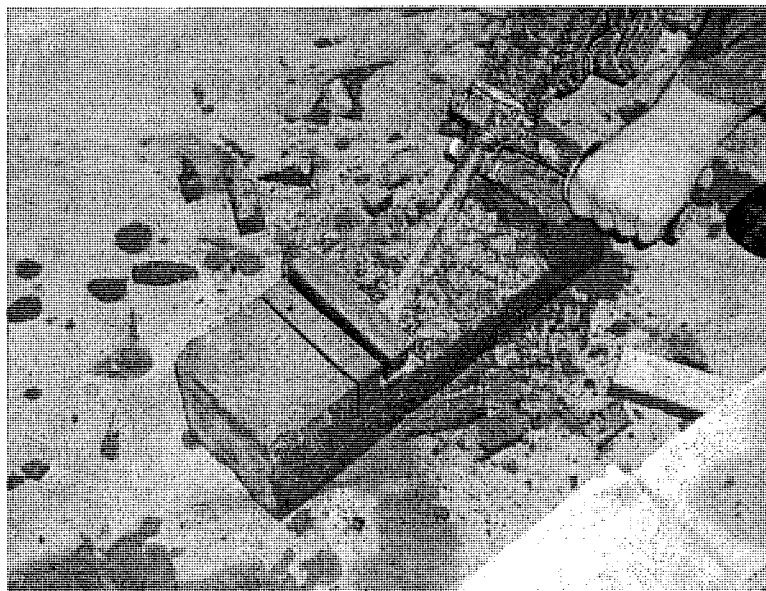


Photo 11-9. Concrete removal progressing across the substrate specimen

11.2.2.8 *Surface Preparation*

Two surface preparation techniques were evaluated. Repair practices commonly require that surface preparation techniques consist of high pressure water blasting or abrasive blasting. While these techniques are known to be effective, surface preparation consisting of brushing with a wire wheel could be another option that may be practical for small repair projects. For this project, testing was performed to determine whether or not an obvious difference existed between abrasive blasting and wire wheel preparation. To make this determination, one specimen was prepared using each method and then viewed under a microscope.

Abrasive blasting was performed on a deep repair specimen in an enclosed abrasive blasting cabinet in the foundry of the Mining and Materials Engineering building at Michigan Tech. Blasting media primarily consisted of 50-70-sieve sand with some similar sized steel shot intermixed in the media. Blasting was performed with the nozzle nearly perpendicular to the removal surface and continued for approximately 30 seconds until there was no noticeable change in the surface appearance. After abrasive blasting, the surface was blown with compressed air at roughly 60 psi until no further airborne debris was observed.

An electric angle grinder was fitted with a wire brush wheel to perform the second surface preparation method. Brushing was performed at full tool speed (approximately 10,000 RPM) and continued until there was no noticeable change in the surface appearance. After brushing, the surface was blown with compressed air at roughly 60 psi until no further airborne debris was observed.

Three surface locations were observed on each specimen using an Olympus SZH10 Zoom Stereo Microscope illuminated with directional lamps. Typically, two normally contoured and one depressed location was observed on each specimen. Photographs of each observation location were captured using an Optronics LX-750 3 CCD Video Camera System and Scion Corporation CG-7 RGB Color Frame Grabber capture card. Images were then downloaded to a Power Macintosh 9600/300 using Scion Image Version 1.62 software. Examples of the surface quality at 20x magnification for each specimen are shown in Photo 11-10 through Photo 11-13. Each photo, regardless of the preparation technique or relative depth on the specimen (depressed or non-depressed region) shows clean aggregate and air pockets within the cement matrix.

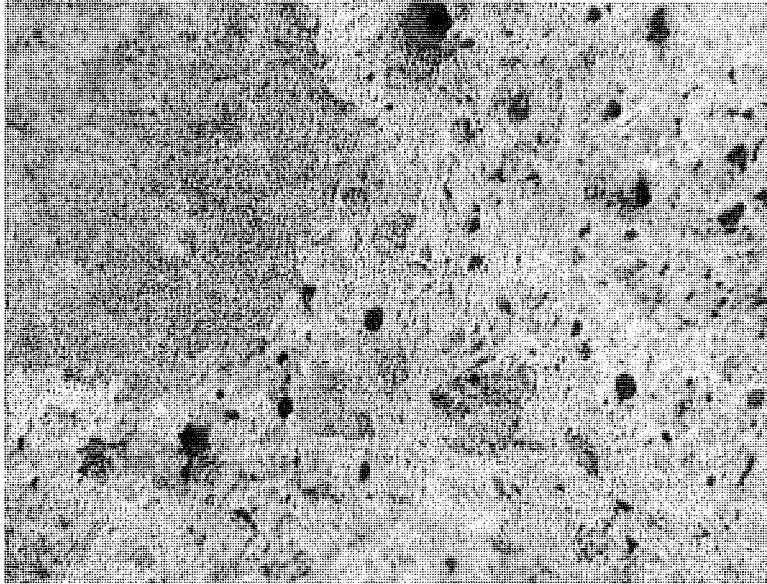


Photo 11-10. Sandblasted concrete surface at 20x magnification, non-depressed region



Photo 11-11. Wire brushed surface profile at 20x magnification, non-depressed region

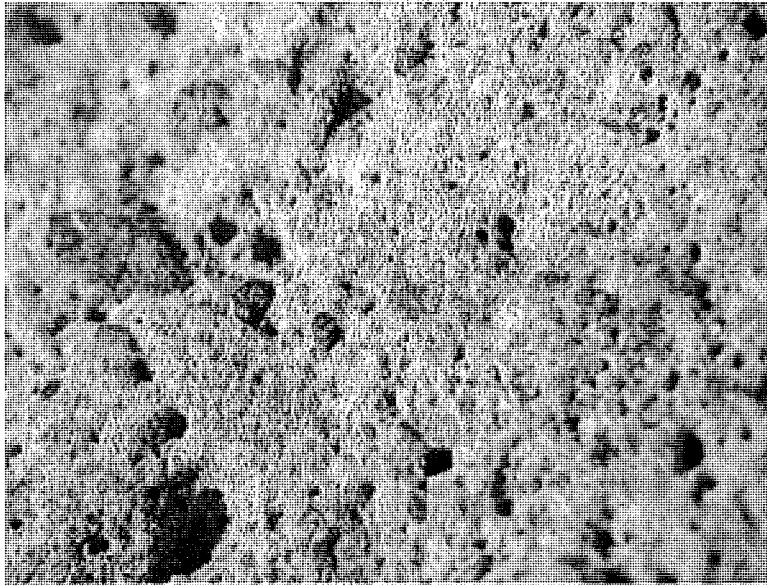


Photo 11-12. Sandblasted surface profile at 20x magnification, depressed region

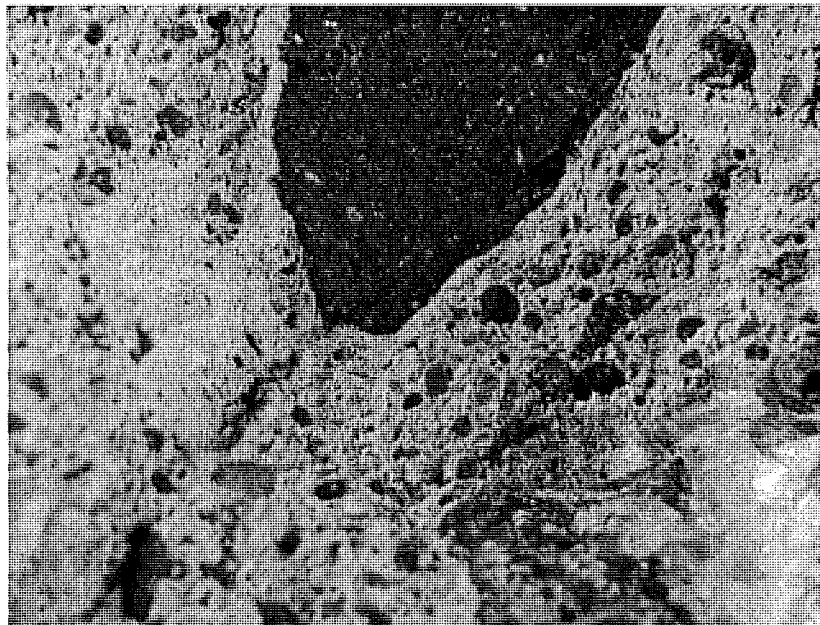


Photo 11-13. Wire brushed surface profile at 20x magnification, depressed region

Based on a visual review of Photo 11-10 through Photo 11-13, there was no obvious difference in the condition of the prepared surface between the sand blasted specimen and the wire brushed specimen. Michigan Tech research scientist Mr. Karl Peterson supported this opinion. Due to the similarity of preparation appearance and greater practicality, the wire brush method was selected to prepare the surface of all substrate specimens.

11.2.3 Repair of Substrate Specimens

Repair of the portland cement concrete specimens was performed in the Dillman Hall laboratories from January 23, 2002 to February 5, 2002. Repairs were typically performed at

room temperature using a two-person repair team. Details on the materials used and practices followed are summarized in the following sections. Thirty-nine specimens were repaired in accordance with Table 11-3.

Table 11-3. Number of Shallow and Deep Repair Specimens per Repair Material

Repair Material	No. of Shallow Repair Specimens	No. of Deep Repair Specimens
Brand X	6	6
Brand Y	6 + 2	6
Brand Z	6 + 1	6
Total No. of Specimens	21	18

11.2.3.1 Specimen Naming

A unique specimen identification system was created for the specimens. A four character alphanumeric designation for all of the repair specimens is shown in Table 11-4.

Table 11-4. Specimen Naming Convention for Vertical Repairs

Label	Description
First Digit: Repair Depth	D = Deep Repair S = Shallow Repair
Second Digit: Post-Curing Conditions	C = Cycled Temperatures A = Laboratory Ambient Temperatures
Third Digit: Repair Mortar Type	S = Brand X E = Brand Y T = Brand Z
Fourth Digit: Specimen No.	1 = Specimen No. 1 2 = Specimen No. 2 3, 4, etc = remaining specimens

As an example, the third shallow depth repair specimen repaired with Brand Y material and conditioned at laboratory ambient temperatures would be named "SAE3".

For accurate tracking, control and reserve specimens were also named. Reserve specimens were labeled with an "R" followed by the specimen number (e.g. R5). Control specimens without patch repairs were labeled with a "C" followed by an appropriate post-curing designation, "C" or "A", followed by the specimen number. For example, the second control sample that was seasoned under thermally cycled conditions would be "CC2".

11.2.3.2 Formwork

Individual multiple-use wood forms were used to form two edges for the repair of the substrate specimens. Pine boards having a 1-inch nominal thickness were selected for this purpose.

For ease of stripping, a release agent was applied to the inside of the forms. This release agent consisted of motor oil and was applied prior to clamping the forms to the sides of the substrate specimens.

11.2.3.3 *Repair Mortar*

For each repair, one of three prepackaged polymer-modified portland cement mortars was used, Sika Top 126 Plus, Emaco R350-CI, or Thoroc HB2. These products are intended for use in vertical and overhead applications where the thickness of the repair material is less than 1-in (overhead repair) to 3-in (vertical repair) (Sika USA, 2002; Chemrex 2002a, 2002b). Technical information on each of the mortars is presented in Table 11-5, based directly on information contained in manufacturer data sheets on each product (Sika USA, 2002; Chemrex 2002a, 2002b). While product information has been provided in this report, a blind study approach was used during testing and to compare results.

The layout of Table 11-5 is in conformance with the recommendations of other researchers in the concrete repair industry (McDonald et al, 2002). The table contains several rows of data for which information was not available, specifically with respect to the composition, physical properties, and performance properties of each material. However, past work has shown that these data are of interest to engineers when specifying repair materials (McDonald et al, 2002).

Table 11-5. Repair Material Data - All Manufacturers

Table 11-5 Repair Material Data - All Manufacturers			
Manufacturer	Sika USA	Master Builder Technologies	ThoRoc
Material	Sika Top 126 Plus	Emaco R350 CI	HB2
1. Repair Material Description			
Recommended Use	Use for fast repairs to overhead and vertical concrete or mortar surfaces on grade, above and below grade. Applicable for use as a repair material for building facades, parking structures, industrial plants, bridges, etc.	The product is ideally suited for patching and/or resurfacing distressed concrete. The lightweight nature of the product allows for excellent build without sagging. Emaco ® R350 CI repair mortar is designed for both interior and exterior use.	HB2 repair mortar can be used for vertical and overhead concrete repairs, around embedded steel reinforcement, where exceptional chloride and where carbon dioxide resistance is required. Product is suitable for interior or exterior use
Benefits	<ul style="list-style-type: none"> • Time/labor-saving material-application up to 3-in on vertical surfaces in one layer. • Application by hand or low-pressure wet-spray method. • Can be applied by hand or low- pressure wet spray equipment. • Factory proportioned packaging ensures constant quality. • High bond strength ensures excellent adhesion. • Good early and ultimate strength. • Increased freeze/thaw durability and resistance to deicing salts. • Enhanced with FerroGard 901, a penetrating corrosion inhibitor – reduces corrosion even in the adjacent concrete. • Low permeability provides protection against carbon dioxide and in water dissolved chlorides. • Compatible with coefficient of thermal • Expansion of concrete - Passes ASTM C884 modified. • Not a vapor barrier. 	<ul style="list-style-type: none"> • Corrosion resistant - contains an integral corrosion inhibitor • One component - easy mixing and handling • Low permeability - resists moisture and chloride intrusion • Low modulus of elasticity - improved compatibility for surface renovation • Economical - excellent yield per bag, low unit weight 	<ul style="list-style-type: none"> • Time/labor saving - can be applied up to 3-in on vertical and 1-1/2-in in overhead areas in one lift • Shrinkage compensated - minimizes shrinkage and stresses on the bond line • High bond strength - polymer component ensures excellent adhesion • Low permeability - provides protection against carbon dioxide and chloride intrusion • Durable - excellent freeze-thaw resistance • Compatible - coefficient of thermal expansion similar to concrete • Reliable - factory proportioned to overcome site-batched variations • Suitable for hand/trowel and low velocity wet spray applications

Table 11-5 Repair Material Data - All Manufacturers

Manufacturer	Sika USA	Master Builder Technologies	ThoRoc
Material	Sika Top 126 Plus	Emaco R350 CI	HB2
Limitations	<ul style="list-style-type: none"> • Application thickness: Minimum: 1/8-in Maximum in one lift: 3-in vertical. 1-1/2-in overhead. • Minimum ambient and surface temperatures: 45F and rising at time of application. • Do not use solvent-based curing compounds. • Size, shape and depth of repair must be carefully considered and consistent with practices recommended by ACI. For additional information, contact Technical Service. • For additional information on substrate preparation, refer to ICRI Guideline No. 03732. • If aggressive means of substrate preparation is employed, substrate strength should be tested in accordance with ACI 503 Appendix A prior to the repair application 	<ul style="list-style-type: none"> • Do not mix partial bags. • Minimum ambient and surface temperatures should be 45°F and rising at the time of application. • Do not use solvent-based curing compounds. • Do not mix longer than 5 minutes. • Featheredging will result in reduced performance. • Do not use in horizontal applications where wheeled traffic is anticipated. 	<ul style="list-style-type: none"> • Do not mix partial bags. • Do not use in horizontal areas subjected to vehicular traffic. • Do not expose to rain or moving water during application. • Exposure to heavy rainfall prior to the final set may result in surface scour. • In cold conditions down to 45°F, maintaining the ThoRoc Polymer Liquid at 80°F is advisable to accelerate strength development. Normal precautions for working with cementitious materials in the winter should then be adopted. Do not apply if the temperature is expected to fall below 45°F within 24 hours of application. • At ambient temperatures above 80°F, the materials should be stored in the shade. Cooling the ThoRoc Polymer Liquid to 60°F is recommended.
2. Composition Data			
Base Material(s)	Two-component, polymer-modified, cementitious ready-to-use repair mortar that contains FerroGard 901 penetrating corrosion inhibitor.	A low-density, one-component, polymer-modified, shrinkage-compensated lightweight renovation mortar that contains an integral corrosion inhibitor.	Two-component, polymer-modified, shrinkage-compensated high-build repair mortar
SO ₃ %: ASTM C563	None Listed	None Listed	None Listed
Alkali Content (lb./cy.)	None Listed	None Listed	None Listed
pH	None Listed	None Listed	None Listed
Air Content	None Listed	None Listed	None Listed
3. Physical Properties			
Unit Weight (lb/cf ³)	None Listed	103 lb / cf	None Listed

Table 11-5 Repair Material Data - All Manufacturers

Manufacturer	Sika USA			Master Builder Technologies			ThoRoc		
Material	Sika Top 126 Plus			Emaco R350 C1			HB2		
Wet Density – ASTM C138	106 lb/cf			None Listed			105 lb / cf		
Strengths (psi):	Test Age (days)			Test Age (days)			Test Age (days)		
	1	7	28	1	7	28	1	7	28
Compressive: ASTM C109	2,500	3,500	5,500	1,500	3,500	5,000	2,300	4,500	5,800
Flexural: ASTM C348	650 (ASTM C496)	None Listed	1,600 (ASTM C496)	250	700	900	None Listed	None Listed	1,000
Tensile: ASTM C496	None Listed	None Listed	700	200	300	600	None Listed	300	500
Modulus: ASTM C469	None Listed			2.0 x 10 ⁶ psi at 28 days			2.0 x 10 ⁶ psi		
4. Performance Properties									
Drying Shrinkage: ASTM C157 (Mod.)	None Listed			None Listed			350 micro strain at 28 days		
Coefficient of Thermal Exp. CRD C 39-81	None Listed			None Listed			4.5 x 10 ⁻⁶ in/in/°F		
F-T Resistance: ASTM C666A	None Listed			100% relative dynamic modulus			100% relative dynamic modulus at 300 cycles		
Comp. Creep: ASTM C512	None Listed			None Listed			None Listed		
Rapid Chloride Permeability: ASTM C1202	Less than 500 coulombs at 28 days, per AASHTO T-277, modified			300 coulombs			941 coulombs		
Sulfate Resistance: ASTM C1012	None Listed			None Listed			None Listed		
Cracking Resistance: Ring Test	None Listed			None Listed			None Listed		
First Crack Age	None Listed			None Listed			None Listed		
Implied Strain	None Listed			None Listed			None Listed		
End of Test Age	None Listed			None Listed			None Listed		

Table 11-5 Repair Material Data - All Manufacturers

Manufacturer	Sika USA	Master Builder Technologies	ThoRoc
Material	Sika Top 126 Plus	Emaco R350 CI	HB2
Cracking Resistance: German Angle	None Listed	None Listed	None Listed
5. Packaging, Storage			
Packaging	Component A: 1-gal. plastic jug; 4/carton. Component B: 53-lb. multi-wall bag.	55-lb. moisture-resistant bags	45 or 225-lb bags for dry component and 1 or 5-gallon containers for liquid component
Volume Yield	0.58 cubic feet / unit	0.61 cubic feet / unit	0.50 cubic feet / unit or 2.50 cubic feet / unit
Shelf Life	12 months	12 months	12 months
Storage Requirements	Store dry at 40 to 95 F. Condition material to 65 to 75 F before using. Protect Component A from freezing. If frozen, discard.	Store under cover in dry conditions between 45 and 90 F.	Transport and store in cool, dry conditions between 40°F and 85°F in the original, unopened containers.
6. How the Material Works			
Description	None Listed	None Listed	None Listed

Table 11-5 Repair Material Data - All Manufacturers

Manufacturer	Sika USA	Master Builder Technologies	ThoRoc
Material	Sika Top 126 Plus	Emaco R350 CI	HB2

7. How to Use the Material

<p>Concrete Surface Preparation</p>	<p>Remove all deteriorated concrete, dirt, oil, grease, and all bond-inhibiting materials from surface. Be sure repair area is not less than 1/8-in. depth. Preparation work should be done by high-pressure water blast, scabber, or other appropriate mechanical means to obtain an exposed aggregate surface with a minimum surface profile of $\pm 1/16$-in. (CSP-5). Saturate surface with clean water. Substrate should be saturated surface dry (SSD) with no standing water during application.</p>	<p>Perform surface preparation in compliance with ICRI Technical Guideline No. 03730 "Guide for Surface Preparation for the Repair of Deteriorated Concrete Resulting from Reinforcing Steel Corrosion." Square cut or undercut the perimeter of the area to be patched to a minimum depth of 1/8-in to prevent featheredges. Do not cut reinforcement. Chip and remove unsound and delaminated concrete within the area to be repaired to a depth of 1/8-in or to whatever additional depth is necessary to reach sound concrete. Limit the size of chipping hammers to 15-lbs. to reduce micro fractures. Hydrodemolition may be used. Remove areas that have been saturated with oil or grease. Remove 3/4-in of concrete behind the corroded reinforcing steel to provide adequate space for preparation and material placement. After concrete removal, thoroughly abrade the roughened surface and exposed reinforcement to remove all bond-inhibiting materials such as rust, dirt, loose chips, and dust.</p>	<p>Concrete substrate must be structurally sound. Loose or unsound concrete should be hammered out. Saw cut the edges of the repair locations to a depth of at least 3/8-in to avoid featheredging and to provide a square edge. Break out the complete repair area to a minimum depth of 3/8-in up to the sawn edge. Clean the surface by removing any dust, unsound or contaminated material, plaster, oil, paint, greases, corrosion deposits or algae. Where breaking out is not required, roughen the surface and remove any laitance by mechanical means or high-pressure water wash. Oil and grease deposits, should be removed by steam cleaning, detergent scrubbing, or the use of a degreaser. To ensure optimum repair results, assess the effectiveness of decontamination by a pull-off test.</p>
--	--	---	---

Table 11-5 Repair Material Data - All Manufacturers

Manufacturer	Sika USA	Master Builder Technologies	ThoRoc
Material	Sika Top 126 Plus	Emaco R350 CI	HB2
Mixing	<p>Pour Component A into the mixing container. Add Component B while mixing continuously. Mix mechanically with a low-speed drill (400 to 600-rpm) and mixing paddle or in an appropriate mortar mixer. Mix to a uniform consistency, maximum 3-minutes. Manual mixing can be tolerated only for less than a full unit. Thorough mixing and proper proportioning of the two components is necessary.</p>	<p>Mechanical mixing is recommended with use of a slow speed drill (400 to 600-rpm) and a Jiffy-type paddle, or in an appropriate size mortar mixer. Add 0.95 to 1.1-gallon of clean potable water per 55-lb. bag of Emaco ® R350 CI. Pour approximately 90 percent of the mix water into the mixing container, then charge the mixer with the bagged material. Add remaining mix water as required for vertical or overhead applications. Mix to a uniform consistency. Typical mixing time is 3 to 5-minutes. Do not mix longer than 5-minutes.</p>	<p>Ensure that ThoRoc " HB2 Repair Mortar is thoroughly mixed. A forced action mixer is essential. Mixing in a suitably sized container using an appropriate paddle and variable speed (400 to 500-rpm) heavy-duty drill is acceptable for the occasional one-bag mix. Free-fall mixers should not be used and mixing of partial bags is not recommended. The material should always be mixed in a clean container. For normal applications, place 3-quarts of ThoRoc Polymer Liquid into the clean mixer for each complete 45-lb. bag of HB2 Repair Mortar and mix for 3 to 5-minutes until fully homogeneous. Avoid over-mixing. Note that the powder should always be added to the liquid. Depending on the ambient temperature and the desired consistency, additional ThoRoc Polymer Liquid may be added up to a maximum liquid content of 1-gallon per 45-lb bag of HB2 Repair Mortar.</p>

Table 11-5 Repair Material Data - All Manufacturers

Manufacturer	Sika USA	Master Builder Technologies	ThoRoc
Material	Sika Top 126 Plus	Emaco R350 CI	HB2
Application and Finish	<p>SikaTop 126 Plus must be scrubbed into the substrate filling all pores and voids. SikaTop 126 Plus can be applied either by hand or low-pressure wet spray process equipment. The mixed SikaTop 126 Plus must be worked well into the primed substrate, filling all pores and voids. Compact well. Force material against edge of repair, working towards the center. Thoroughly compact the mortar around ex-posed reinforcement. After filling repair, consolidate, then screed. Finish with steel, wood or plastic floats, or damp sponges, depending on the desired surface texture. Where multiple lifts are required, score top surface on each lift to produce a roughened substrate for next lift. Allow preceding lift to harden before applying fresh material. Saturate surface of the lift with clean water. If previous layers are over 48-hours old, mechanically prepare the substrate. Dampen and apply bonding agent or scrub coat prior to the mortar.</p>	<p>Remove excess water from the saturated surface dry (SSD) substrate and apply while taking proper consideration for compaction around reinforcing steel. Scrub a bond coat of Emaco ® R350 CI repair mortar into the prepared surface with a stiff bristle broom or brush. Emaco ® R350 CI repair mortar must be placed before the bond coat dries. When applying in multiple lifts, scratch the preliminary lift before initial set. Apply the next lift after the preliminary lift has reached final set. If the next lift is not to be immediately placed, keep the surface continually moist. Cut off or level as required to match the original concrete elevation. Maximum application thickness is 2-3/4-in. Where rapid drying conditions exist (e.g., hot, dry, windy conditions) use Confilm ® evaporation reducer. Finish the final surface as required.</p>	<p>Substrate should be SSD (saturated surface dry) with no standing water. Using a stiff brush, scrub a thin coat of the mixed material thoroughly into the surface to ensure sufficient bonding. Before bond coat dries, thoroughly compact the mortar onto the substrate and around the exposed reinforcement. HB2 Repair Mortar can be applied in sections up to a 3-in thickness in vertical locations and up to a 1-1/2-in thickness in overhead locations in a single lift and without the use of formwork. Thicker sections should be built up in layers, but are sometimes possible in a single application depending on the actual configuration of the repair area and the volume of exposed reinforcing steel. If sagging occurs during application, HB2 Repair Mortar should be completely removed and reapplied at a reduced thickness onto the correctly re-primed substrate. HB2 Repair Mortar is finished by striking off with a straight edge and closing with a steel float. Wooden or plastic floats or sponges may also be used to achieve the desired surface texture. The completed surface should not be overworked.</p>

Table 11-5 Repair Material Data - All Manufacturers

Manufacturer	Sika USA	Master Builder Technologies	ThoRoc
Material	Sika Top 126 Plus	Emaco R350 CI	HB2
Curing	<p>As per ACI recommendations for portland cement concrete, curing is required. Moist cure with wet burlap and polyethylene, a fine mist of water or a water based*, compatible curing compound. Curing compounds adversely affect the adhesion of following lifts of mortar, leveling mortar or protective coatings. Moist curing should commence immediately after finishing. If necessary protect newly applied material from direct sunlight, wind, rain and frost.</p> <p>*Pre-testing of curing compound is recommended.</p>	<p>Proper curing is extremely important and should be conducted in accordance with ACI 308, "Standard Practice for Curing Concrete." Apply a curing compound which complies with the moisture retention requirements of ASTM C 309, such as Masterkure ® 100W or 200W curing compounds. Apply curing materials as soon as the surface cannot be marred by the application. Sheeting material, wet burlap, or fog spray may be used in lieu of curing compounds. Minimum curing time for wet curing is three days. Give mortar extra time for curing in temperatures below 50°F.</p>	<p>Proper curing is extremely important. HB2 Repair Mortar should be cured immediately after finishing in accordance with good concrete practice (ACI 308) to approach peak performance of the repair. Proper curing is of particular importance when ambient conditions may cause rapid moisture loss (high temperature, low humidity, or moderate to high winds). The use of ThoRoc Acrylic Modifier, or an appropriate ASTM C 309 compliant curing compound, sprayed on to the surface of the finished repair in a continuous film, is recommended. Large areas of greater than 5-sq. ft. should be cured as troweling progresses without waiting for completion of the entire area. Other curing options include a fine mist of water, application of wet burlap (burlap must be kept continuously moist), application of polyethylene sheeting taped down at the edges, or a combination of the above to keep the finished repair moist for a minimum of 7-days. In cold conditions, the finished repair must be protected from freezing. If doubts arise concerning proper curing procedures, consult ACI guidelines.</p>

Table 11-5 Repair Material Data - All Manufacturers

Manufacturer	Sika USA	Master Builder Technologies	ThoRoc
Material	Sika Top 126 Plus	Emaco R350 CI	HB2
Cleanup	In case of spillage, scoop or vacuum into appropriate container, and dispose of in accordance with current, applicable local, state and federal regulations. Keep container tightly closed and in an upright position to prevent spillage and leakage. Mixed components: Uncured material can be removed with water. Cured material can only be removed mechanically.	This product when discarded or disposed of is not listed as a hazardous waste in federal regulations. Dispose of in a landfill in accordance with local regulations. For additional information on personal protective equipment, first aid, and emergency procedures, refer to the product Material Safety Data Sheet (MSDS)	HB2 Repair Mortar should be removed from tools, equipment and mixers with clean water immediately after use. Cured material can only be removed mechanically. Clean hands and skin immediately with soap and water or industrial hand cleaner.

Table 11-5 Repair Material Data - All Manufacturers

Manufacturer	Sika USA	Master Builder Technologies	ThoRoc
Material	Sika Top 126 Plus	Emaco R350 CI	HB2
Safety	<p>Component A - Irritant - May cause skin/eye/respiratory irritation. Avoid breathing vapors. Use with adequate ventilation. Avoid skin and eye contact. Safety goggles and rubber gloves are recommended.</p> <p>Component B - Irritant; suspect carcinogen - Contains portland cement and sand (crystalline silica). Skin and eye irritant. Avoid contact. Dust may cause respiratory tract irritation. Avoid breathing dust. Use only with adequate ventilation. May cause delayed lung injury (silicosis). IARC lists crystalline silica as having sufficient evidence of carcinogenicity in laboratory animals and limited evidence of carcinogenicity in humans. NTP also lists crystalline silica as a suspect carcinogen. Use of safety goggles and chemical resistant gloves is recommended. If PELs are exceeded, an appropriate, NIOSH/MSHA approved respirator is required. Remove contaminated clothing.</p> <p>In case of skin contact, wash thoroughly with soap and water. For eye contact, flush immediately with plenty of water for at least 15 minutes, and contact a physician. For respiratory problems, remove person to fresh air.</p>	<p>Eye irritant. Skin irritant. Causes burns. Lung irritant. May cause delayed lung injury. Avoid contact with eyes. Wear suitable protective eyewear. Avoid prolonged or repeated contact with skin. Wear suitable gloves. Wear suitable protective clothing. Do not breathe dust. In case of insufficient ventilation, wear suitable respiratory equipment. Wash soiled clothing before reuse. Wash exposed skin with soap and water. Flush eyes with large quantities of water. If breathing is difficult, move person to fresh air.</p>	<p>Product is alkaline on contact with water and may cause injury to skin or eyes. Ingestion or inhalation of dust may cause irritation. Contains free respirable quartz, which has been listed as a suspected human carcinogen by NTP and IARC. Repeated or prolonged overexposure to free respirable quartz may cause silicosis or other serious and delayed lung injury.</p> <p>Precautions: Prevent contact with skin and eyes. Prevent inhalation of dust. Do not take internally. Use only with adequate ventilation. Use impervious gloves, eye protection and if the TLV is exceeded or used in a poorly ventilated area, use NIOSH/MSHA approved respiratory protection in accordance with applicable federal, state and local regulations. In case of eye contact, flush thoroughly with water for at least 15 minutes and seek immediate medical attention. In case of skin contact, wash affected areas with soap and water. If irritation persists, seek immediate medical attention. Remove and wash contaminated clothing. If inhalation causes physical discomfort, remove to fresh air. If discomfort persists or any breathing difficulty occurs or if swallowed, seek immediate medical attention.</p>

11.2.3.4 Repair Fabrication

11.2.3.4.1 General Practices

Certain practices were followed during repair fabrication, regardless of the repair material, thickness, or orientation. All surfaces of the substrate specimen to receive the repair material were re-cleaned with compressed air at roughly 60-psi until no further airborne debris was observed. This cleaning often resulted in the noticeable removal of concrete dust and at times small (less than 1/4-in diameter) concrete chips. Specimen orientation, vertical or overhead, was maintained during the repair and curing processes.

Forms were secured to the sides of the specimen using adjustable clamps (see Photo 11-14). The repair area of the substrate specimens was then wetted to a near saturated surface dry (SSD) condition. Multiple applications of water mist from a garden hose or hand held spray bottle were used to maintain this state prior to the installing the repair material.

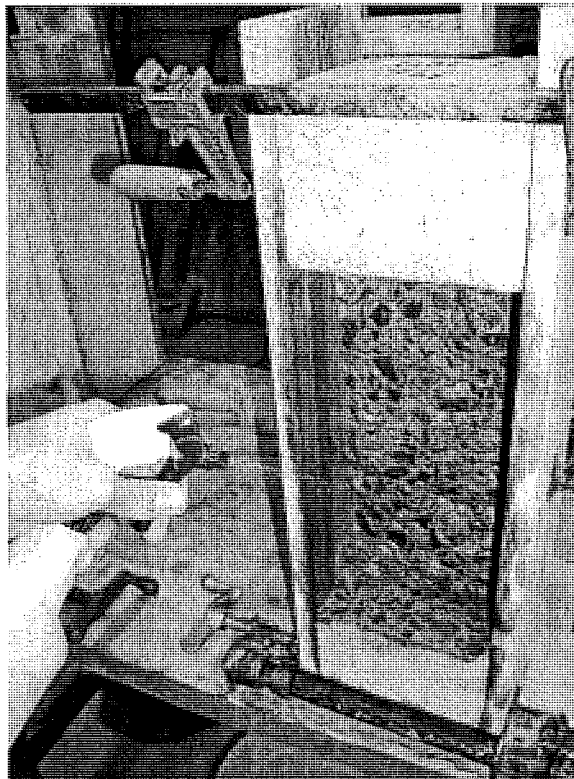


Photo 11-14. Formwork in place on a substrate specimen and wetting of prepared surface

Repair mortar was mixed in partial units in a Hobart Manufacturing Company Model N-50 variable speed stand mixer as shown in Photo 11-15. The quantities and limits of liquid component and dry component were pre-determined, measured with scales or graduated cylinders in clean containers, and added to the mixing bowl. Proportions used for each repair depth are presented in Table 11-6 through Table 11-8.

Table 11-6. Mixture Proportions for Brand X Repair Mortar

Brand X Component	Proportions for Shallow Repair	Proportions for Deep Repair
Dry Mortar	6.28-lb	16.34-lb
Polymer Liquid	15.2 oz	39.6 oz

Table 11-7. Mixture Proportions for Brand Y Repair Mortar

Brand Y Components	Proportions for Shallow Repair	Proportions for Deep Repair
Dry Mortar	6.22-lb	16.22-lb
Water	13.7 oz to 15.6 oz	35.7 oz to 40.7 oz

Table 11-8. Mixture Proportions for Brand Z Repair Mortar

Brand Z Components	Proportions for Shallow Repair	Proportions for Deep Repair
Dry Mortar	6.19-lb	16.11-lb
Polymer Liquid	13.0 oz to 17.7 oz	33.9 oz to 46.0 oz

For every batch of mortar mixed, the liquid component was always added prior to the dry component. The start of mixing was documented once the dry component was added to the mixing bowl. Mixing was performed with the mixer at low speed (agitator speed: 136 RPM, attachment speed: 60 rpm) for 3 (Brand X) or 5-minutes (Brand Y and Z). Mix times and batch quantities were documented and varied from batch to batch depending on the mortar manufacturer recommendations. After mixing, the fresh mortar was either transferred to stainless steel bowls or remained in the mixing bowl prior to placement. Repair material from each batch was placed within approximately 10 to 30 minutes after mixing.



Photo 11-15. Equipment used for preparing repair mortar

With the mortar freshly mixed, hand held stiff bristle brushes were used to scrub repair mortar into the SSD substrate (see Photo 11-16). Brush size and bristle stiffness varied, however a palm-sized plastic bristle brush was generally used for the bulk of the scrubbing and a toothbrush-sized steel bristle brush was used for corners and depressed areas.

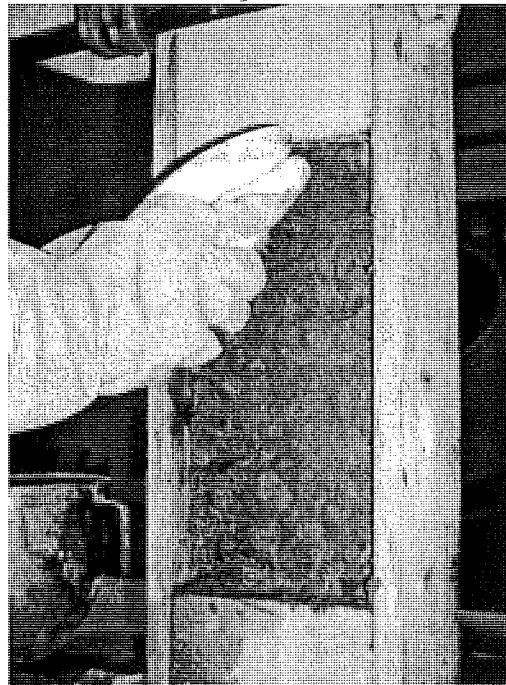


Photo 11-16. Scrubbing mortar into the prepared substrate surface

Several methods were attempted for placing the repair material into the void. These methods were by hand, putty knife, and steel trowel. A majority of the specimens were repaired by placing repair mortar with a 2-in steel putty knife (see Photo 11-17). The size of the knife alone required that small amounts of mortar be placed at a time.

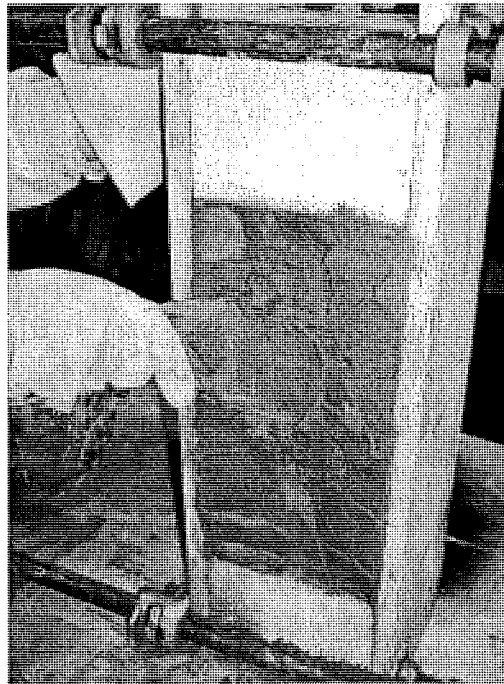


Photo 11-17. Applying repair mortar with a putty knife

The plastic repair material was consolidated in-place by a variety of methods. Tools used included fingers, round-nosed steel bars, flat steel bars, the pressure of the knife, and blunt-end bars. In general, a well-distributed pattern of penetration points was followed, regardless of the tool used, with the exception of the knife-pressure approach. Repair material placed for shallow repairs was generally consolidated once, after the full thickness of the repair had been achieved. Consolidation with tools having a large surface area (e.g. the flat side of a putty knife compared to a round-nosed rod) tended to produce the densest repairs. Deep repairs were generally consolidated twice, at the mid-depth thickness and again after the full thickness of the repair had been achieved. Applying additional mortar with the pressure of the knife closed depressions in the mortar that remained after consolidation.

Specimens were finished with a steel trowel as shown in Photo 11-18. Finishing operations were kept to a minimum, aiming to achieve surface uniformity without causing sagging of the repair material.

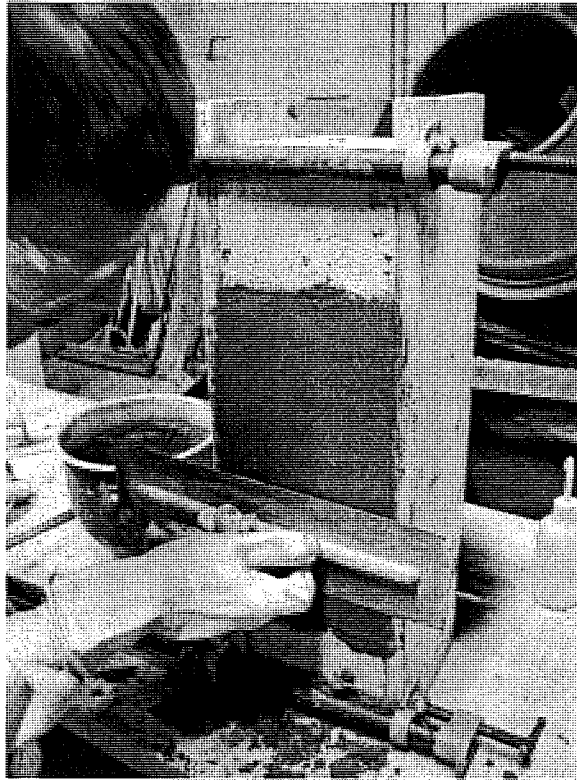


Photo 11-18. Finishing repair specimens with a steel trowel

11.2.3.4.2 Shallow Repair: Vertical Placement

Twenty-one shallow repairs cast in the vertical position were in general conformance with the procedures described above. The overall size of this repair type was 6-in by 12-in at a 1-in nominal repair depth. Substrate specimens were set atop a 3.5-ft high workbench to aid in placement of the mortar.

In general, mortar was placed first at the top of the specimen and progressed downward and outward to the finished surface. Specimens remained in the vertical position until initial set (approximately 30 minutes) whereby they were temporarily turned horizontal for setting of instrumentation points.

Due to bonding problems noticed during installation of repair material on one specimen, "SCE1", an additional specimen was fabricated. For this specimen, a reserve substrate specimen was prepared for a shallow depth repair and repaired using the Brand Y repair material in the vertical position. This specimen was thermally cycled after initial curing and was labeled "R1".

11.2.3.4.3 Shallow Repair: Overhead Placement

Two specimens were repaired in the overhead position, each using a different repair material. These specimens were in addition to the original 39 specimens cast for this experiment. As such, two of the reserve specimens, "R2" and "R5" were selected for the substrate specimens. The Brand Z and Brand Y materials were arbitrarily selected for the "R2" and "R5" specimens, respectively. Specimen "R2" was further designated to have post-curing thermal cycling while specimen "R5" was placed in a laboratory ambient post-curing environment.

The overall size of this repair type was 6-in by 12-in at a 1-in nominal repair depth. The intent of performing these repairs was to validate the feasibility and performance of a repair mortar applied in the overhead position.

In the laboratory, overhead repair specimens were set between two tables of equal height, approximately 3.5 feet off the floor of the laboratory (see Photo 11-19). Formwork application, surface preparation, mortar mixing, mortar placement, and mortar finishing then proceeded similarly to that for the vertical repair of shallow depth specimens with few exceptions. The most notable exception was that the mortar was not consolidated in-situ, other than with the consolidation provided by the pressure of the knife (see Photo 11-20).

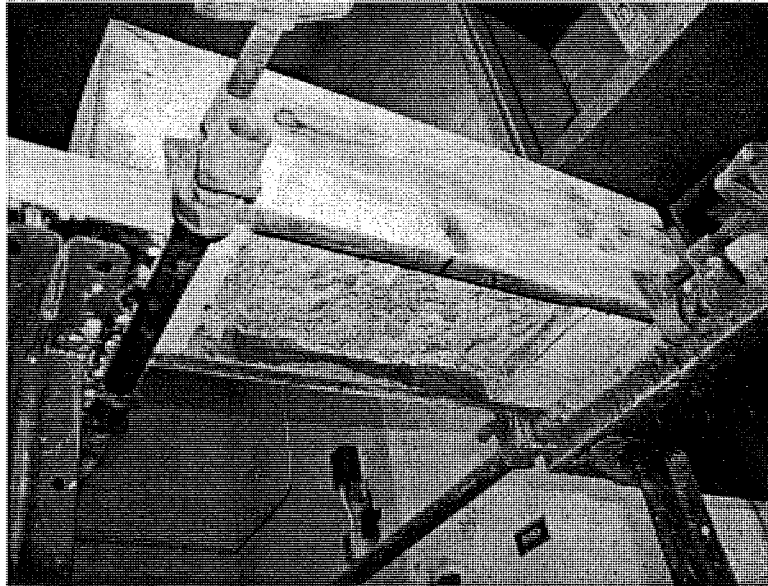


Photo 11-19. Specimen in the overhead position prior to initiating repairs

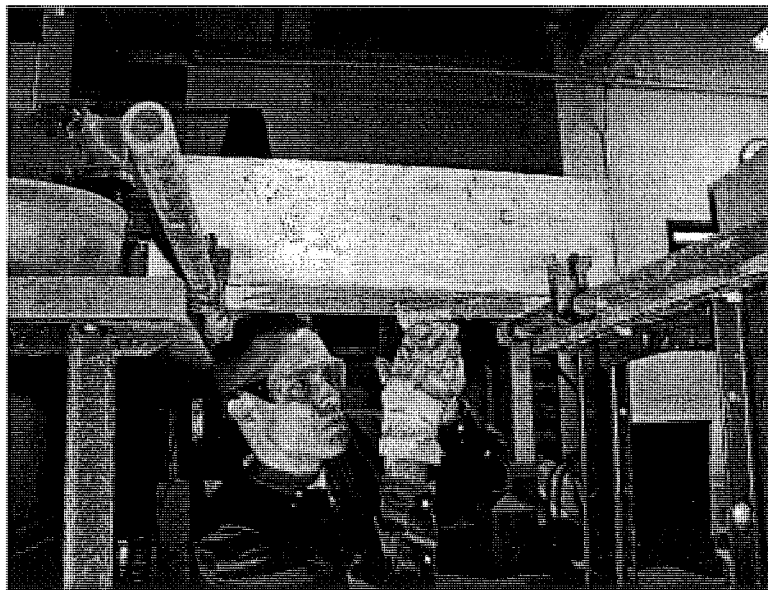


Photo 11-20. Placing repair material in the overhead position

Specimens remained in the overhead position until initial set (approximately 30 minutes) and were then temporarily turned upright for setting of instrumentation points.

11.2.3.4.4 Deep Repair: Vertical Placement

Eighteen deep repairs cast in the vertical position were in general conformance with the procedures described above. The overall size of this repair type was 6-in by 12-in at a 3-in nominal repair depth. Substrate specimens were set atop a 3.5-ft high workbench to aid in placement of the mortar.

Due to outward sagging of the repair material at a full-height placement of trial repairs, deep repair specimens needed to be repaired in two successive 6-in vertical lifts. In general, the lower mortar lift was first placed at the bottom of the specimen and progressed upward and outward to the finished surface. Edges of the formwork were clearly marked at the intended inter-lift height for reference during repair material placement. Typically, the lower lift was over-filled by one inch. After some hardening of the mortar, the excess was cut off with the knife to the inter-lift height. The top surface of the lower-lift mortar was then etched with an awl in a random pattern to improve bond between each lift.

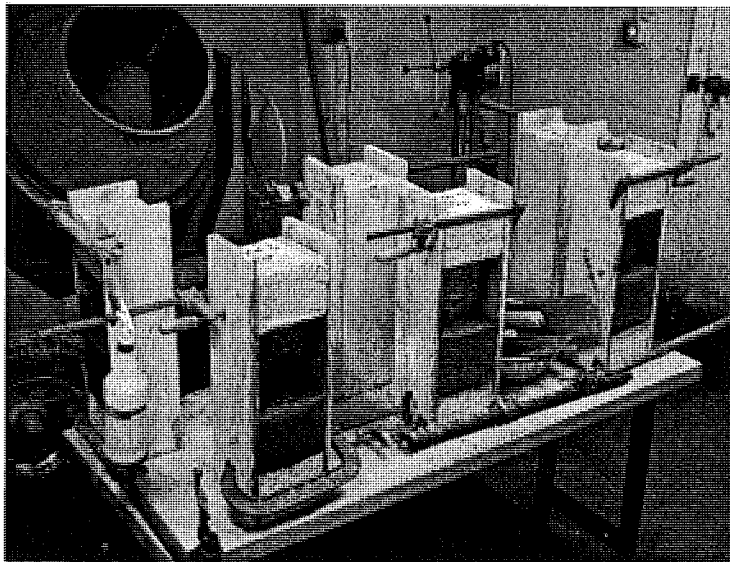


Photo 11-21. Deep repair specimens with the bottom lift in place

The upper lift of mortar was placed after the lower lift had hardened sufficiently to support the next lift (approximately 2-1/2 hours). Loose mortar that remained on the top surface of the lower lift was removed with compressed air prior to repair material placement. Repairs then proceeded in a similar fashion to those used for the shallow depth vertical specimens, including a mortar scrub of the top edge of the lower repair surface. After surface preparation, the void for the upper lift was filled from the top down, with the repair progressing downward and outward to the finished surface, in the opposite direction of the lower lift repair. These procedures were per the manufacturers technical support for deep repairs. These techniques would also be used for proper placement of repair mortar in the field.

Specimens remained in the vertical position until initial set of the upper lift (approximately 3 hours from start of lower lift) and were then temporarily turned horizontal for setting of instrumentation points.

11.2.3.5 Instrumentation

Each repair specimen was fitted with six pairs of DETachable MEChanical (DEMEC) points after the last lift of repair material had achieved initial set. By measuring the change in distance between each pair of DEMEC points, shrinkage information of the mortar and substrate was to be gathered and assessed. The points were mounted on the surface of the specimen that received the repair mortar with the specimen in the horizontal position. Figure 11-1 previously illustrated the typical setting pattern used on each repair specimen.

Points were set in pools of Devcon 5-minute epoxy gel on the surface of each specimen and kept parallel to one another by steel bar stock spacer bars. Spacer bars were secured to each point pair with machine screws and removed from the pair within at least one day.

11.2.3.6 Curing

Moist curing methods were used to cure the repair materials selected for this study. Moist curing was selected as the curing method since it was appropriate for each of the three repair materials and could be performed in the field (Sika USA, 2002; Chemrex, 2002a; Chemrex, 2002b). In the field, moist curing of beam end repairs could be achieved with burlap blankets and intermittent water sprinkling.

Moist curing was initiated after the epoxy for the instrumentation points had set sufficiently (approximate set time of 15 minutes). With the epoxy set, the specimens were returned to the vertical or overhead position and transported to a moist cure room. The moist cure room used for this project was located on the ground level of Dillman Hall. This room is equipped with water misting nozzles at the ceiling, emitting spray on specimens set below. Specimen temperatures inside the cure room ranged between 55 to 60 degrees Fahrenheit.



Photo 11-22. Repair specimens undergoing initial curing in a moist cure room

Moist curing was conducted for 2 to 7 days inside the cure room, depending on the repair mortar manufacturer's minimum recommended curing time. At the conclusion of moist curing, the specimens were removed from the moist cure room and stored in Dillman Hall at laboratory ambient conditions. Specimens remained in laboratory ambient temperature and humidity conditions until one of the two designated starting dates for documenting post-curing conditions, February 7, 2002 (first 33 specimens repaired: lot 1), or February 13, 2002 (last 6 specimens repaired: lot 2). Specimens in lot 2 included R1, R2, R5, DCE3, DCT2, and DCT3. The time between removal from the curing room to the commencement of post-curing conditions for lot 1 specimens ranged from 7 to 12 days. Lot 2 specimens were in laboratory ambient temperature and humidity conditions for 1 to 6 days prior to commencement of post-curing conditions.

11.2.3.7 *Post-Curing Conditions*

Roughly half of the specimens were designated for laboratory ambient post-curing conditions with the other half reserved for thermally cycled conditions. The specimens designated for laboratory ambient post-curing conditions were stored in the vertical or overhead position until preparation for direct tension testing as described in Section 11.3.3.3. Specimens continually remained in their as-repaired position except when bi-weekly strain measurements were obtained.

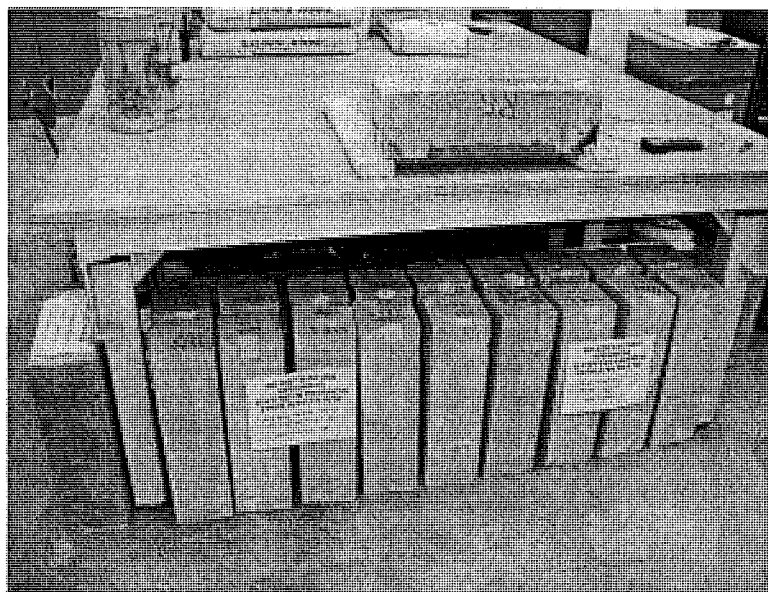


Photo 11-23. Storage of repair specimens undergoing laboratory ambient post-curing conditions

The remaining specimens were transported to a thermal chamber located in the Dow Environmental Science and Engineering Building. The thermal chamber used for this project was manufactured by Bally Refrigerated Boxes and equipped with a CAN-TROL Environmental Systems Ltd. control panel. Specimens were stored in the vertical or overhead

position until March 24, 2002 (lot 1) or March 30, 2002 (lot 2). Specimens continually remained in their as-repaired position except when bi-weekly strain measurements were obtained.



Photo 11-24. Exterior of thermal chamber

The features of the chamber control panel required that the temperatures be manually cycled on a daily basis. A log of the daily-programmed chamber temperature, previous chamber temperature, and previous chamber setting is included in Appendix G of Kasper's report (Kasper, 2002). Chamber temperatures were typically set at 32 or 95 degrees Fahrenheit. However, actual chamber temperatures ranged from 32 to 88 degrees Fahrenheit 24 hours after manually changing the chamber temperature.

Each specimen was in the chamber for 44 days. Because the chamber was not cycled for one weekend, the specimens were subjected to 21 high-low-high temperature cycles.

Specimens were subjected to visual inspection of repair surfaces (Section 11.3.2), strength evaluation (Section 11.3.3) including isolated material tests, and shrinkage evaluation (Section 11.3.4).

11.3 Experimental Results and Observations

In this section, the results of the experimental study conducted are presented. In addition to numerical data and analysis, a portion of this section includes observations made during fabrication and a discussion of the surface condition of the repairs at the conclusion of post-curing conditioning. Test procedures used in the study will be briefly described, along with the results and significance of the test data. Where testing procedures have deviated from established standards, the actual practices used have been described.

11.3.1 Fabrication Observations

11.3.1.1 Substrate Specimens

Fabrication of the substrate specimens followed engineering judgment and construction practice as previously described in this chapter. Substrate specimens generally exhibited sufficient consolidation, as evidenced by infrequent bugholes on the sides of the specimens. The addition of the No. 4 reinforcing bar opposite of the repaired face appeared to have provided sufficient ductility and durability to the substrate specimen, as no specimens were damaged during selective demolition. The surface finish of the substrate specimens was generally rough and at times, uneven. This finish and texture was difficult to match when placing repair material within the substrate specimen. The use of polystyrene blanks in the face of the substrate specimens did not adversely affect the casting of the substrate specimen and accelerated concrete removal operations.

Cutting concrete with a diamond saw blade was found to be a practical and effective method for sound concrete removal. Although the saw used for this study was a stationary unit, it is anticipated that similar results could be achieved with hand held equipment. Sawing provides a way of eliminating feathered edges of repairs by providing a square edge at the limit of the repair. If in future work a more effective means of concrete removal is found, sawing may still be desirable to produce desired substrate edges at the limits of the repair. However, bond between the repair material and substrate at the smooth interface may be of concern. Bond at this location was not evaluated in this study.

A rotary hammer was proven to be a practical and effective tool for removing sound, scored concrete. The rotary hammer used for this study had an approximate weight of 14 pounds and generated 4.4 ft-lbs of impact energy (S-B Power Tool Company, 2002). Other rotary hammers are commercially available with a range of hammer weight and impact energy characteristics. These tools may also be suitable for concrete removal. However, based on the bond tensile strength results discussed later in the sections *Bond Tensile Strength of Repairs* and *Bond Tensile Strength of Substrate*, the use of the rotary hammer may have had an adverse effect on the bond of the repair material to the substrate. This is evidenced by the lower failure stress of those repair specimens that failed entirely within the concrete substrate compared to the failure stress of the control substrate-only specimens.

Surface preparation with a wire wheel brush may or may not be an effective method of preparing a concrete substrate prior to repair. This inconclusive observation is made because the preparation quality was sufficient to allow failure within the substrate in roughly 5-percent

of the bond tensile strength tests, but that over 75-percent of the repair bond tensile strength failures occurred at the repair-substrate interface.

11.3.1.2 *Repair Specimens*

Manufacturer installation instructions for each of the three prepackaged repair materials permitted user variation in repair mortar consistency (Sika USA, 2002; Chemrex, 2002a; Chemrex, 2002b). Placing mortars that were mixed at the lower range of recommended water or polymer to cement ratios ($w-p/c$) were difficult to place. This was evidenced by the installation of repair mortar in specimens SAT1 and SAT2. The liquid component for these repairs was at the lower limit of the $w-p/c$ ratio of other specimens. The stiff consistency not only made for difficult material placement, but also was difficult to consolidate and finish.

Manufacturer installation instructions for each of the repair materials also suggest that the dry and liquid components of the repair mortar be mixed in “full-bag” portions (Sika USA, 2002; Chemrex, 2002a; Chemrex, 2002b). However, for this study, roughly 20 individual batches of repair mortar were produced from each full-bag of dry repair material. It was found that the individual batches were similar in terms of initial mortar consistency and workability based on observations during repair. In addition, it was observed that the repair mortars became difficult to work as the material was used during repair. Depending on the level of experience of the person or team working with the repair material, environmental conditions, repair geometry, and mixing equipment, partial bag mixing may be a more efficient use of repair material. If full bag batches are used, waste material can be expected due to the material attaining set prior to installation.

Sagging of plastic repair mortar can be a problem in shallow and deep repairs. Sagging is an outward progression of the repair mortar from the intended exterior limit of the repair. In general, mixes with a stiffer consistency were found to sag less than those mixes that exhibited greater flow. Sagging was reduced in shallow depth vertical repairs by placing the mortar at the top of the specimens first and progressing to the sides and bottom of the repair. Sagging was a significant problem in deep repairs, as evidenced by observations of the first deep repairs attempted in this study (DAT1, DAT2). A suggestion from the technical representatives at Chemrex to minimize sagging was to build the deep repairs from the bottom up with individual lifts of material. This approach worked marginally well when using two subsequent 6-in vertical lifts of repair mortar. The lower lift was typically allowed to set approximately 2-1/2-hours prior to placing the upper lift. However, sagging did occur in the lower lift of some specimens. Smaller lifts and/or longer times between successive lifts may have produced even less sagging and therefore better results, but the time required to make multiple lift repairs can make this approach undesirable.

Manufacturer installation instructions for each of the three prepackaged repair materials did not state how to achieve consolidation of the repair mortar. Numerous types of consolidation procedures for the repair mortar were attempted on the vertical repairs. Consolidation was attempted with a flat bar, by hand, putty knife pressure, round-nosed dowels, and blunt-ended bars. Using tools with a relatively large contact area such as a putty knife or blunt-ended bars worked the best for consolidating mortar into the repair area. However, excessive consolidation of the repair mortar, regardless of the tool used, resulted in sagging.

Each of the three repair materials generally finished well with the steel trowel. Repeated finishing in an effort to achieve maximum surface uniformity often contributed to sagging. It

was therefore desirable to finish the specimens with as little effort as possible. Finishing with a “dry” trowel tended to split or tear the exterior surface of the repairs, especially for repairs using polymer liquid components.

11.3.2 Visual Review of Repair Surfaces

A visual review of the repair surface for each specimen was conducted after obtaining final distance measurements between the DEMEC points and prior to performing bond tensile strength testing. The examination was performed to document obvious repair conditions such as the presence of cracking, sagging, spalling, finishing defects, and delaminations. Cracks were visually documented with the aid of a crack comparator and delaminations were located by tapping on the repair surface with a mason’s hammer. Laboratory logs were completed for each set of three specimens cast for a particular material, repair depth, and post-curing condition and are included in Appendix H of Kasper’s report (Kasper, 2002).

Observations were performed on March 26, 2002 (lot 1 specimens) and March 30, 2002 (lot 2 specimens). A discussion of observations follows, separated per repair material.

11.3.2.1 *Brand X Repaired Specimens*

Twelve specimens were repaired with Brand X. Two-thirds of these specimens exhibited cracking at the bottom repair-substrate joint for specimens in the vertical position. For deep repair specimens, crack widths were on the order of 2-mils. Three of the cracked shallow repair specimens had cracking at the bottom repair-substrate joint in the range of 2 to 13 mils in width, however two other shallow repair specimens exhibited cracking of greater widths. These specimens, SCS1 and SCS2, exhibited relatively wide cracking, possibly severe enough to be considered a void, at the bottom repair-substrate joint. This crack or void resembled a surface retreat of the mortar away from the substrate. The width of the cracking was on the order of 16 mils to 1/16-in and the depth of the crack was approximately 1/16-in.

Specimens SCS2, SAS1, SAS2 had signs of edge spalling along the length of the repairs (see Photo 11-25, note that the specimens have been drilled for bond tensile strength testing). Additionally, specimens SCS1, SCS3, SAS2, and DCS3 exhibited diagonal cracking along the long repair edge of the finished face. Both of these distresses are possibly due to early form removal and/or insufficient release agent on the repair formwork that was noticed after form removal.

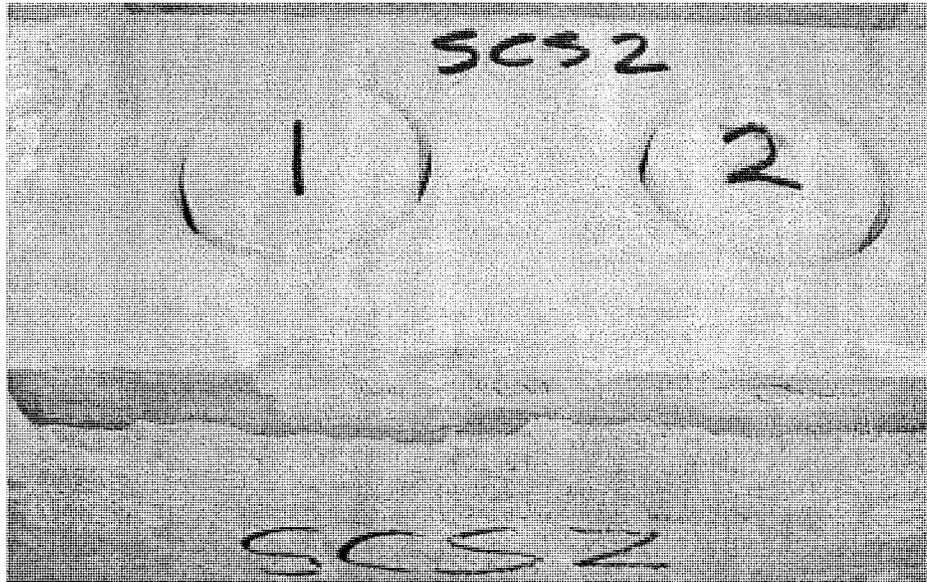


Photo 11-25. Typical edge spalling on repair specimens

Surface cracks that resembled a tearing of the surface were observed on specimens DAS3, DCS1, SAS3, and SCS1. Tearing cracks are suspected to be attributed to finishing the repair material after it had excessively hardened or excessive friction between the trowel and repair mortar.

Acoustic impact testing was performed to assess the presence of delamination between the repair mortar and concrete substrate. Testing was accomplished by tapping the surface of the repair mortar with a mason's hammer. The frequency and damping characteristics of the resulting sound gives an indication of the presence of defects (ACI, 1994). Delaminations were not detected in specimens repaired with Brand X material.

11.3.2.2 *Brand Y Repaired Specimens*

Thirteen specimens were repaired with Brand Y repair material. Most developed pattern cracking at roughly three weeks after installing the repair materials. Deep and shallow repairs made with the Brand Y material exhibited fine openings on the concrete surface that were generally parallel and normal to the length of the specimen (see Appendix H of Kasper, 2002, and Photo 11-26). Pattern cracking on the order of 2 to 3 mils in width was observed on 12 of the 13 specimens that were repaired with Brand Y material. Estimation of crack width was made using a hand-held crack comparator. An example of typical pattern cracking observed is shown in Photo 11-26. Cracks in Photo 11-26 were wetted with water to better show their presence. Reasons for pattern-cracking formation are not specifically known, however, mix proportions (dry to liquid component) and mixing time were similar between specimens that exhibited cracking and the specimen that did not crack.

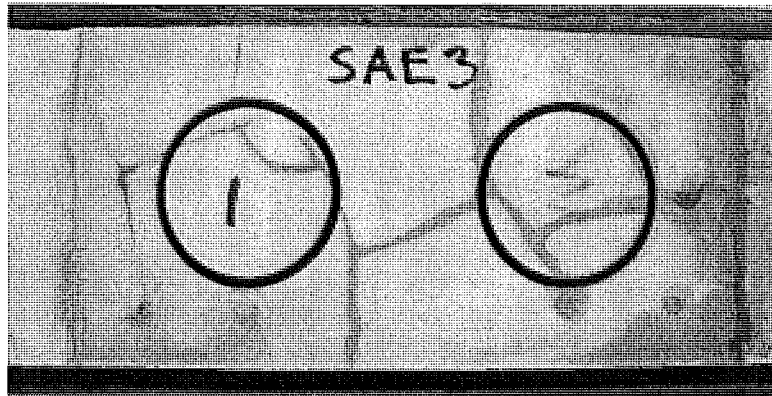


Photo 11-26. Typical pattern cracking observed on Brand Y specimens

Deep repair specimens exhibited an additional crack at the lift joint between the bottom and top halves of the repair area. Similar to the pattern cracking, the lift joint crack was documented to be on the order of 2 to 3 mils, as estimated by a crack comparator. This crack is due to shrinkage of one or both lifts of repair material. Cracks on the order of 2 to 3 mils were also present on 5 of the 6 of the deep repair specimens at the bottom repair-substrate joint of the vertical specimens.

Shallow depth repair specimens exhibited larger crack widths than did the deep repair specimens for the Brand Y repair material, especially at the bottom repair-substrate joint. Cracks at the bottom repair-substrate joint in the shallow repair vertical specimens were on the order of 10 to 60 mils in width for two-thirds of the specimens and less than 5 mils in width for the remaining two specimens. It is possible that the geometry of the shallow repairs influenced the more severe cracking compared to the deep repair specimens. One of the shallow repair specimens, SAE3, exhibited relatively wide cracking, possibly severe enough to be considered a void, at the bottom repair-substrate joint of the vertical specimen. This crack or void resembled a surface retreat of the mortar away from the substrate. The width of the cracking was roughly 50 mils and the depth of the crack was on the order of 1/16 to 1/8-in. The formation of this crack or void may be attributed to the placing the specimens too early in the curing room, before the material had sufficiently set to resist washout from curing moisture. Surface cracks that resembled a tearing of the surface were observed on specimen SAE2. Tearing cracks are likely attributed to finishing the repair material after it had excessively hardened or excessive friction between the trowel and repair mortar.

Mortar sagging near the lift joint was observed on 4 of the 6 deep repair specimens fabricated with Brand Y material. Sagging either extended on both sides of the lift joint or was present in the top lift only. The overall height of the sagging, as measured normal to the length of the specimen, was on the order of 1 to 3-in. Sagging is likely attributed to excessive weight of the plastic mortar on the lower regions of the repair, prior to these lower regions attaining sufficient set to support the plastic mortar above it.

Acoustic impact testing was performed to assess the presence of delamination between the repair mortar and concrete substrate. Delaminations were revealed through the testing on 2 of the 6 Brand Y material shallow repair specimens and are shown as hatched areas on Photo 11-27 and Photo 11-28.

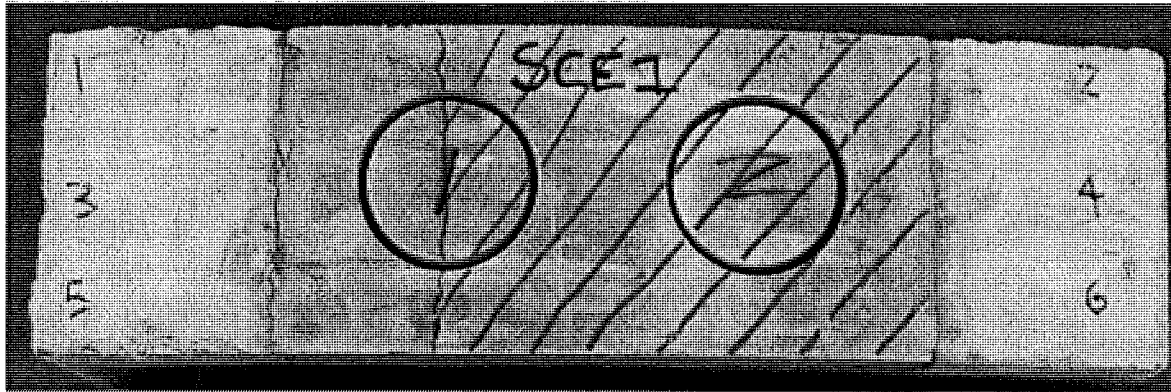


Photo 11-27. Hatched, delaminated region of specimen SCE1

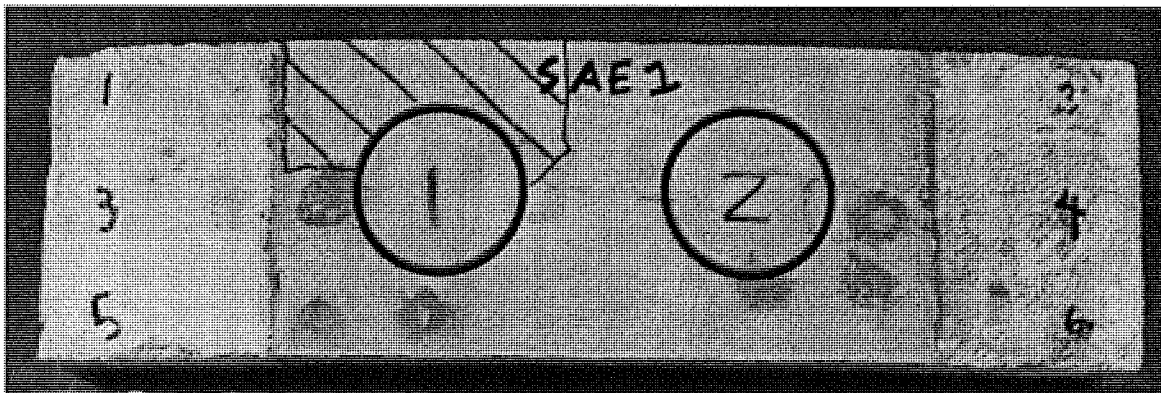


Photo 11-28. Hatched, delaminated region of specimen SAE1

Not shown in Photo 11-28 is a delaminated region of test location no. 1, which is roughly the top half (photo orientation) of core location no. 1. The potential for repair material delamination of specimen SCE1 was suspected during fabrication, as problems arose with the repair adhering to the substrate. It was suspected that the mortar scrub coat had dried on this specimen prior to application of the repair material.

11.3.2.3 Brand Z Repaired Specimens

Twelve specimens were repaired with Brand Z material. A condition unique to these specimens was a deposit of precipitate at the bottom repair-substrate joint of the vertical specimens. The precipitate was only present on shallow repair specimens and could be seen on 5 of the 6 shallow repair specimens. An example of the precipitate formation is shown in Photo 11-29. As shown in this photo, the precipitate tended to form trails toward the bottom of the specimen, possibly indicating that internal moisture was drawn out from the bottom joint. It is possible that the moisture then leaked down the side of the specimen assisted in creating the formations. It should be noted that the polymer liquid component used to mix the Brand Z repair material was white in color. While it is not suspected that presence of the precipitate has an immediate adverse effect on load carrying capacity, continual formation may degrade the overall integrity of the repair.

Similar to other repair materials, half of the Brand Z deep repair specimens exhibited sagging of the repair mortar. The bottom 4-in of repair area for specimens DAT 2 and DAT3 as well as the upper 4-1/2-in of the top half of the bottom lift of specimen DAT1 exhibited the sagging. Sagging is likely attributed to excessive weight of the plastic mortar on the lower regions of the repair, prior to these lower regions attaining sufficient set to support the plastic mortar above it.

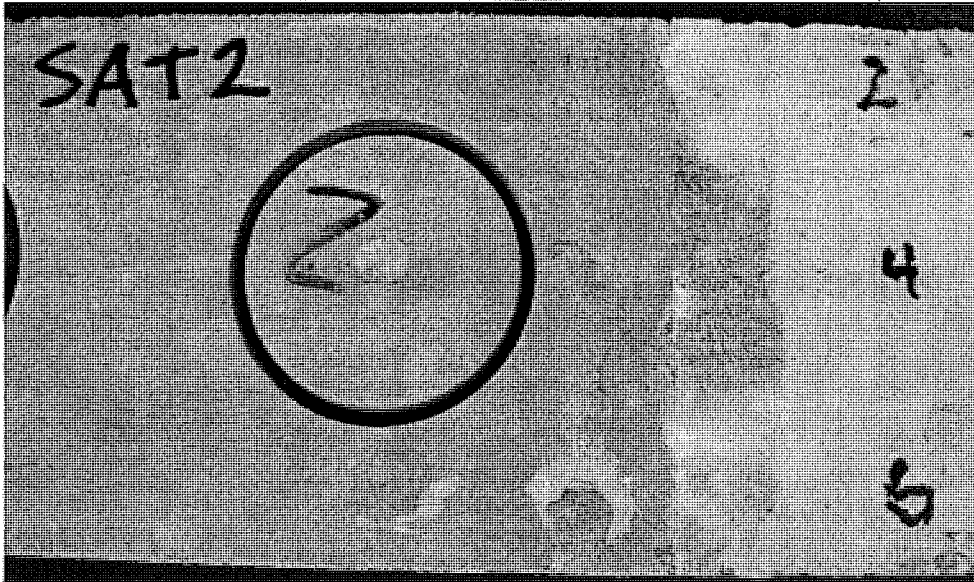


Photo 11-29. Typical white precipitate leaching from the bottom repair-substrate joint

Surface cracks that resembled a tearing of the surface mortar were observed on specimens DAT2, DAT3, SCT2, and SAT1. Tearing cracks were on the order of 2 to 16 mils in width and was likely attributed to finishing the repair material after it had excessively hardened or excessive friction between the trowel and repair mortar.

Perhaps of greater importance is the presence of wider cracking, possibly severe enough to be considered a void, at the lift joint and the bottom repair-substrate joint of some Brand Z vertical specimens. This crack or void resembled a surface retreat of the mortar away from the substrate, possibly resembling erosion of repair material at the affected location. Specimens affected by this condition included DCT2, DCT3, SAT3, and SCT3. The width of the cracking was on the order of 25 mils to 3/32-in and the depth of the cracking was roughly 1/16 to 1/8-in.

Lift joint locations were often difficult to visually distinguish on the finished surface of the Brand Z deep repair specimens. One of the six deep repair specimens exhibited cracking at the lift joint. The width of this crack was on the order of 16-mils, maximum.

Acoustic impact testing was performed to assess the presence of delamination between the repair mortar and concrete substrate. Delaminations were not detected on specimens repaired with the Brand Z repair material.

11.3.2.4 Performance Evaluation Based on Visual Observations

Probably of greatest interest is the formation of cracking and more specifically pattern and joint cracking. If a concrete member were free in space, it would expand and contract with changes in moisture and temperature (ACI, 1990). Expansion and contraction of the unrestrained member would occur without distress to the member and no stresses would be induced. However, if say two or more edges of the member were fixed (restrained), the member would develop tensile stresses. If the tensile stresses exceed the tensile strength of the material, cracking will occur. Cracks allow more rapid ingress of contaminants (e.g.: moisture, carbon dioxide, deicers) into the member, or in the case of this study, the repair.

ACI has suggested maximum crack widths for reinforced concrete structures, based on their service condition (ACI, 1990). These crack widths are summarized in Table 11-9.

Table 11-9. Suggested maximum crack widths for in-service structures (ACI, 1990)

Exposure Condition	Crack Width
Dry air, protective membrane	16 mils
Humidity, moist air, soil	12 mils
Deicing chemicals	7 mils
Seawater and seawater spray, wetting and drying	6 mils
Water retaining structures	4 mils

Beam-ends in locations of defective transverse deck joints could be considered to be in a wetting and drying environment. As such, a crack width of 6 mils is considered detrimental to the performance of repair materials, based on the ACI recommendations. This crack width also corresponds to a moderate crack from the vulnerability assessment in Chapter 4. Crack widths or voids greater than 6 mils were observed on 21 of the 39 repair specimens in this study (54 percent of samples), based on visual observations. Deep repair specimens exhibited cracking greater than 6 mils less frequently than shallow repair specimens based on a percentage of the total number of samples in each repair depth category. Deep repair specimens constituted 7 of the 21 specimens that had crack or void widths greater than 6 mils. These cracks are located within the repair itself and at the top and bottom of the vertical specimen. However, the expansion and contraction of the substrate impacts the repair performance in terms of cracking, including the repair-substrate joints. Not considering cracking or voids that were at the repair-substrate joints, surface cracks or voids were present on 14 of the 39 repair specimens fabricated (36 percent of samples). Cracks or voids on these specimens ranged from 7 to 60 mils in width. Comparing the quantity of specimens with cracks or voids in the region outside of the repair-substrate joints, one of the three materials clearly exhibited better performance than the others, as shown in Figure 11-2. However, the Brand Y repaired specimens had fine pattern cracking, as opposed to larger cracks. Fine pattern cracking may be detrimental to future performance if crack widths increase or the integrity of the repair is further reduced by the presence of the cracks.

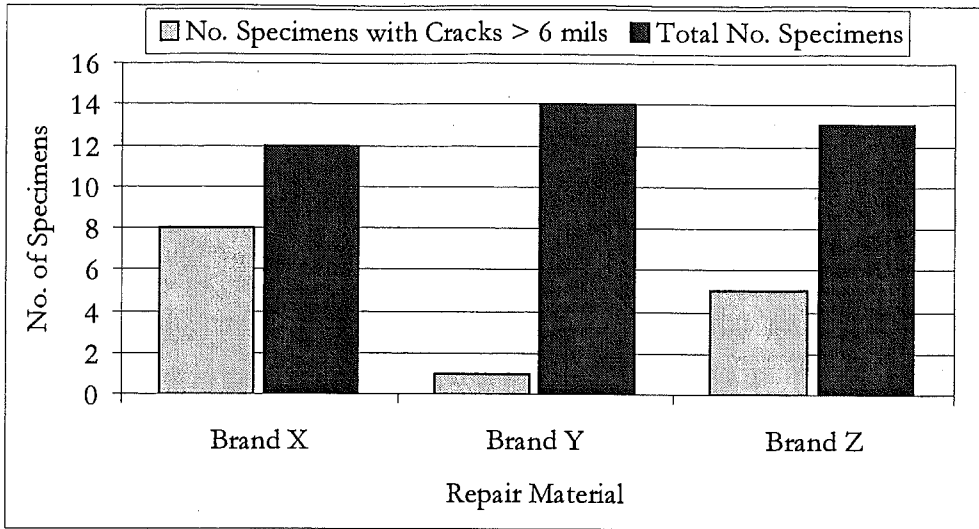


Figure 11-2. Number Of Specimens with Cracking Greater Than 6 mils Outside the Repair-Substrate Joint (Per Repair Material)

The depth of repair or type of post-curing environment appears to have little effect on the performance of the repairs, in terms of cracks greater than 6 mils in width. This is shown in Figure 11-3 and Figure 11-4.

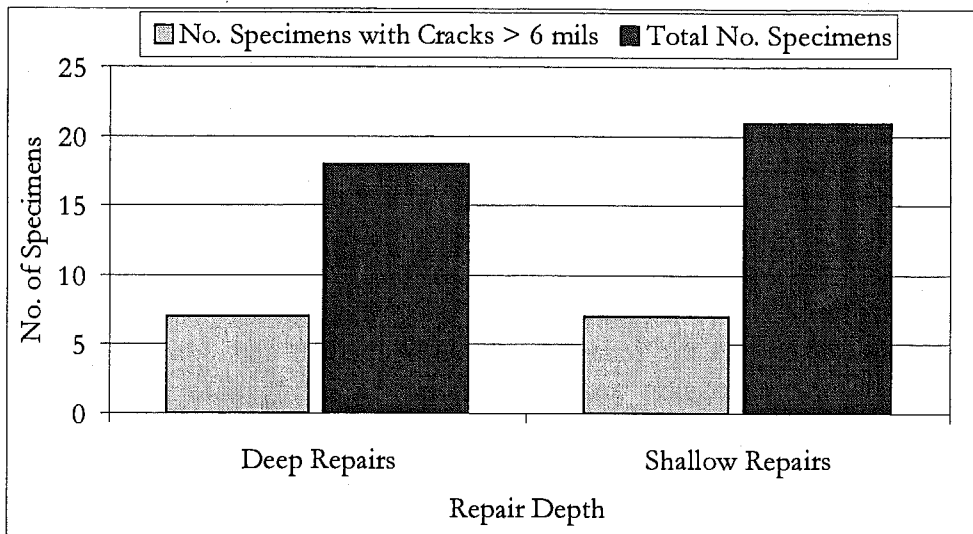


Figure 11-3. Number Of Specimens with Cracking Greater Than 6 mils Outside the Repair-Substrate Joint (Per Repair Depth)

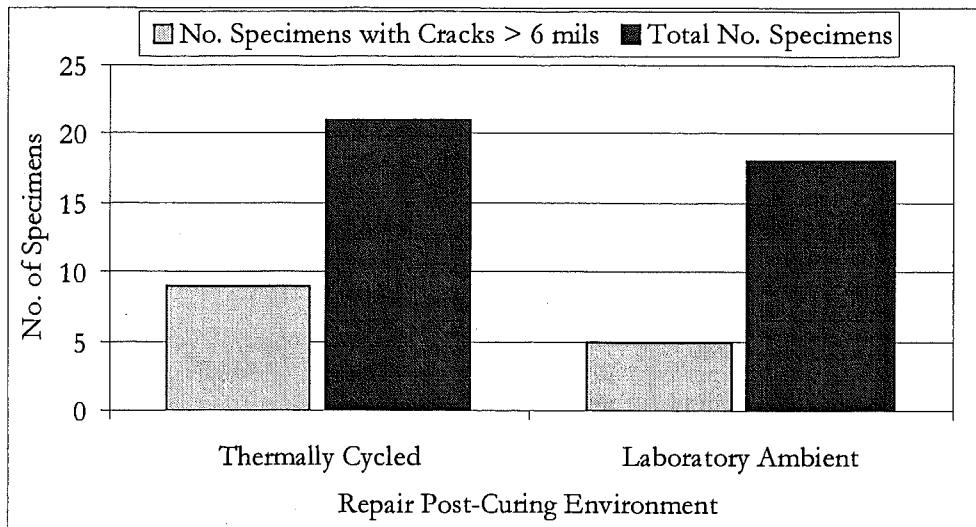


Figure 11-4. Number Of Specimens with Cracking Greater Than 6 mils Outside the Repair-Substrate Joint (Per Repair Post-Curing Environment)

General expectations of the repairs prior to application were that they not be cracked or delaminated from the substrate after the post-curing period. As evidenced in the previous discussion, cracking and delamination of many repairs did occur. If the repair adhered to the prepared substrate during patching, the repairs did not delaminate with exception of one specimen. From a finishing standpoint, it was expected that finishing would take place without damage to the repair. The development of tearing cracking and increased tendency for sagging with over-finishing indicates that the repair materials did not perform as expected.

11.3.3 Strength Evaluation

Three types of strength evaluations were performed for this study. Two evaluations were performed to assess compressive strength while a third test was performed to determine bond tensile strength. Compressive strength testing was performed on standard-sized concrete cylinders and repair mortar cubes in accordance with ASTM testing standards.

11.3.3.1 Concrete Cylinders - Compressive Strength

Testing of the freshly mixed concrete was performed during casting of the substrate specimens. Testing included casting sixteen test compressive strength specimens per ASTM C31/C31M-00e1 (ASTM, 2001). Specimens were cured similarly to the curing procedures used for the substrate concrete described earlier. The specimens were scheduled for testing as indicated in Table 11-10.

Table 11-10. Schedule for Testing Substrate Compressive Strength Specimens

No. of Cylinders to be Tested	Conditioning	Test Age
3 + 1 spare	Wet Cure + Ambient (repair installation) before thermal cycling	30 days
3 + 1 spare	Wet Cure + Ambient	28 days
3 + 1 spare	Wet Cure + Ambient (repair installation) + Thermal Cycling	75 days
3 + 1 spare	Wet Cure + Ambient (repair installation) + Ambient (companion to above)	75 days

Due to space restrictions in the wet curing environment, the spare compressive strength specimens could not experience the same initial curing as the other specimens and were therefore discarded. Compressive strength testing was performed in general conformance with ASTM C39-01 (ASTM, 2001). Testing was conducted using a Baldwin Materials Testing Equipment Model 300CT test machine located in the Dillman Hall Laboratory. Individual strength results of the 6-in by 12-in cylinders are shown in Table 11-11.

As shown in Table 11-11, the mean 24-day compressive strength was within 70-psi or 1.4 percent of the targeted compressive strength for the substrate mixture, i.e. 5,000-psi. The coefficient of variation, COV, is defined as the standard deviation divided by the mean, and is listed in the table as percent. The mean strength of the specimens that were thermally cycled after initial curing was 10-psi less than the mean strength of those specimens that were placed in laboratory ambient conditions after initial curing.

A t-test was performed to determine whether or not there was any reason to believe that the substrate concrete (i.e., “28-day” compressive strength from Table 11-11) came from a population having a mean other than 5000-psi (Ayyub and McCuen, 1997). The use of this test requires that the two samples under consideration be independent, and normally distributed. Both assumptions were made for statistical t-tests in this study. A level of significance of 5 percent was selected for the test. This represents the probability of making a Type I error. A Type I error occurs when the null hypothesis is rejected when in fact it is actually true. The significance level of 5 percent was chosen because this is typically an acceptable level for a Type I error. The null hypothesis was that the mean 28-day compressive strength was equal to the design compressive strength 5000-psi. The alternate hypothesis was that the 28-day compressive strength was not equal to the design compressive strength, i.e., a two-sided t-test. The result of the t-test indicated that there is no statistical reason to believe that the “28-day” compressive strength of the substrate was from a population with a mean other than 5000-psi.

A two-sided t-test was also performed to determine if there was any reason to believe that the mean compressive strengths were not equal between the “End of Post-Curing Compressive

Strength - Thermally Cycled” specimens and the “End of Post-Curing Compressive Strength – Laboratory Ambient” specimens (see Table 11-11). Because no population variance data were available, a statistical F-test was performed first to determine if the sample means came from populations with unequal and unknown or equal and unknown variances. For the F-test a level of significance of 10-percent was used. The F-test indicated that there was no statistical reason to believe that the two samples came from populations with unequal variances. Therefore, it was assumed that the population variances were equal when performing the two-sided t-test of the means. For the t-test, a level of significance of 5-percent was again used. The result of the t-test indicated that there was no statistical reason to believe that the thermally cycled and laboratory ambient test cylinders came from populations with unequal means.

Table 11-11. Concrete Compressive Strength at Various Test Ages and Post-Curing Conditioning

Specimen No.	Cast	Test Date	Age (days)	Load (lb)	Stress (psi)	Mean (psi)	COV
"28-Day" Compressive Strength							
C1	1/8/02	2/1/01	24	143000	5060	5070	0.23%
C2	1/8/02	2/1/01	24	143000	5060		
C3	1/8/02	2/1/01	24	143500	5080		
Start of Post-Curing Compressive Strength							
C4	1/8/02	2/7/02	30	141500	5010	5020	0.30%
C5	1/8/02	2/7/02	30	142500	5040		
C6	1/8/02	2/7/02	30	142000	5020		
End of Post-Curing Compressive Strength - Thermally Cycled							
C7	1/8/02	3/24/02	75	147000	5200	5170	1.35%
C8	1/8/02	3/24/02	75	144000	5090		
C9	1/8/02	3/24/02	75	147500	5220		
End of Post-Curing Compressive Strength – Laboratory Ambient							
C10	1/8/02	3/24/02	75	149000	5270	5180	1.46%
C11	1/8/02	3/24/02	75	145000	5130		
C12	1/8/02	3/24/02	75	145500	5150		

Target Design Strength = 5000-psi

11.3.3.2 Repair Mortar Cube Compressive Strength

Compressive strength cubes were cast for each repair material used in the study. Cubes were cast in general conformance with ASTM C109/C109M-99 (ASTM, 1999). Curing of the mortar cubes consisted of a two to seven day moist curing period. Duration of moist curing was in conformance with each repair material manufacturer’s recommendations, similar to the procedure used for the repair specimens. Moist curing was performed in the Dillman Hall moist curing room. After initial curing, mortar cubes were either placed in thermally cycled or laboratory ambient temperature conditions, similar to the conditions provided for the repair specimens. The temperature of the moist cure room was not formally documented for this portion of the work but was estimated to be on the order of 55 to 60 degrees Fahrenheit daily, based on measurements obtained for other portions of this study.

Strength testing of the cubes was in general conformance with ASTM C109/C109M-99 (ASTM, 1999). Load to the specimens was applied by an MTS 810 material test system.

Force and displacement data were obtained during the test by MTS Test Star II hardware and processed with MTS Test Ware SX software.

Dates when each of the repair mortars was cast, ages at testing, and compressive strength test results are indicated in Table 11-12 through Table 11-14. Shaded data in Table 11-12 through Table 11-14 had been eliminated from calculating the mean compressive strength in accordance with ASTM C109/C109M -99 because these tests fall outside the permitted range of test results (ASTM, 1999).

Table 11-12. Brand X Compressive Strength at Various Test Ages and Post-Curing Conditioning

Specimen No.	Cast	Test Date	Age (days)	Load (lbf)	Stress (psi)	Mean (psi)	COV
"28-Day" Compressive Strength							
M1	2/7/02	3/7/02	28	28589	7150	7630	4.26%
M2	2/7/02	3/7/02	28	30966	7740		
M3	2/7/02	3/7/02	28	30948	7740		
M4	2/7/02	3/7/02	28	31517	7880		
Start of Post-Curing Compressive Strength							
M5	2/7/02	2/13/02	6	11581	2900	4200	2.29%
M6	2/7/02	2/13/02	6	17164	4290		
M7	2/7/02	2/13/02	6	16887	4220		
M8	2/7/02	2/13/02	6	16397	4100		
End of Post-Curing Compressive Strength - Thermally Cycled							
M9	2/7/02	3/30/02	51	31699	7920	7530	7.42%
M10	2/7/02	3/30/02	51	28503	7130		
M11	2/7/02	3/30/02	51	27088	6770		
M12	2/7/02	3/30/02	51	32768	8190		
End of Post-Curing Compressive Strength - Laboratory Ambient							
M13	2/7/02	3/30/02	51	28858	7210	7720	6.48%
M14	2/7/02	3/30/02	51	30998	7750		
M15	2/7/02	3/30/02	51	32826	8210		

Target 28-day strength, cured per ASTM C109 = 5500-psi (per manufacturer)

Table 11-13. Brand Y Compressive Strength at Various Test Ages and Post-Curing Conditioning

Specimen No.	Cast	Test Date	Age (days)	Load (lbf)	Stress (psi)	Mean (psi)	COV
S1	2/11/02	3/11/02	28	25294	6320	6100	3.16%
S2	2/11/02	3/11/02	28	24622	6160		
S3	2/11/02	3/11/02	28	24235	6060		
S4	2/11/02	3/11/02	28	23446	5860		
Start of Post-Curing Compressive Strength							
S5	2/11/02	2/13/02	2	10265	2570	2520	2.81%
S6	2/11/02	2/13/02	2	8743	2190		
S7	2/11/02	2/13/02	2	9888	2470		
S8	2/11/02	2/13/02	2	10954	2740		
End of Post-Curing Compressive Strength - Thermally Cycled							
S9	2/11/02	3/30/02	47	24040	6010	6590	0.21%
S10	2/11/02	3/30/02	47	26407	6600		
S11	2/11/02	3/30/02	47	28680	7170		
S12	2/11/02	3/30/02	47	26334	6580		
End of Post-Curing Compressive Strength - Laboratory Ambient							
S13	2/11/02	3/30/02	47	27892	6970	5050	0.98%
S14	2/11/02	3/30/02	47	20339	5080		
S15	2/11/02	3/30/02	47	20052	5010		

Target 28-day strength, cured per ASTM C109 = 5000-psi (per manufacturer)

Table 11-14. Brand Z Compressive Strength at Various Test Ages and Post-Curing Conditioning

Specimen No.	Cast	Test Date	Age (days)	Load (lbf)	Stress (psi)	Mean (psi)	COV
T1	2/5/02	3/5/02	28	29635	7410	7820	6.65%
T2	2/5/02	3/5/02	28	32110	8030		
T3	2/5/02	3/5/02	28	33800	8450		
T4	2/5/02	3/5/02	28	29460	7370		
Start of Post-Curing Compressive Strength							
T5	2/5/02	2/13/02	8	19276	4820	4390	9.66%
T6	2/5/02	2/13/02	8	16000	4000		
T7	2/5/02	2/13/02	8	18744	4690		
T8	2/5/02	2/13/02	8	16361	4090		
End of Post-Curing Compressive Strength - Thermally Cycled							
T9	2/5/02	3/30/02	53	27781	6950	8970	0.76%
T10	2/5/02	3/30/02	53	35689	8920		
T11	2/5/02	3/30/02	53	35816	8950		
T12	2/5/02	3/30/02	53	36213	9050		
End of Post-Curing Compressive Strength - Laboratory Ambient							
T13	2/5/02	3/30/02	53	39031	9760	Retest Required	
T14	2/5/02	3/30/02	53	14621	3660		
T15	2/5/02	3/30/02	53	23583	5900		

Target 28-day strength, cured per ASTM C109 = 5800-psi (per manufacturer)

The mean 28-day compressive strength of each repair mortar exceeded the 28-day compressive strength stated on mortar manufacturer's technical data sheet (Sika USA, 2002; Chemrex 2002a; Chemrex 2002b) on the order of 600 to 2,200-psi. As with the concrete cylinders, F-tests and t-tests were performed for each repair material to determine if there was any statistical reason to believe that the 28-day repair mortar strengths were not representative of a population having a mean compressive strength as stated on the manufacturer data sheets (the null hypothesis). As before, F-tests were performed prior to performing the t-tests in order to determine, with a 10-percent level of significance, if the population variances can be assumed to be unknown and equal or unknown and not equal. The result of the F-test determined which t-test was to be performed (i.e., test with unknown and equal population variances or test with unknown and unequal population variances). The F-test indicated that there was no statistical reason to believe that the two samples came from populations with unequal variances. Therefore, it was assumed that the population variances were equal when performing the two-sided t-test of the means. Using a level of significance of 5-percent, the t-test indicated that for each repair material the null hypothesis should be rejected. In other words, for each repair material, there was reason to believe that the mean 28-day compressive strength was representative of a population with a mean different than that indicated on the repair manufacturer data sheet (see Appendix F of Kasper's report (Kasper, 2002)).

Depending on the repair material, the post-curing strength may be greater for the laboratory ambient or thermally cycled test cubes. The difference in mean compressive strength between the two post-curing environments ranged from 190 to 1540-psi depending on the repair material. It should be noted however that, as shown in Table 11-14, an end of laboratory ambient post-curing mean compressive strength for Brand Z material could not be calculated per ASTM C109/C109M. An insufficient amount of individual test results were available to determine a mean compressive strength if outlying test results are not considered.

As with the concrete cylinders, t-tests were performed to determine if, for each repair material, there was a statistical difference between the post-curing mean compressive strengths. These tests were performed on sample means based on the corrected strength data (see ASTM C109/C109M). As such, a t-test was not performed on the Brand Z material because one of the two means could not be calculated due to excessive outlying data.

For these tests, the alternate hypothesis was that the population means were not equal. As there was no information available on the population variance for each material, F-tests were performed first to determine if the samples were from populations with equal or unequal variances, again assuming a 10-percent level of significance. The results of the F-test indicated that there was no statistical reason to believe that the samples came from populations with different variances. With information known, the t-tests were performed. The statistical tests indicated that for the Brand Y material, there was no reason to believe that the mean post-curing compressive strengths were from populations having different means. However, the t-test performed for the Brand X material indicated that the null hypothesis should be rejected. In other words, there the samples come from populations with unequal means. As such, a conclusive relationship could not be established between post-curing thermal conditions and mortar compressive strength.

11.3.3.2.1 Performance Evaluation for Compressive Strength of Repair Mortars

One of the objectives of this study was to determine whether the repair materials could develop sufficient compressive strength to assist the substrate in carrying loads. Test results indicated that each of the 28-day repair mortar compressive strengths was in excess of the strength of the substrate, and presumably, therefore, of many in-service structures (see Table 2-3). It should be noted that although the test procedures used to cast the specimens were in accordance with ASTM standards, the specimen sizes and overall preparation methods were considerably different. No relationship is known that normalizes one test procedure to another, nor is it known if one is needed.

Therefore, based on compressive strength data alone, it is not possible to make a statement on how the strength of a material relates to repair performance. However, relationships may exist between compressive strength and other properties that can be better related to performance. This is examined in a future section of this report, *Bond Tensile Strength of Substrate*.

11.3.3.3 Bond Tensile Strength of Repairs

Bond tensile strength testing was performed on each of the repaired specimens and on four non-repaired control specimens. The practices recommended in British Standard 1881 : Part 207 (BSI) were followed to assess the bond tensile strength of either the repair material to the concrete substrate or the substrate itself (British Standard Institution, 1992). In general, the test involves predrilling the repair and substrate, preparing the testing surface, securing a steel disk to the repair, advancing a core around the disk into the repair and substrate, and applying a tensile load to the disk from a testing instrument.

For the purposes of this study two test locations were created on each repair specimen as shown in Figure 11-5.

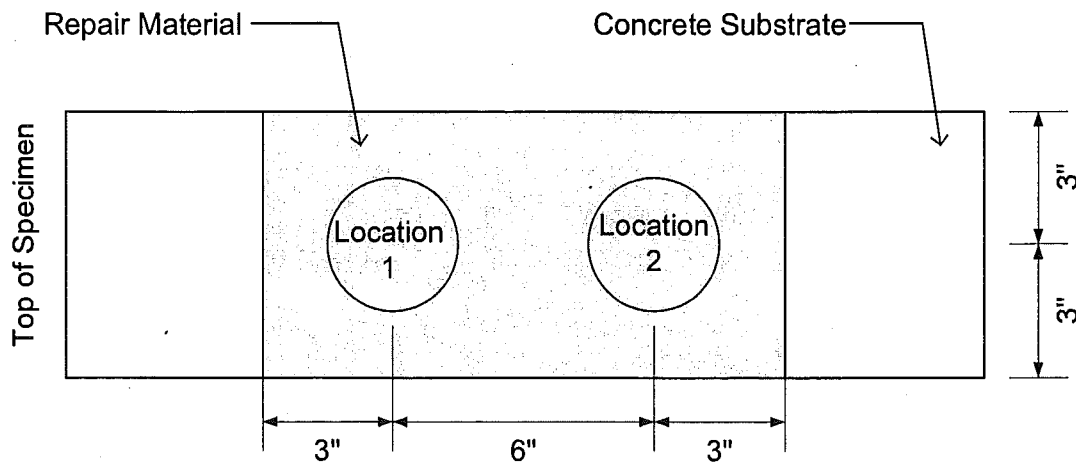


Figure 11-5. Repair Specimen Bond Tensile Strength Locations

For vertically repaired specimens, test location no. 1 was designated as the test location on the top half of the specimen. Test location no. 2 was located in the bottom half of the repair area. For specimens cast, cured, and conditioned in the overhead position, test location no. 1 was

positioned closest to the odd numbered DEMEC point locations, similar to the practice used for the vertical specimens.

For this study, coring of the specimen was performed first, followed by surface preparation, disk application, and load testing. In order to conduct the test, it was first necessary to drill through the repair material into the substrate. A 3-in inside diameter wet cut diamond core bit fitted on a 20-amp Milwaukee Diamond Coring motor attached to a Milwaukee Dymorig coring rig was used to advance the hole into the specimen. Along with the coring rig, a treated wood drilling platform and guide fence were fabricated, leveled, and bolted to the laboratory's concrete floor (see Photo 11-30). Leveling was performed using a torpedo level in an effort to produce a core with an axis perpendicular to that of the repair surface. With the specimens positioned on the drilling platform and core bit advanced to the repair surface, a guide stop was clamped to set the rig mast to the required drilling depth.



Photo 11-30. Drilling rig and platform used for the study

Nominal drilling depths were set to 4-in for deep repair specimens or 2-in for shallow repair specimens. These depths result in a nominal drilling depth of 1-in into the concrete substrate, which was the drilling depth used in the control specimens. BSI specifications require that the annulus of the core not be closer than the maximum nominal aggregate size from reinforcement (British Standards Institute, 1992). The BSI core depth requirement was exceeded for this study with the deep repair specimens, with the annulus approximately 1/4-in from the reinforcing steel. A distance of 1/2-in between the core annulus and the reinforcement would have met the BSI specification. In addition, other researchers have

suggested that the depth of drilling into the substrate should be 1-in or one-half the core diameter, whichever is larger (Vaysburd and McDonald, 1999).

Test locations on the specimen for this study also met the BSI specification for required geometry (British Standard Institution, 1992). BSI specifications require that the center of test locations be at least two core hole diameters apart. In addition, the specification states that the center of a test location should not be closer than one core diameter from an edge. Given that the cores for this study were 3-in in diameter, both geometry requirements of the specification were satisfied.

Surface preparation for the repair specimens consisted of first scrubbing the test surface with a wire brush and then blowing surface debris free with compressed air. The majority of repair specimens had a repair surface that was generally planar, however some specimens had surface irregularities (e.g. sagging) that were either ignored or partially remedied by filling depressions with adhesive. A plane surface, normal to that of the axis of the core, was desired to be able to apply a uniform axial load to the test location.

After the surface had been prepared, 3-in diameter, 1-in thick steel disks were adhered to the test surface using a fast-setting epoxy supplied by Germann Instruments, Evanston, Illinois. Generally, the adhesive was mixed to a fluid paste consistency and evenly distributed on the disk with a steel dowel (see Photo 11-31). Once placed on the test location, rotating the disk several times under pressure and then placing a weight on the top of the disk adequately seated the disks. Disk rotation during seating was performed to distribute the adhesive over the test location. Excess adhesive around the perimeter of the disk was removed with the steel dowel once seating was complete. Curing of the adhesive was accelerated by heating the adhesive and steel disk with a hot air gun for 10-minutes.

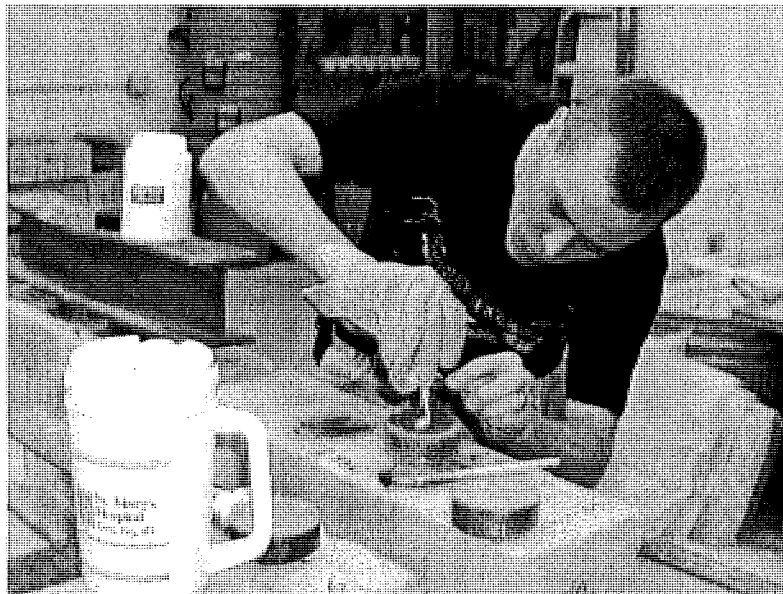


Photo 11-31. Application of adhesive to the steel disk

Test locations were loaded using a Germann Instruments BOND-TEST testing instrument. The instrument attached to the adhered disk through a pull bolt assembly (see Photo 11-32)

and applied load by reacting against the surrounding material via a counter pressure frame (see Photo 11-33).

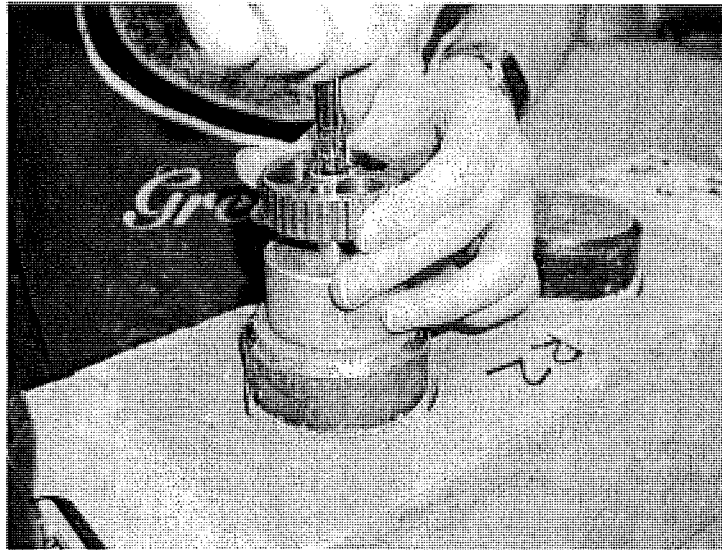


Photo 11-32. Securing the pull bolt to the steel disk

Test load was applied by hand at a rate of approximately 3-psi per second (0.1-kN per second per instrument display) until failure as shown in Photo 11-33. Specimens were air-dried at the time of testing. The rate of load application was in conformance with the BSI test specifications of 3 to 11-psi per second (British Standard Institution, 1992).

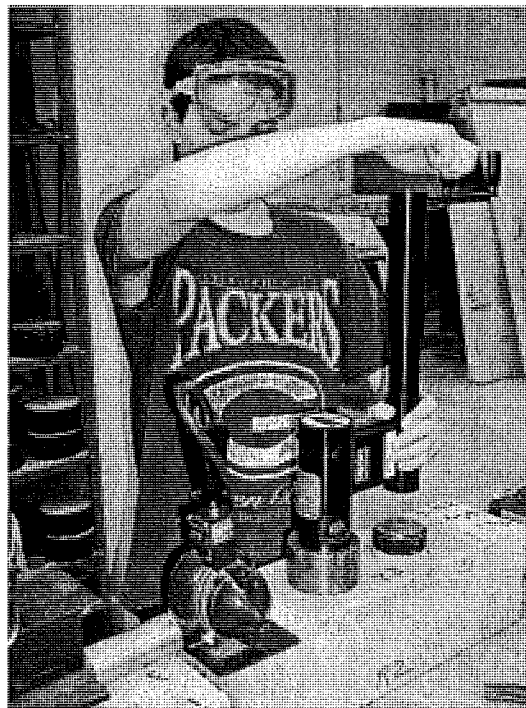


Photo 11-33. Bond tensile strength testing in progress

The failure stress was determined by matching the failure force to a stress calibration chart for the instrument. The calibration chart is included in Appendix I of Kasper's report (Kasper, 2002). Test results for each specimen, including information at various testing stages, failure loads, equivalent stresses, failure modes, and observations are included in Appendix J of Kasper's report (Kasper, 2002).

11.3.3.3.1 Failure Modes

When a direct tensile load is applied to a repair on a substrate, one of six potential failure modes is possible. These modes are:

- Mode A. Bond failure at steel disk-repair interface,
- Mode B. Cohesive failure of the repair mortar,
- Mode C. Adhesive bond failure at the repair-substrate interface,
- Mode D. Partial adhesive failure at the repair-substrate interface and cohesive failure of the repair mortar,
- Mode E. Partial adhesive failure at the repair-substrate interface and cohesive failure of the substrate, and
- Mode F. Cohesive failure of the substrate

Illustrations of each of these failure types are shown in Figure 11-6.

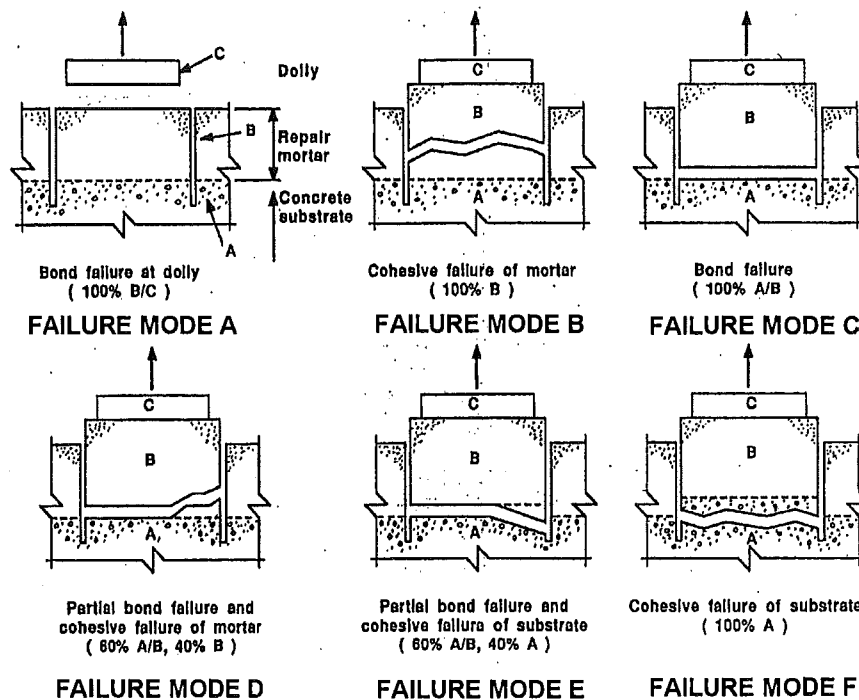


Figure 11-6. Bond Tensile Strength Test Failure Modes (Vaysburd and McDonald, 1992)

Figure 11-6 shows a smooth interface between the substrate (labeled A) and the repair mortar (labeled B). However, the actual interface for specimens in this study was rough, as would be expected in field repairs. Because of the texture at the repair-substrate interface, it was often

difficult to distinguish between failure modes C, D, and E. A common feature of failure modes C, D, and E is that each of the failures occurs near the interface of the repair and substrate. Therefore, for the purposes of comparing the test data, test failures corresponding to either a mode C, D, or E failure were designated as one mode: C-D-E. BSI as well as Vaysburd and McDonald have suggested that mode "A" failures not be included when calculating the mean bond tensile strength (British Standard Institution, 1992; Vaysburd and McDonald, 1999). Where disk-repair interface failures were encountered (mode A), efforts to perform at least one retest were made, with the exception of specimen SAS2, test location no. 2. As shown in the summary tables (Table 11-15 through Table 11-19), two of the test locations exhibited mode "A" failures at the conclusion of testing. Because the number of these failure types was relatively small, they were included when averaging the mean failure stress of a repair material per a given depth of repair and post-curing conditioning.

11.3.3.3.2 Bond Tensile Strength Test Results

Summary tables of the mean bond tensile strength tests are presented in Table 11-15 through Table 11-19. Table 11-15 includes tests results for all specimens, regardless of repair depth or type of post-curing environment. Individual test data are included in Appendix J of Kasper's report (Kasper, 2002).

Table 11-15. Summary of Bond Tensile Strength Test Statistics - All Depth and Post-Curing Specimens

Failure Mode	Statistic	Material			Total
		X	Y	Z	
A	No. Failures	1	-	1	2
	Mean (psi)	128		180	154
	COV	-		-	24%
B	No. Failures	-	8	4	11
	Mean (psi)		141	159	147
	COV		50%	84%	59%
C-D-E	No. Failures	22	18	16	56
	Mean (psi)	147	150	185	159
	COV	66%	47%	42%	53%
F	No. Failures	1	-	3	4
	Mean (psi)	226		297	279
	COV	-		7%	14%
All Modes	No. Failures	24	26	24	
	Mean (psi)	149	147	195	
	COV	63%	46%	46%	

Alternate ways of viewing the data presented in Table 11-15 are shown in Table 11-16 through Table 11-19. These tables examine the mean bond tensile strength test results when considering the four different repair and post-curing scenarios possible for this study.

Table 11-16. Summary of Bond Tensile Strength Test Statistics – Deep Repair, Thermally Cycled Post-Curing Specimens

Failure Mode	Statistic	Material			Total
		X	Y	Z	
A	No. Failures	-	-	1	1
	Mean (psi)			180	180
	COV			-	-
B	No. Failures	-	2	-	2
	Mean (psi)		105		105
	COV		71%		71%
C-D-E	No. Failures	6	4	2	12
	Mean (psi)	225	197	265	222
	COV	15%	18%	53%	26%
F	No. Failures	-	-	3	3
	Mean (psi)			297	297
	COV			7%	7%
All Modes	No. Failures	6	6	6	18
	Mean (psi)	166	225	267	219
	COV	39%	15%	30%	33%

Table 11-17. Summary of Bond Tensile Strength Test Statistics – Deep Repair, Ambient Post-Curing Specimens

Failure Mode	Statistic	Material			Total
		X	Y	Z	
A	No. Failures	-	-	-	0
	Mean (psi)				
	COV				
B	No. Failures	-	4	2	6
	Mean (psi)		187	173	182
	COV		23%	62%	32%
C-D-E	No. Failures	5	2	4	11
	Mean (psi)	169	162	238	193
	COV	24%	8%	25%	29%
F	No. Failures	1	-	-	1
	Mean (psi)	226			226
	COV	-			-
All Modes	No. Failures	6	6	6	18
	Mean (psi)	178	178	216	191
	COV	24%	20%	35%	28%

Table 11-18. Summary of Bond Tensile Strength Test Statistics – Shallow Repair, Thermally Cycled Post-Curing Specimens

Failure Mode	Statistic	Material			Total
		X	Y	Z	
A	No. Failures	-	-	-	0
	Mean (psi)				
	COV				
B	No. Failures	-	2	-	2
	Mean (psi)		87		87
	COV		37%		37%
C-D-E	No. Failures	6	6	6	18
	Mean (psi)	41	103	155	100
	COV	163%	76%	27%	77%
F	No. Failures	-	-	-	0
	Mean (psi)				
	COV				
All Modes	No. Failures	6	8	6	20
	Mean (psi)	41	99	155	98
	COV	163%	68%	27%	74%

Table 11-19. Summary of Bond Tensile Strength Test Statistics – Shallow Repair, Ambient Post-Curing Specimens

Failure Mode	Statistic	Material			Total
		X	Y	Z	
A	No. Failures	1	-	-	1
	Mean (psi)	128			128
	COV	-			-
B	No. Failures	-	-	2	2
	Mean (psi)			146	146
	COV			141%	141%
C-D-E	No. Failures	5	6	4	15
	Mean (psi)	157	163	138	154
	COV	75%	44%	46%	53%
F	No. Failures	-	-	-	0
	Mean (psi)				
	COV				
All Modes	No. Failures	6	6	6	18
	Mean (psi)	152	163	140	152
	COV	70%	44%	74%	59%

It should be noted that the mean failure stress for the two specimens repaired in the overhead position (R2 and R5) was 134-psi with a coefficient of variation (COV) of 57-percent. Three failures were at the repair interface (mode C-D-E) and one failure was observed within the repair material itself (mode B).

11.3.3.3.3 Discussion of Bond Tensile Strength Results

The relatively high COV indicates that there is a wide dispersion of test data about the calculated mean. Other researchers have experienced coefficients of variation on the order of 17 to 26 percent when performing bond tensile strength testing of concrete repair materials with this type of equipment (Vaysburd and McDonald, 1999). The higher COV's for this study are likely due to the large number of failures at the repair-substrate interface, and the variable results due to bond quality at this failure location. Examining the study by Vaysburd and McDonald (1999), it is seen that their work was performed on specimens in the horizontal position on relatively large slabs using repair mortars and concretes.

Bond tensile strength results for the repair specimens could not be compared to any existing data using the same materials and procedures. In addition, repair material manufacturers report different types of bond strength tests and not necessarily test results per the BSI test standard.

In light of the wide dispersion of test data, some statistical observations can be made. Of particular interest in this study are the effects of repair depth and post-curing conditioning. In

general, the mean bond tensile strength of deep repairs was greater than that of shallow repairs, regardless of the test material used. Depending on the material, the range of mean bond tensile strength difference was on the order of 15 to 126-psi between deep and shallow repairs for a given post curing conditioning.

To statistically examine the impact of these variables in the repair specimen bond tensile strengths, t-tests were performed at a significance level of 5-percent. When comparing repair materials of different depth and the same post-curing conditioning, an alternate hypothesis was selected such that the population mean of variable 1 was less than the population mean of variable 2 (i.e., $H_A: \mu_1 < \mu_2$). However, when performing t-tests between repairs of similar depth and different post-curing conditioning, the alternate hypothesis was stated such that the population means were not equal (i.e., $H_A: \mu_1 \neq \mu_2$). As before, F-tests were performed prior to performing the t-tests in order to determine, with a 10-percent level of significance, if the population variances can be assumed to be unknown and equal or unknown and not equal. The result of the F-test determined which t-test was to be performed (i.e., test with unknown and equal population variances or test with unknown and unequal population variances). The results of the F and t-tests are presented in Table 11-20 through Table 11-22.

Table 11-20. t-Test Results for Brand X Material

Material: Brand X			Variable 1			
Depth Comparison	<i>t-Test:</i>	$H_0: \mu_1 = \mu_2$	Shallow Cycled		Shallow Ambient	
		$H_A: \mu_1 < \mu_2$	<i>F-test Result</i>	<i>t-Test Result</i>	<i>F-test Result</i>	<i>t-Test Result</i>
	Variable 2	Deep Cycled	$\sigma_1^2 = \sigma_2^2$	$\mu_1 < \mu_2$		
		Deep Ambient			$\sigma_1^2 \neq \sigma_2^2$	$\mu_1 = \mu_2$
Post-Curing Comparison	<i>t-Test:</i>	$H_0: \mu_1 = \mu_2$	Deep Ambient		Shallow Ambient	
		$H_A: \mu_1 \neq \mu_2$	<i>F-test Result</i>	<i>t-Test Result</i>	<i>F-test Result</i>	<i>t-Test Result</i>
	Variable 2	Deep Cycled	$\sigma_1^2 = \sigma_2^2$	$\mu_1 = \mu_2$		
		Shallow Cycled			$\sigma_1^2 = \sigma_2^2$	$\mu_1 = \mu_2$

Note: F-test hypothesis were $H_0: \sigma_1^2 = \sigma_2^2$ and $H_A: \sigma_1^2 \neq \sigma_2^2$

Table 11-21. t-Test Results for Brand Y Material

Material: Brand Y			Variable 1			
Depth Comparison	<i>t-Test:</i>	$H_0: \mu_1 = \mu_2$	Shallow Cycled		Shallow Ambient	
		$H_A: \mu_1 < \mu_2$	<i>F-test Result</i>	<i>t-Test Result</i>	<i>F-test Result</i>	<i>t-Test Result</i>
	Variable 2	Deep Cycled	$\sigma_1^2 = \sigma_2^2$	$\mu_1 < \mu_2$		
		Deep Ambient			$\sigma_1^2 = \sigma_2^2$	$\mu_1 = \mu_2$
Post-Curing Comparison	<i>t-Test:</i>	$H_0: \mu_1 = \mu_2$	Deep Ambient		Shallow Ambient	
		$H_A: \mu_1 \neq \mu_2$	<i>F-test Result</i>	<i>t-Test Result</i>	<i>F-test Result</i>	<i>t-Test Result</i>
	Variable 2	Deep Cycled	$\sigma_1^2 = \sigma_2^2$	$\mu_1 = \mu_2$		
		Shallow Cycled			$\sigma_1^2 = \sigma_2^2$	$\mu_1 = \mu_2$

Note: F-test hypothesis were $H_0: \sigma_1^2 = \sigma_2^2$ and $H_A: \sigma_1^2 \neq \sigma_2^2$

Table 11-22. t-Test Results for Brand Z Material

Material: Brand Z			Variable 1			
Depth Comparison	<i>t-Test:</i>	$H_0: \mu_1 = \mu_2$	Shallow Cycled		Shallow Ambient	
		$H_A: \mu_1 < \mu_2$	<i>F-test Result</i>	<i>t-Test Result</i>	<i>F-test Result</i>	<i>t-Test Result</i>
	Variable 2	Deep Cycled	$\sigma_1^2 = \sigma_2^2$	$\mu_1 < \mu_2$		
		Deep Ambient			$\sigma_1^2 = \sigma_2^2$	$\mu_1 = \mu_2$
Post-Curing Comparison	<i>t-Test:</i>	$H_0: \mu_1 = \mu_2$	Deep Ambient		Shallow Ambient	
		$H_A: \mu_1 \neq \mu_2$	<i>F-test Result</i>	<i>t-Test Result</i>	<i>F-test Result</i>	<i>t-Test Result</i>
	Variable 2	Deep Cycled	$\sigma_1^2 = \sigma_2^2$	$\mu_1 = \mu_2$		
		Shallow Cycled			$\sigma_1^2 \neq \sigma_2^2$	$\mu_1 = \mu_2$

Note: F-test hypothesis were $H_0: \sigma_1^2 = \sigma_2^2$ and $H_A: \sigma_1^2 \neq \sigma_2^2$

As shown in Table 11-20 through Table 11-22, the null hypothesis was rejected when comparing the population means of the shallow cycled specimens to the deep cycled specimens for each of the three repair materials. In other words, given a 5-percent level of significance, the population mean of the shallow cycled specimens is less than the population mean of the deep cycled specimens. For all other bond tensile strength mean comparisons, the null hypothesis was accepted, meaning that there was no statistical reason to believe that the population means are not equal.

Prior to performing bond tensile strength testing, it was expected that there might be a difference between the specimens of different post curing conditions. It was thought that thermally cycling two different materials, with presumably different thermal expansion coefficients, would result in shearing stresses across the repair-substrate interface. These stresses could negatively impact bond tensile strength. However, results did not indicate this to be the case, as evidenced by the t-tests.

In addition, no statistical difference was expected between different depth repairs subjected to the same post curing conditions. However, thermal cycling does appear to have had an impact on the mean bond tensile strength with repairs of different thickness. A reason has not been established as to why the lower mean bond tensile strength was observed in the shallow repair specimens.

11.3.3.3.4 Comparison of Bond Tensile Strengths Based on Failure Mode

Overall, a majority of the bond tensile strength failures occurred at the repair-substrate interface (see Table 11-15). To determine whether the mean failure stress at the repair-substrate interface was lower than the mean failure stress of failures entirely within the repair mortar or substrate, t-tests were performed. The alternate hypothesis was structured such that $H_A: \mu_1 < \mu_2$ with variable 1 being the mode C-D-E failures and variable 2 being either the mode B or mode F failures. See Figure 11-6 for an illustration of the failure modes.

T-tests were performed for failures within the same repair material and for all repair materials. Due to a large number of interface failures, mean bond tensile strength results for Brand X material could not be compared between failure mode C-D-E and modes B or F. Similarly, a mean comparison between the mode C-D-E and mode F failures for Brand Y material could not be performed.

As before, F-tests were performed prior to conducting the t-tests because the population variances for each of the failure modes were unknown. For each F-test, the result indicated that the null hypothesis should be accepted; therefore the population variances were assumed to be equal, but unknown.

The results of the t-tests are shown in Table 11-23.

Table 11-23. t-Test of Bond Tensile Strength Per Failure Mode

Material: Brand Y			Variable 1	
Failure Mode Comparison	<i>t-Test:</i>	$H_0: \mu_1 = \mu_2$	Failure Mode C-D-E	
		$H_A: \mu_1 < \mu_2$	<i>F-test Result</i>	<i>t-Test Result</i>
Variable 2		Failure Mode B	$\sigma_1^2 = \sigma_2^2$	$\mu_1 = \mu_2$
		Failure Mode F	Insufficient Data	
Material: Brand Z			Variable 1	
Failure Mode Comparison	<i>t-Test:</i>	$H_0: \mu_1 = \mu_2$	Failure Mode C-D-E	
		$H_A: \mu_1 < \mu_2$	<i>F-test Result</i>	<i>t-Test Result</i>
Variable 2		Failure Mode B	$\sigma_1^2 = \sigma_2^2$	$\mu_1 = \mu_2$
		Failure Mode F	$\sigma_1^2 = \sigma_2^2$	$\mu_1 < \mu_2$
Material: All Repair Materials			Variable 1	
Failure Mode Comparison	<i>t-Test:</i>	$H_0: \mu_1 = \mu_2$	Failure Mode C-D-E	
		$H_A: \mu_1 < \mu_2$	<i>F-test Result</i>	<i>t-Test Result</i>
Variable 2		Failure Mode B	$\sigma_1^2 = \sigma_2^2$	$\mu_1 = \mu_2$
		Failure Mode F	$\sigma_1^2 = \sigma_2^2$	$\mu_1 < \mu_2$

The results of the t-tests indicated that there was no reason to believe that, given a 5-percent level of significance, there is any difference between the population means of the failures at the repair-substrate interface (mode C-D-E) and failures within the repair mortar (mode B). However, the alternate hypothesis was accepted when comparing interface and substrate failure modes. In other words, the population means of the mode F failures is greater than the population mean of the mode C-D-E failures. As indicated in Table 11-23, these statements are true when comparing the mean failure stresses of all repair materials as well as the mean failure stresses of the Brand Y and Z repairs.

11.3.3.4 *Bond Tensile Strength of Substrate*

In order to assess the effects of selective demolition on a substrate and determine the bond tensile strength of the substrate, four specimens were cast for the specific purpose of performing bond tensile strength tests. These control specimens were cast at the same time, followed the same initial curing procedures, and were subjected to each type of post-curing conditions as the repair substrate specimens. For this study, half of the control specimens were placed in a laboratory ambient post-curing environment and the others were subjected to thermally cycled post-curing conditions.

Additional surface preparation above that used for performing bond tensile strength testing on repair specimens was required in order to perform testing on the control specimens. Due to the very rough surface on the control specimens, the outer 1/8 to 1/4-inch of the finished surface was removed by passing the specimen through the masonry saw. The resulting surface was, in most cases, level enough to permit sufficient adhesive bond between the substrate and the steel disk. However, one test location, CA2-3, was noted to have an uneven surface after sawing. Not surprisingly, this test location produced a mode "A" failure during bond tensile strength testing.

After the outer surface of the control specimens had been sawn, the test locations were drilled following a procedure similar to that used for the repair specimens. Unlike the repair specimens, three test locations were created on the control specimens centered at 4, 10-1/2, and 17-in from the top of the specimen. These test locations were designated as no. 1, 2, and 3, from the top of the specimen, down. A depth of drilling into the substrate of 1-in was used for the control specimens, which matches the desired substrate drilling depth in all repair specimens in this study.

Procedures for test location cleaning, steel disk application, adhesive curing, and loading were similar to those followed for testing of the repair specimens. Refer to the earlier section in this chapter, *Bond Tensile Strength of Repairs*, for additional information on these procedures. Testing procedures also match those previously described. Test results for each specimen, including information at various testing stages, failure loads, equivalent stresses, failure modes, and observations are included in Appendix K of Kasper's report (Kasper, 2002).

Bond tensile strength failure modes for the control specimens were, by design of the test, limited to a mode A or mode F failure, because no repair material was present. Please refer to the earlier section in this chapter, *11.3.3.3.1 Failure Modes*, for illustrations of these failure modes. Mode A failures constitute a bond failure at the disk-repair interface while mode F failures are a cohesive failure of the substrate.

A summary of test statistics for bond tensile strength tests performed on the control specimens is provided in Table 11-24.

Table 11-24. Summary of Bond Tensile Strength Test Statistics – Substrate Control Specimens

Failure Mode	Statistic	Post-Curing		Total
		Cycled	Ambient	
A	No. Failures		1	1
	Mean (psi)		361	361
	COV			
F	No. Failures	6	5	11
	Mean (psi)	461	387	426
	COV	4%	22%	16%
All Modes	No. Failures	6	6	
	Mean (psi)	461	382	
	COV	4%	20%	

The mean of all bond tensile strength tests performed on thermally cycled control specimens was 461-psi, with a coefficient of variation of 16 percent. This corresponds to a value of roughly $6.5\sqrt{f_c}$, where f_c is the 28-day compressive strength. Expressed in different terms, the bond tensile strength was roughly 9 percent of f_c . This generally corresponds to the expected range of concrete tensile strength being within 8 to 15 percent of f_c (MacGregor, 1992).

It is apparent from Table 11-24 that cycled control specimens had fairly uniform bond tensile strength test results. Greater dispersion about the mean ambient bond tensile strength was also observed. With only one low outlying mode F test result disregarded from the ambient bond tensile strength data, the mean increases to 411-psi with a coefficient of variation of 8 percent.

11.3.3.5 Comparison of Bond Tensile Strength to Mean Mortar Compressive Strength

Results from the bond tensile strength testing were compared to the mortar compressive strength data for each repair material to see if any trends exist between the two variables. Scatter plots were used to make a comparison between the end of post-curing mean compressive strength (thermally cycled and laboratory ambient strengths for each repair material) versus the mean bond tensile strength for each repair material with a given repair depth and post-curing conditioning. These plots are presented in Figure 11-7 through Figure 11-10.

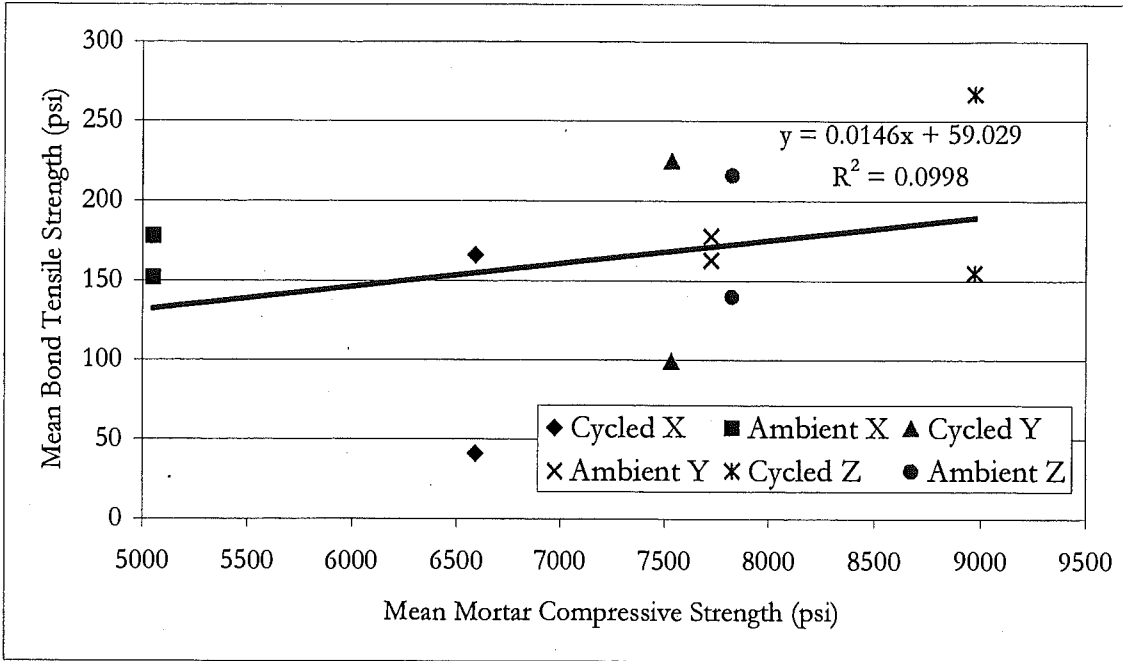


Figure 11-7. Mean Bond Tensile Strength vs. Mean Mortar Compressive Strength - All Specimens

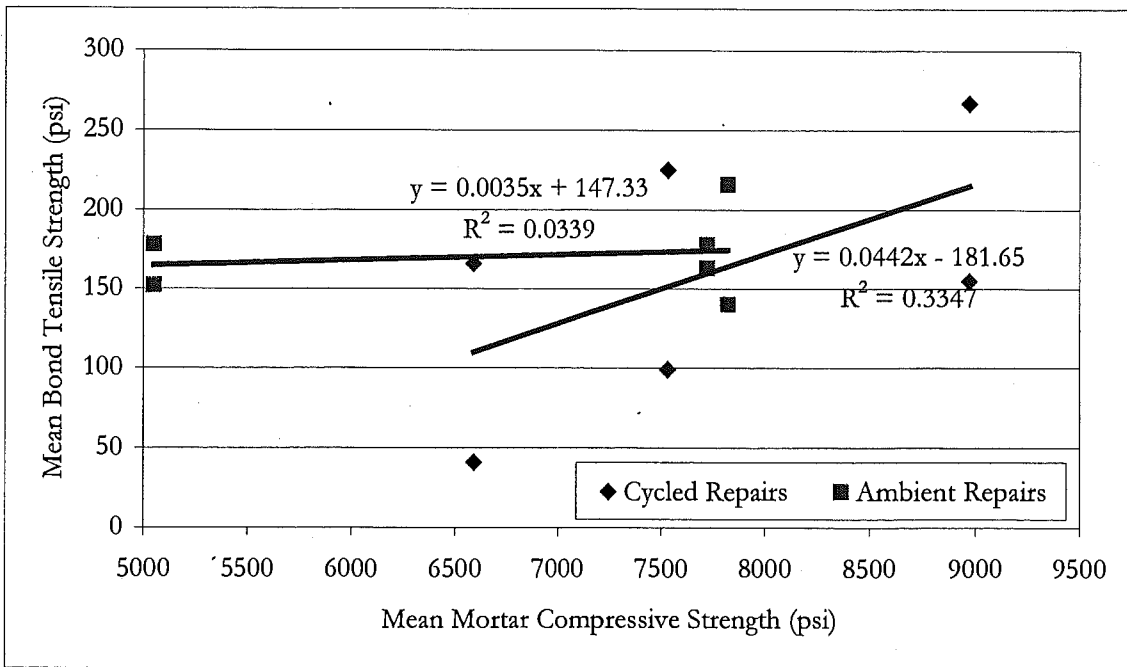


Figure 11-8. Mean Bond Tensile Strength vs. Mean Mortar Compressive Strength – Cycled vs. Ambient Post-Cured Specimens

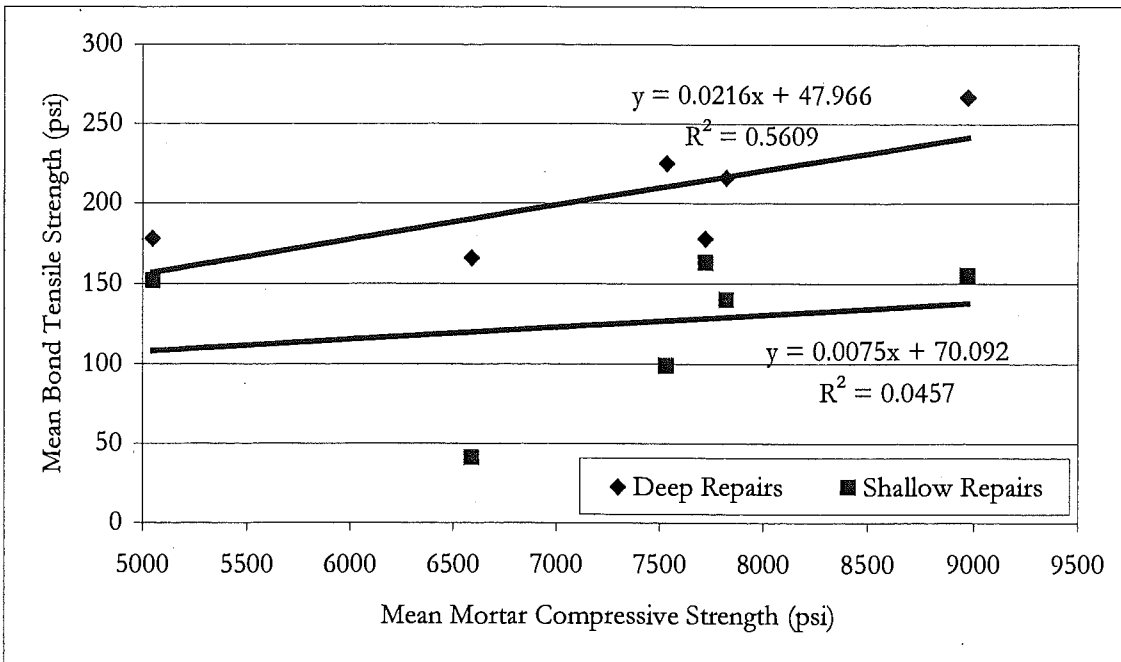


Figure 11-9. Mean Bond Tensile Strength vs. Mean Mortar Compressive Strength – Shallow vs. Deep Repair Specimens

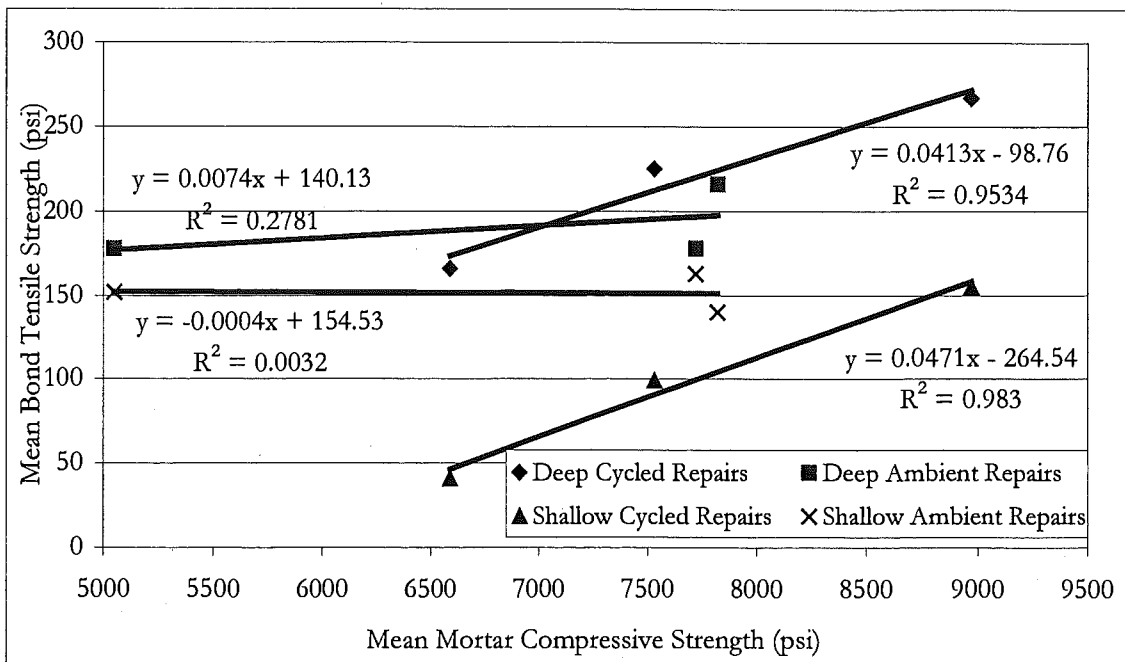


Figure 11-10. Mean Bond Tensile Strength vs. Mean Mortar Compressive Strength – Individual Depth and Post-Curing Conditions

Figure 11-7 shows a scatter plot generated from the mean compressive strength and mean bond tensile strength data. The compressive strength of the Brand Z specimens that were

post-cured in laboratory ambient conditions has been estimated to equal the 28-day compressive strength, because a mean strength could not be obtained from the actual test data. This strength (7820 psi) was used in all bond tensile vs. compressive strength plots for this study. A linear regression analysis was performed on the data in Figure 11-7 and indicates slowly increasing mean bond tensile strengths with increasing mean compressive strength. However, the data was spread widely about the regression function, as evidenced by the coefficient of determination, R^2 , which was approximately 0.1. The coefficient of determination can range from 0 to 1. An R^2 value of 1 indicates that there is no variation of the data about the regression line. In contrast, a R^2 value of 0 indicates that the best estimate of the data is the mean.

Linear regression analyses generate the rate of change in one variable compared to another. This rate of change is the slope of the regression line (b_1) where the regression line can be described by the general relationship: $y = b_1x + b_0$. For Figure 11-7, b_1 was calculated to be 0.0146. A t-test was performed to evaluate whether b_1 is equal to zero or not. If the slope of the regression line was found to be statistically equal to zero, then one could say that the best estimate of any mean bond tensile strength for a given mean mortar compressive strength would be the mean bond tensile strength. For this test, the null hypothesis was stated such that $H_0: \beta_1 = 0$, where β_1 was the slope of the population of mean bond tensile strength. The alternate hypothesis was structured such that $H_A: \beta_1 \neq 0$. Assuming a 5-percent level of confidence, the t-test indicated that the null hypothesis be accepted and that, considering all test data, the best estimate of any mean bond tensile strength for a given mean mortar compressive strength would be the mean bond tensile strength. That is, with a line slope equal to zero, the bond tensile strength is constant over the compressive strength range tested, and the best estimate is the mean of the bond tensile strength.

Another comparison was made with the data, this time looking at the specimens that were thermally cycled after curing compared to those that were in laboratory ambient conditions after curing. This plot is shown in Figure 11-8. A linear regression analysis was again performed on this data and showed, for repairs that were conditioned in laboratory ambient conditions after curing, there was little gain in mean bond tensile strength, with increasing mean compressive strength, regardless of repair depth. A t-test was also performed on each set of data in Figure 11-8 to determine if the slope of the regression line for the data was representative of a slope with a population mean equal to zero. Testing was performed similar to the analysis used for the regression of all compressive strength – bond tensile strength data points (Figure 11-7). The t-test indicated that the null hypothesis should be accepted for each regression analysis in Figure 11-8; the best estimate of any mean bond tensile strength for a given mean mortar compressive strength would be the mean bond tensile strength of the cycled or ambient post-cured repairs. However, the coefficient of determination of each regression analysis (0.33 and 0.03) indicated that the linear regression did not explain the mean bond tensile strength well.

As shown in Figure 11-9, the strength data was re-evaluated, this time considering the different depths of the repair and not considering the post-curing conditions. Linear regression analyses performed on this data indicate a general trend of increasing bond tensile strength with increasing compressive strength. t-testing of the regressions shown in Figure 11-9 was performed, similar to the analysis used for the regression of all mean compressive strength – mean bond tensile strength data points (Figure 11-7). The t-test indicated that the

null hypothesis should be accepted for each regression analysis in Figure 11-9; the best estimate of any mean bond tensile strength for a given mortar compressive strength would be the mean bond tensile strength. However, the coefficient of determination of each regression analysis (0.56 and 0.05) indicated that the linear regression did not explain the mean bond tensile strength well.

Lastly, a means comparison was performed for each repair depth and post-curing scenario. This scatter plot is shown in Figure 11-10. Linear regression analyses was performed on these four data sets and indicated an overall poor relationship between the mean bond tensile strength for the deep and shallow ambient repairs compared to the mortar compressive strength. This is indicated by the low coefficients of determination, 0.28 and 0.00 for the deep and shallow ambient repairs, respectively. A strong relationship between the mean bond tensile strength and mean mortar compressive strength can be observed in Figure 11-10 for the deep and shallow cycled repairs; R^2 for these data were 0.95 and 0.98, respectively. t-testing of the regressions shown in Figure 11-10 was performed, similar to the analysis used for the regression of all mean compressive strength – mean bond tensile strength data points (Figure 11-7). The t-test indicated that the null hypothesis should be accepted for each regression analysis in Figure 11-10; the best estimate of any mean bond tensile strength for a given mortar compressive strength would be the mean bond tensile strength.

An alternate presentation of the data in Figure 11-7 through Figure 11-10 is to compare individual bond tensile strength data, rather than the mean strengths. As the data in Figure 11-10 appeared to show the most promise for providing the most conclusive results, the regression analyses in this Figure were re-calculated, based on the actual test data, rather than the mean strengths. These plots are presented in Figure 11-11 through Figure 11-14.

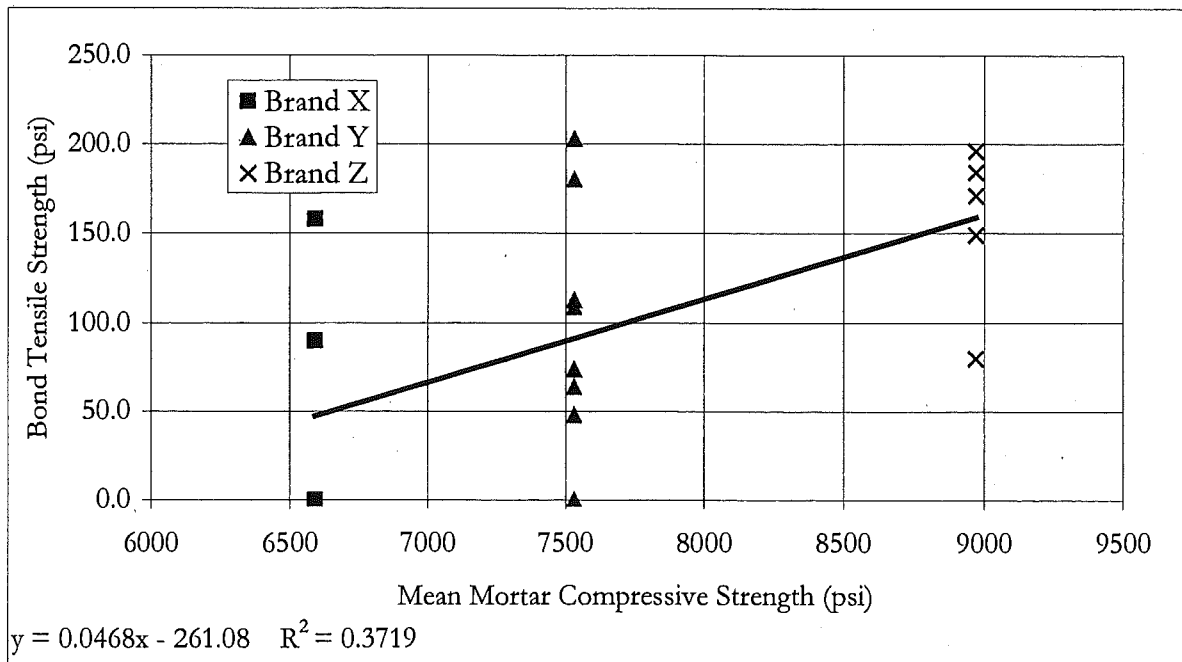


Figure 11-11. Bond Tensile Strength Data vs. Mean Mortar Compressive Strength - Shallow Cycled Specimens

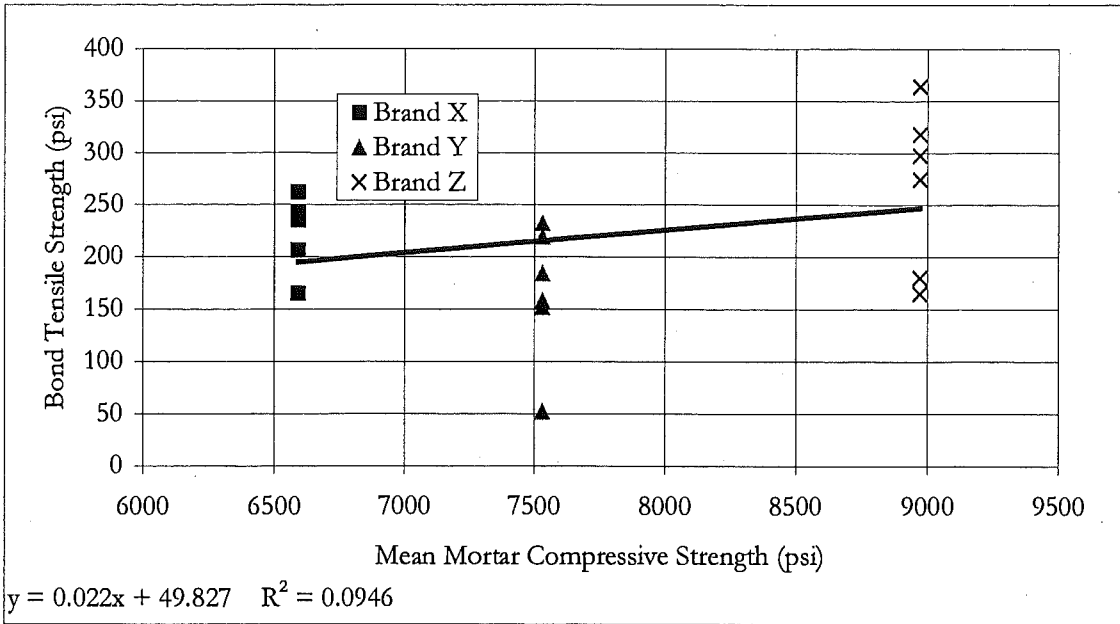


Figure 11-12. Bond Tensile Strength Data vs. Mean Mortar Compressive Strength - Deep Cycled Specimens

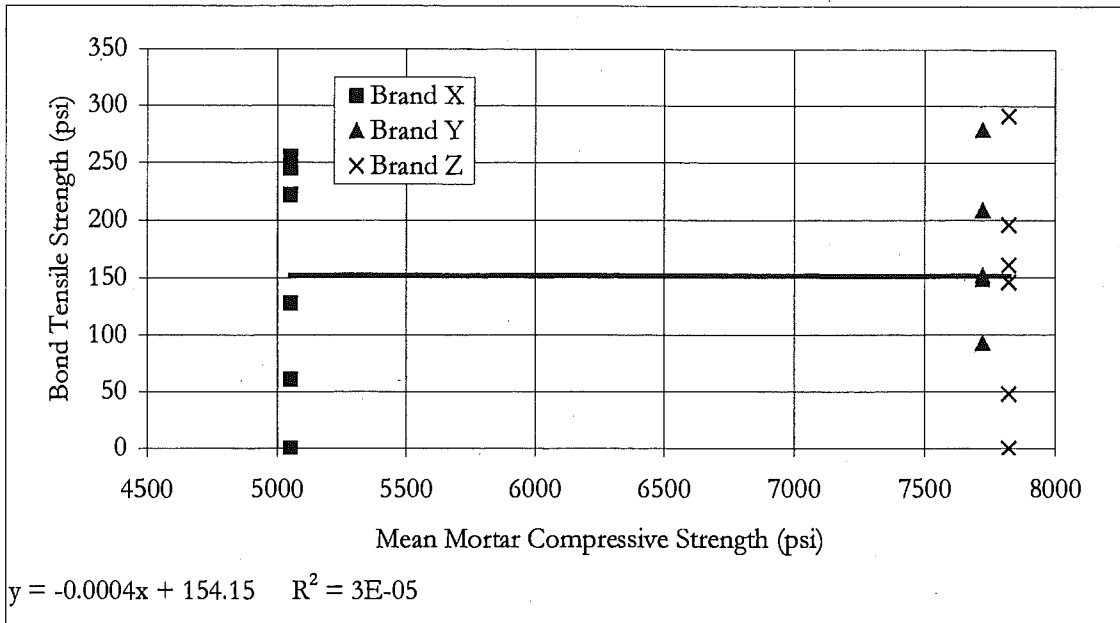


Figure 11-13. Bond Tensile Strength Data vs. Mean Mortar Compressive Strength - Shallow Ambient Specimens

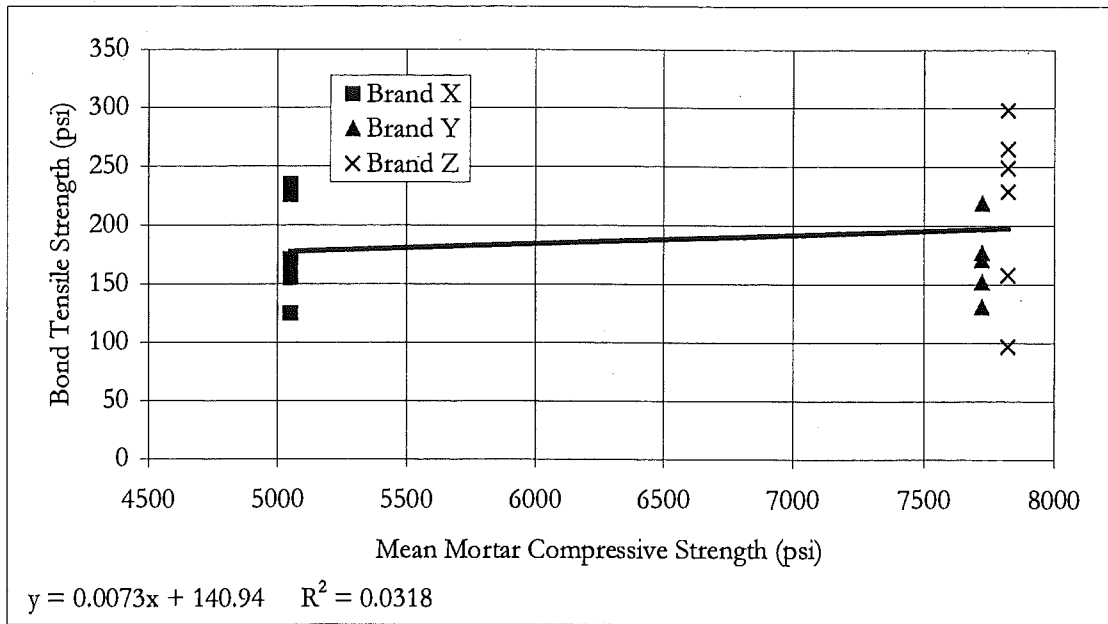


Figure 11-14. Bond Tensile Strength Data vs. Mean Mortar Compressive Strength – Deep Ambient Specimens

A trend that is present in the bond tensile strength data scatter plots compared to the mean bond tensile strength plots is that the slope of the regression lines generally remained the same. However, the goodness of fit of the regression functions decreased significantly for linear regression analyses performed on individual bond tensile strength data. Table 11-25 summarizes a comparison between the t-test results, the regression slope, and the coefficient of determination for both the mean and individual bond tensile strength data.

Table 11-25. Comparison of Test Statistics and Regression Analyses - Mean vs. Individual Bond Tensile Strength Data

Specimen Group	Mean Bond Tensile Strength Data			Individual Bond Tensile Strength Data		
	t-test of b_1	Regression Slope	R^2	t-test of b_1	Regression Slope	R^2
Deep Cycled	$\beta_1=0$	0.0413	0.9534	$\beta_1=0$	0.0220	0.0946
Deep Ambient	$\beta_1=0$	0.0074	0.2781	$\beta_1=0$	0.0073	0.0318
Shallow Cycled	$\beta_1=0$	0.0471	0.9830	$\beta_1 \neq 0$	0.0468	0.3719
Shallow Ambient	$\beta_1=0$	-0.0004	0.0032	$\beta_1=0$	-0.0004	0.00003

In summary, it was found that based on the mean bond tensile failure stress for each repair depth and post curing conditioning, there appears to be a trend for increasing mean bond tensile strength with increasing mean compressive strength for specimens that had been in a

thermally cycled post-curing environment. Trends for all other comparisons showed no significant increase in mean bond tensile strength with increasing mean mortar compressive strength. T-tests performed on the slope of the linear regression function for each mean-mean comparison indicated that the null hypothesis should be accepted; the best estimate of any mean bond tensile strength for a given mean mortar compressive strength would be the mean bond tensile strength. Statistically, mean mortar compressive strength has no impact on the mean bond tensile strength. Coefficient of determination statistics calculated for the regression analyses shown in Figure 11-7 through Figure 11-10 generally indicated a poor fit of the regression line to the data. Exceptions to this observation are evident in specimens that were thermally cycled after curing, especially when considering different repair depths individually. R^2 statistics for these regression analyses approached 1, indicating little variation about the regression line.

Additional poorly fit regressions were observed when plotting actual bond tensile strength data to the mean mortar compressive strength. Table 11-25 shows how the quality of the regression model decreased with the second comparison. The results of the t-tests on the individual bond tensile strength data indicated that there was no statistical difference between the regression line slope and a slope of zero, except for the shallow repair that were thermally cycled after curing. In other words, for each case, the best estimate of the bond tensile strength for each case corresponds to the mean of all failure modes as listed in Table 11-16 through Table 11-19 (e.g., deep repair specimens undergoing thermal cycles can be expected to have a bond tensile strength of 219 psi from Table 11-16).

11.3.3.5.1 Performance Evaluation Based on Bond-Tensile Strength of Repairs

In the introduction to this chapter, it was stated that one of the requirements of a repair material was to develop sufficient bond to assist the parent member in carrying load and at a minimum not de-bond from the substrate. The long-term success of a repair material cannot be based on one test alone; however, past research has also shown that, in general, improved performance of repair materials can be expected with increasing tensile strength (McDonald et al, 2002). Analysis to determine a required bond tensile strength value for a particular condition is beyond the scope of this study. However, a minimum bond tensile strength of 400-psi has been suggested for non-structural or protective repairs (McDonald et al, 2002). While the BSI 1881: Part 207 test was used for bond tensile strength in this study, the procedure does not list a minimum performance criterion for strength. As such, the limit suggested by McDonald was employed.

None of the repair materials tested met the 400 psi performance criteria for bond tensile strength. In fact, less than 3 percent of the repair specimens (2 out of 78 tests) yielded bond tensile strengths greater than 300 psi. If repair material and repair-substrate interface strengths are improved, bond tensile strengths greater than 400 psi can be attained. This is evident from review of the control specimen strength data. Unless preparation, placement, and curing procedures are modified from those followed for this study, it appears that suggested minimum bond tensile strength cannot be reached.

An earlier section in this chapter, *Brand Y Repaired Specimens*, discussed how delamination of the repair material had occurred on two specimens. Delaminated regions can be considered to have zero bond tensile strength to the substrate. Spalling of these repairs is likely in a field situation, such as a beam-end beneath a defective transverse deck joint.

11.3.4 Shrinkage Evaluation

As stated in the *Visual Review of Repair Surfaces* section of this chapter, an important property in the performance of concrete repairs is the ability to resist cracking (McDonald et al, 2002). This requires dimensional compatibility between the repair material and concrete substrate, because the repair material and concrete substrate are physically connected to the same structure, but yet may have significantly different material properties.

As mentioned in the section *Performance Evaluation Based on Visual Observations*, cracking of a restrained material will occur if the tensile stresses generated exceed the tensile strength of the material. In the case of a restrained repair, such as the one used in this study, the amount of tensile stress that develops will depend on many properties. These include the amount of shrinkage, quality of bond on all bonded edges, creep or relaxation properties of the repair, and thermal expansion properties of mortar and substrate (ACI, 1990). It is not well understood how material properties affect dimensional compatibility, how material properties interrelate, and what values should be specified to achieve durable repairs (McDonald et al, 2002).

This component of the study attempted to evaluate the restrained shrinkage properties of various repair materials in different repair geometries and post-curing temperature conditions. Various tests exist for measuring the restrained shrinkage of a portland cement concrete material (McDonald et al, 2002). These tests include casting concrete rings, prisms, or bars (Emmons and Vaysburd, 1995). These tests commonly either use cracking or deflection as the performance measure of the material. However, none of these tests were used in this study, primarily because they are performed on separately cast test specimens that are not part of an actual repair itself. In other words, this study aimed to observe the in-situ restrained shrinkage performance rather than on an isolated test specimen.

The intended performance measure for this component of the study was to record dimensional changes at the repair-substrate joint, such as cracking, by performing periodic measurements between surface mounted monuments (DEMEC points). The locations of the monuments were shown in Figure 11-1. They were positioned to document lengths, and therefore length changes over time on the substrate, repair material, and at the substrate-repair joint. Monuments were placed at these locations in an effort to later subtract contributions to the crack width from substrate activity at the conclusion of the experiment (i.e. after final distance measurements were obtained).

However, in developing the model for analyzing the data after the experiment was completed, two large sources of experimental error were found. The first of these error sources was that relative humidity measurements were not obtained during the course of the study. Relative humidity has a significant impact on drying shrinkage and swelling of portland cement concrete (Nawy, 2000). The second error was the position of the monuments on the specimen. As shown in Figure 11-1, the monuments were located at various distances from the free edges of the substrate or repair material. The distance of a monument to a free edge can impact localized moisture in the specimen (e.g. moisture content closer to a free edge can be different than moisture content at a distance into the specimen) and therefore impact distance measurements. This error, when combined with the impacts of relative humidity, makes the data impractical to analyze at this time.

11.4 Summary

11.4.1 Overview

Although the integrity and durability of a repair can generally never be as good as the original member, repairs are recognized for their ability to extend service life in the short-term at an attractive cost. A significant portion of this study involved laboratory experiments that focused on the performance of concrete repairs for corrosion-induced beam-end deterioration. Research has been conducted recently that looked at the performance of various concrete repair materials for repair depths similar to those used in this study (McDonald et al, 2002). However, this study was unique in that the specimen fabrication, selective demolition, repair, curing, conditioning, and testing were done using methods similar to those that would actually be used in the field on distressed beam ends. An example of one of the more unique aspects of this research is that the repairs were performed in vertical and overhead positions, something that was not discussed in any literature reviewed for this study. Major variables in the fabrication of the repair specimens included shallow (1-in nominal) and deep (3-in nominal) repairs as well as laboratory ambient and cycled post-curing temperatures. Some important findings during fabrication of the repairs were:

- Concrete selective demolition can be performed with conventional hand-held tools, however concrete breakers should be less than a 15-lb. class of hammer to reduce damage to the substrate.
- A surface microscopic evaluation of substrates prepared by mechanical wire brushing and sandblasting did not reveal a significant difference in surface characteristics between the two surface preparation methods.
- Concrete repair in the vertical and overhead position with prepackaged repair mortars is feasible. Each of the materials evaluated in this study were equally easy to work with in small batches.
- Shallow repairs should be completed from the top down to reduce sagging. Deep repairs must be completed in successive lifts to reduce sagging.
- Consolidation of repair mortars with tools having a large surface area (e.g. flat side of a putty knife compared to a round-nosed rod) tended to produce the densest repairs. Over-consolidation can result in repair mortar sagging.
- Improper finishing can lead to sagging and tearing of the finished repair surface.
- Sufficient release agent must be applied to formwork. Removal of forms or initiation of wet curing prior to sufficient set can damage the repairs.

Although a concrete repair must have many properties in order to be durable in-service, perhaps two of the most important properties are crack resistance and substrate adhesion (bond). Crack resistance is needed to prohibit ingress of contaminants that can adversely affect the performance of the repair. Adhesion is required to assist the parent member in carrying loads as well as protecting the parent member (or repair) steel reinforcement from corrosion. A performance evaluation of the repairs was also conducted for this study and

focused on evaluating crack development and repair bond tensile strength at the conclusion of the post-curing period. Repair mortar compressive strength testing was also performed in this study to verify conformance to manufacturer specifications. In addition, compressive strength testing is relatively easy to perform. It was therefore desirable to see if any relationships exist between mortar compressive strength and other performance tests (i.e. bond tensile strength).

The performance measure for repair cracking width for this study was 6-mils, based on industry recommendations (ACI, 1990). Based on the relatively short time in which the repairs needed to perform (approximately 60 days), it could be argued that this criteria is unconservative and that any cracking or finer crack widths would be cause for finding a repair unsatisfactory.

Visual observations of repair condition at the conclusion of the post-curing period revealed cracking within the repair material itself and at the repair-substrate joints (i.e. top and bottom repair joints). Not considering the cracking at these joints, some observations made were:

- All brands of repair material showed cracking greater than 6-mils in width.
- Those specimens with fine-width (2-mil) pattern cracking generally did not exhibit cracks within the repair greater than 6-mils in width.
- Those specimens repaired with materials produced with a liquid polymer exhibited more cracking than the material mixed with potable water (Figure 11-2).
- Repair depth did not have an impact on frequency of cracked specimens relative to the total number of specimens tested (Figure 11-3). About one-third of each repair depth group exhibited cracking greater than 6 mils.
- Post-curing environment showed 43% of specimens exceeded the 6-mil performance measure, whereas 28% of ambient cured specimens exceeded the measure (Figure 11-4).

For bond tensile strength, two sets of performance measures were observed. First, repairs cannot delaminate from the substrate and second, a bond tensile strength of 400 psi was required. As discussed in this chapter, over 1/3 of the repair specimens did not meet the cracking performance criteria and none of the specimens were able to develop a bond tensile strength of greater than 400 psi.

From statistical analysis of the mean bond tensile strength data, the following conclusions can be made for the different materials, repair depths, and post-curing conditions used in this study:

- For each repair material, the population mean bond tensile strengths were equal between the:
 - Shallow ambient and deep ambient repairs
 - Deep ambient and deep cycled repairs
 - Shallow ambient and shallow cycled repairs
- For each repair material, the population mean bond tensile strength of the shallow cycled specimens was less than the population mean of the deep cycled specimens.

One of six failure modes is possible for the bond tensile strengths performed in this study (see Figure 11-6). The majority of failures (77-percent) were at the repair-substrate interface. Statistically evaluating the bond tensile strength results on the basis of failure mode, the following conclusions can be drawn:

- The population mean bond tensile strengths were equal between mode B (repair material) and mode C-D-E (repair-substrate interface) failures for the:
 - Brand Y repair material
 - Brand Z repair material
 - All materials together (independent of brand)
- The population mean bond tensile strength for mode F failures (substrate) were greater than the mode C-D-E (repair-substrate interface) failures for the:
 - Brand Z repair material
 - All All materials together (independent of brand)

Compressive strength testing performed on the concrete substrate and repair mortar was also evaluated statistically. From these analyses, the following observations can be drawn:

- The 28-day compressive strength of the substrate used for this study is from a population having a compressive strength of 5000-psi.
- The end of post-curing compressive strength test results for the substrate concrete cycled and ambient are from the same population.
- The end of post-curing compressive strength test results for the Brand Y material cycled and ambient are from the same population.
- The end of post-curing compressive strength test results for the Brand X material cycled and ambient are not from the same population (Brand Z was inconclusive.)

Some trends can be drawn when relating mean bond tensile strength to mean mortar compressive strength. These trends are evident by evaluating the data in a scatter plot and performing linear regression analyses. Additional statistical testing of the rate of change in mean compressive strength to mean bond tensile strength (slope of regression, b_1) revealed that, considering all repair materials, and each unique repair depth / post-curing combination:

- The best estimate of any bond tensile strength data for a given mean mortar compressive strength would be the mean bond tensile strength for:
 - Deep cycled specimens (219-psi, Table 11-16)
 - Deep ambient specimens (191-psi, Table 11-17)
 - Shallow ambient specimens (152-psi, Table 11-19)
 - Shallow cycled specimens did not meet the criteria, see next comment.
- There is reason to believe that the slope of the regression is not equal to zero for the shallow cycled specimens.

- The coefficient of determination for each linear regression performed on a bond tensile strength data vs. mean mortar compressive strength was less than 0.4. In other words, the regression functions do not explain the individual data very well, but do indicate overall trends.
- Trends in the regression analyses performed indicate relatively little change in bond tensile strength (mean or individual data) with increasing mortar compressive strength for laboratory ambient post-cured specimens.
- Trends in the regression analyses performed indicate increasing bond tensile strength (mean or individual data) with increasing mortar compressive strength for thermally cycled post-cured specimens.

11.4.2 Significance and Limitations of Results

Findings and techniques from this experimental study will likely be used in aiding other engineers to make better-educated decisions on which techniques to use and why. For example, this study synthesized many available preventive maintenance and repair alternatives both currently and not currently being used by state departments of transportation. Appendix J contains a summary of the techniques identified in the literature review and state surveys separated into the four different approaches for addressing corrosion-induced deterioration of prestressed concrete I-beam ends. It should be stressed that if the mechanism of deterioration is not from corrosion-induced deterioration by deicer penetration significantly different approaches for preventive maintenance and repair will be needed. Appendix J can be used as a quick reference to see what alternatives are available.

Overall, the performance of the repairs was not favorable. Cracking, sagging, delaminations, and lower-than-expected bond tensile strengths suggest that at best, repairs can provide only short-term increased service life. It must be noted that the poor overall performance cannot be attributed to any one material, each had conditions or properties that were less than desirable for durable repairs. In addition, there were a multitude of different approaches that could have been taken while performing the repairs: different demolition, surface preparation, material placement, and curing.

Based on the findings and procedures used in this experimental study, those persons specifying one of the three repair materials evaluated in this study can expect the repairs to crack. The severity, frequency, and location of cracking will likely vary based on the repair material used. However, the repairs should develop a bond tensile strength of approximately 200-psi (\pm 100-psi) and not delaminate from the substrate shortly after placement. Because repairs to beam-ends are in a thermally cycled environment, specifiers should expect to see increased bond tensile strength with increasing repair material compressive strength, especially for deeper repairs. In addition, the mean bond tensile strength of deep repairs should be expected to be greater than mean bond tensile strength of shallow repairs in a thermally cycled environment.

12.0 Bridge Management for I-Girder End Condition

12.1 Introduction

One specific goal of this research is to develop an inspection or health monitoring procedure for prestressed concrete I-beam bridges and to develop/recommend protection and repair techniques corresponding to each state of health. The primary expectation from the health monitoring procedure is to identify the prestressed concrete I-beams that are vulnerable to end deterioration, including tendon corrosion. The health monitoring procedure is based on an extensive analysis of the Michigan bridge inventory and condition data, a multi-state survey in the US to learn about the experience of other State Departments of Transportation, and the detailed field inspection¹¹ of twenty highway bridges in Michigan.

It is also important to relate the protection and repair techniques to funding categories specified as "Capital Scheduled Maintenance (CSM)", "Capital Preventive Maintenance (CPM)", "Rehabilitation (R1)" and "Replacement (R2)". CSM activities are for sustaining the current condition of the bridges, CPM is to address the needs of bridges in fair condition, and R1 and R2 are for improving the condition of the bridges.

The long-term bridge health-monitoring goal in Michigan is to utilize fleet management tools and procedures in planning and scheduling maintenance and repair activities. In fleet-management tools, analytical models are incorporated for predicting service life of bridge components, specifically with respect to corrosion-initiated distress (Enright and Frangopol 2000). Practical issues such as traffic control and re-routing necessitate that the repair and maintenance activities be performed on highway corridors. In this approach, repair and maintenance are performed only on the bridges along and on the corridors planned for that budget year. The objective of the bridge repair and maintenance activities is to improve the condition of all the components to above "satisfactory." Keeping this reality in mind, the health monitoring procedure includes a table with maintenance and repair techniques for each common distress state found in the ends of prestressed concrete I-beams. The distress states are described in Chapter 6 and tabulated in Table 6-2. The maintenance repair procedures, when implemented, will improve the girder condition from its current state to a "good" condition.

12.2 I-Beam End Management

As described, the maintenance and repairs on the bridges are currently scheduled along selected corridors. The bridges with distresses that cannot be deferred and which are not on the repair schedules are often dealt with temporary shoring and strengthening procedures until the corridor bridges are scheduled. When bridges on a corridor are scoped, the beam-end conditions described in Table 6-2 are often observed. In order to help with the maintenance/repair replacement decision for the beam-ends from the scoping reports, a process is developed.

In this process the twelve condition states identified for the beam-end described in Chapter 6 are lumped into the following five General Condition Categories:

1. No Obvious Distress
2. Corrosion
3. Corrosion with Delamination and/or Spall
4. Loss of Deformability (Non-Functional Bearing)
5. Reduction in Beam Capacity

In order to assist with the necessary corrective action and the available means, Table 12-1 and Table 12-2 are presented. Table 12-1 shows the relation between the condition states (presented in Table 6-3) and the General Condition Categories. The goals presented in Table 12-1 would be achieved if the preventative maintenance and/or repair techniques given in Table 12-2 were enacted.

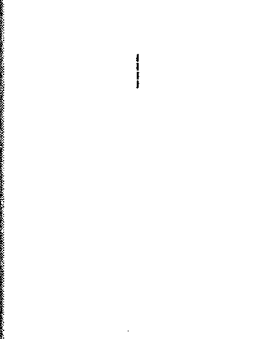
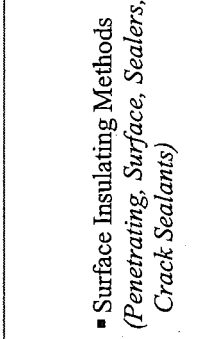
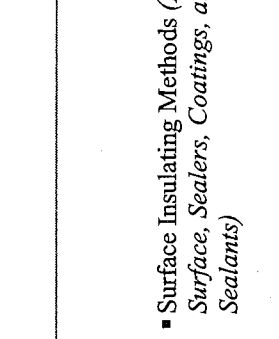
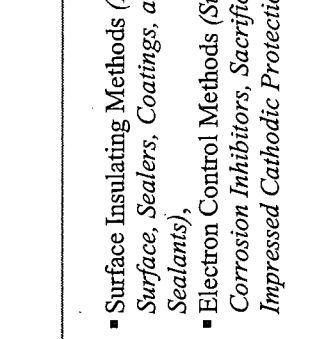
Table 12-2 was generated to provide a link between beam-end distress and common repair and maintenance procedures specific to that distress. Utilizing the twelve condition states that were established in Chapter 6.0, techniques are applied to the prestressed concrete I-beam bridge fleet. The maintenance and repair activity required for each condition state is identified as shown in the Table 12-2. Also shown is the relationship between the condition states developed and those specified by FHWA for safety assessment of the bridge. It should be noted that the FHWA requirement is to assure bridges are at least in fair condition.

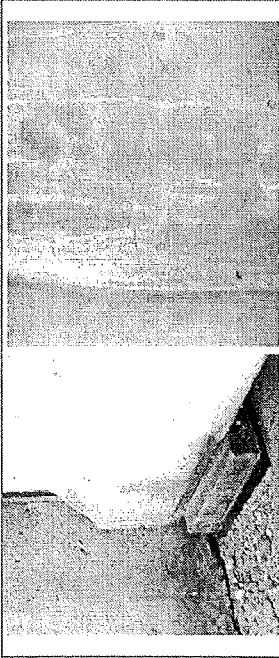
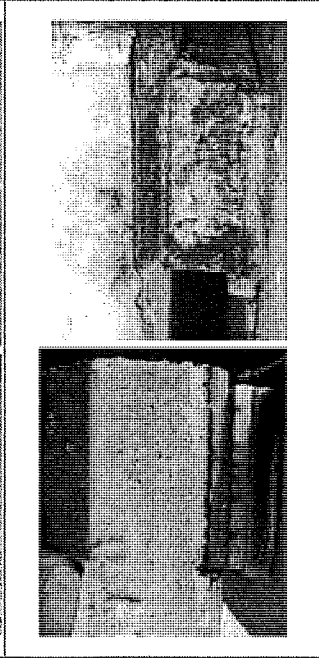
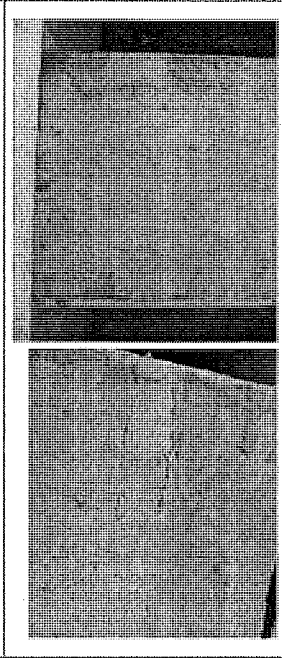
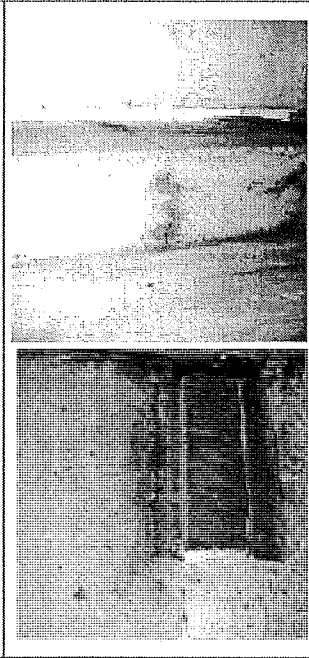
Table 12-1. General Condition Categories

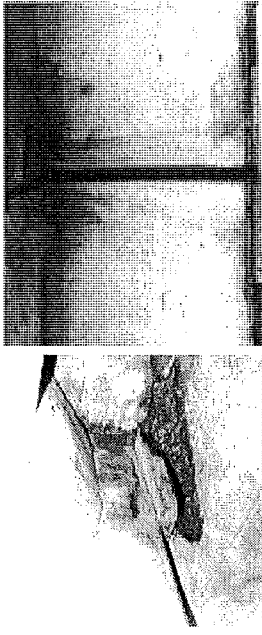
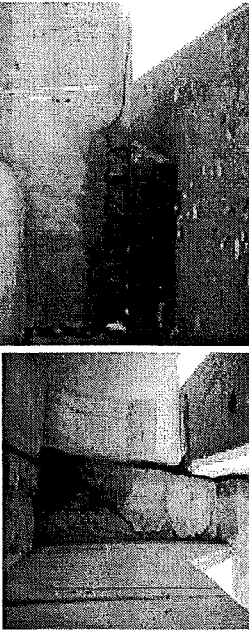
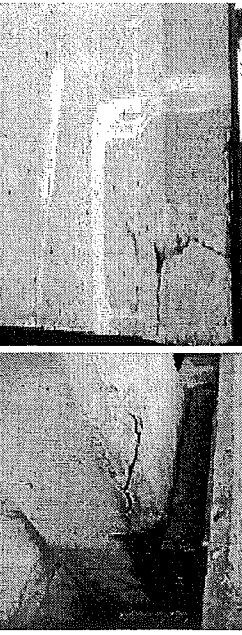
General Condition Categories	Condition States	Goals		
No Obvious Distress	1	Prevent Corrosion Initiation	-	-
Corrosion	2,3,4,5,7,8,9	Stop Corrosion	Prevent Corrosion Reinitiation	-
Corrosion with Delamination and/or Spall	10,11	Stop Corrosion	Prevent Corrosion Reinitiation	Esthetic Restoration of Beam-end
Loss of Deformability (Non-Functional Bearing)	6	Stop Corrosion	Restore Functionality	-
Reduction in Beam Capacity	12	Replace Beam-end	Prevent Corrosion Initiation	-

For beam-ends in the most severe condition state, Michigan has already developed and utilized an overcasting repair procedure. Prior to encasing the beam end, the Michigan procedure specifies removal of deteriorated web and flange concrete. The overcast section on the beam-end is also integrated with a new diaphragm. Repair concrete for this design is MDOT Grade D polymer (latex) modified concrete. MDOT plans were prepared detailing an end repair method for prestressed concrete I-beams with and without end blocks. This repair technique was executed in 1999 in Lower Michigan. The cost of repairing prestressed concrete I-beam ends using this procedure was reported to be 35 to 69 percent of full-replacement cost (Needham, 2000). These tables provide categories for the condition of I-beam end and the appropriate preventative maintenance or repair technique.

Table 12-2. Condition States of Prestressed Concrete I-Beam Ends with Suggested Preventative Maintenance & Repair Techniques

Condition State	Photos Describing the Condition State	FHWA Condition Rating and Description	Preventative Maintenance / Repair Technique
<p>1</p> <p>No cracks observed, No staining</p>		<p>N - NOT APPLICABLE & 9 & 8 - EXCELLENT CONDITION</p>	<p>---</p>
<p>2</p> <p>Efflorescence, water-stains, and/or corrosion</p>		<p>7 - GOOD CONDITION</p>	<ul style="list-style-type: none"> ▪ Surface Insulating Methods (<i>Penetrating, Surface, Sealers, Coatings, and Crack Sealants</i>)
<p>3</p> <p>Hairline cracks: horizontal, vertical, and/or diagonal</p>			<ul style="list-style-type: none"> ▪ Surface Insulating Methods (<i>Penetrating, Surface, Sealers, Coatings, and Crack Sealants</i>)
<p>4</p> <p>Map Cracks</p>			<ul style="list-style-type: none"> ▪ Surface Insulating Methods (<i>Penetrating, Surface, Sealers, Coatings, and Crack Sealants</i>), ▪ Electron Control Methods (<i>Surface Applied Corrosion Inhibitors, Sacrificial Anodes, Impressed Cathodic Protection</i>),

5	Hairline Cracks with efflorescence, water-stains, and/or corrosion with a horizontal crack propagating from the sole plate			<ul style="list-style-type: none"> ▪ Surface Insulating Methods (<i>Penetrating, Surface, Sealers, Coatings, and Crack Sealants</i>), ▪ Electron Control Methods (<i>Surface Applied Corrosion Inhibitors, Sacrificial Anodes, Impressed Cathodic Protection</i>), ▪ Environment Modifying Methods
6	Cracked and deformed neoprene pad, probably non-functional		<p>6 - SATISFACTORY CONDITION</p>	<ul style="list-style-type: none"> ▪ Remove Rust from Bearing ▪ Replace Neoprene Pad
7	Moderate Cracks			<ul style="list-style-type: none"> ▪ Electron Control Methods (<i>Surface Applied Corrosion Inhibitors, Sacrificial Anodes, Impressed Cathodic Protection</i>) ▪ Surface Insulating Methods (<i>Penetrating, Surface, Sealers, Coatings, and Crack Sealants</i>), Reinforcement Surface Preparation (<i>Epoxies, Liquid Corrosion Inhibitors, Zinc-rich Paint</i>)
8	Moderate cracks with efflorescence, water-stains, and/or corrosion			<ul style="list-style-type: none"> ▪ Secondary Framing Modification (<i>Replace Diaphragms</i>), ▪ Surface Sealers, ▪ Re-alkalization, Chloride Ion Extraction, ▪ Concrete Surface Preparation (<i>Compressed Air, High Pressure Water, Grit and Sand Blasting, Scrubbing, Wire Brushing</i>), ▪ Electron Control Methods (<i>Surface Applied Corrosion Inhibitors, Sacrificial Anodes, Impressed Cathodic Protection</i>)

<p>9</p> <p>Major Cracks with efflorescence, water-stains, and/or corrosion</p>			<ul style="list-style-type: none"> ▪ Support Member Modification (<i>New Haunch and New Bearing</i>), ▪ Primary Framing Modification (<i>Supplemental Beam, Full Beam Replacement</i>), ▪ Environment Modification Methods (<i>Re-Alkalinization, Chloride Ion Extraction, DC Current Impressed, and Surface Applied Barriers</i>) ▪ Partial Depth Beam Repair (<i>Concrete Removal, Concrete Surface Preparation, Reinforcement Cleaning, Reinforcement Surface Preparation</i>),
<p>10</p> <p>Delamination with moderate and/or major cracks</p>		<p>5 -FAIR CONDITION</p>	<ul style="list-style-type: none"> ▪ Support Member Modification ▪ Deck Modifications (<i>Joint Repair, New Joint, Overlay, New CLL Deck</i>), ▪ Primary Framing Modification (<i>Supplemental Beam, Full Beam Replacement</i>), ▪ Electron Control Methods (<i>Surface Applied Corrosion Inhibitors, Sacrificial Anodes, Impressed Cathodic Protection</i>), ▪ Environment Modification Methods ▪ Partial Depth Beam Repair (<i>Concrete Removal, Concrete Surface Preparation, Reinforcement Cleaning, Reinforcement Surface Preparation, Partial Depth Patching</i>)
<p>11</p> <p>Spall, delamination, corrosion, and cracks</p>		<p>4 -POOR CONDITION</p>	<ul style="list-style-type: none"> ▪ Environment Modification Methods ▪ Partial Depth Beam Repair (<i>Concrete Removal, Concrete Surface Preparation, Reinforcement Cleaning, Reinforcement Surface Preparation, Partial Depth Patching</i>) ▪ Chip and Overcast procedure used by MDOT R-1373 and RR-1380. ▪ Replacement of the superstructure and substructure elements
<p>12</p> <p>Spall, exposed reinforcement and corrosion</p>			

13.0 Conclusions

The study had three components: field inspection, experimental study, and analytical modeling. The purpose of the field inspection was to document the beam-end distress states and collect data in order to understand the causes of girder-end distress. The experimental study dealt with evaluating shallow and deep patches for beam-end repair. The analytical study looked into the influence of prestressing actions and additional live and intrinsic loads on girder-end distress. The research procedure had five steps: first—document the level and extent of beam-end distress; second—develop a hypothesis for determining the cause(s) of beam-end distress; third—develop a test for the hypothesis; fourth—analyze the impact of beam-end distress on bridge safety; and fifth—perform experiments for developing viable repair methods for moderate levels of beam-end distress.

The major conclusions are described below:

1. The prestressed concrete I-beam ends are often cracked. The cracking with the presence of moisture accelerates the girder-end deterioration primarily by accelerating the chloride ingress process and corrosion initiation of shear reinforcement and prestressing tendons.
2. The recent deck design using the continuous for live-load system eliminates the expansion joint and consequently provides a roof over the beam-end. Moisture access to the beam-end and the ingress of chlorides is subsequently reduced. However, spray from traffic below and new diaphragm details, which encase the beam-end and traps moisture, still make beam-ends a vulnerable portion of the I-beam bridges. The diaphragm in this configuration also conceals the beam-end, which makes visual inspection impossible. The primary approach for improving beam durability should be the elimination or reduction of beam-end cracking. In all existing bridges, beam ends with any width cracks should be sealed.
3. Analytical models showed that the cracking potential is very high on straight and draped prestressed strand girders. The cracking potential is lower but still exists in sheathed or debonded girders, which affect the more recent manufacturing process. Prestressed concrete beam-end cracking is due to the transverse and shear stresses generated by axial load change along transfer length. These loads cannot be eliminated, but cracking can be minimized with the use of confinement steel near beam-ends. Further study is needed to determine the exact arrangement and size of confinement steel.
4. Conclusions related to full bridge analysis include the effect of diaphragms and bearings on the stresses at the beam-ends. The purpose of diaphragms is for girder stability during erection and transfer of shear between girders under live loads. It is seen in the analyses that

the diaphragm geometry and material properties do not generate significant influence on the beam-end stresses. The recent diaphragm design and material properties may require changes. Steel X bracings may be a proper alternative, which provide ventilation for the beam-ends. An efficient detail with steel X-braced girders and beam-ends free of diaphragm should be further investigated.

5. The beam-end stresses are amplified due to neoprene bearing, which is sometimes nonfunctional. Analytical studies show that beam-end vulnerability is a concern for bridge safety for two reasons. First, the deteriorated portion of the girder-end is often within the path of live load transfer to the bearings. Second, the loss of bond near the ends reduces the prestressing force affecting the moment capacity. Load path is established under dead and service loads to assess when the deteriorated portions of beam-end intrude into the load-path.
6. Shallow and deep patch repairs on delaminated girder ends can be a way of restoring the cross-section and preventing further progression of tendon corrosion. All patching materials, however, are not equal and may show significant differences in expected performance. The three repair materials evaluated herein showed non-acceptable cracking, and none met the minimum adhesion criteria through bond tensile strength testing.
7. The bridge scoping, assessment, maintenance, and rehabilitation are often currently performed on roadway corridors. The scoping inspections are performed within a designated corridor. Beam-ends at various condition states can be encountered. Utilizing the inspection data and further studies using the Pontis database, common beam-end distress are categorized into twelve condition states. The first six of these conditions can be dealt with using Capital Preventive Maintenance.

14.0 Recommendations for Future Work

14.1 Introduction

This research provides a solid foundation for understanding issues related to the deterioration of prestressed concrete I-beam ends used in Michigan bridges. The focus of this work has been the maintenance and repair of prestressed concrete I-beam bridges. We established girder condition states and recommended repair and maintenance procedures for each condition state. We also tested patch techniques for the repair of spalled/delaminated beam-ends. We attempted to understand the reasons for the beam-end vulnerability by developing analytical models and conducting response analysis for discrete girders as well as full bridges.

However, as with most research projects, several questions remain unanswered and deserve future attention. The following discussion constitutes a list of research items that should be considered.

The focus of the next phase of work should be safety assessment. In order to understand the relation between girder-end condition states and their load performance, the approach should be the development of an analytical model for various bridge types calibrated by the full-scale testing of decommissioned girders. In order to successfully implement this approach, future research will have an analytical and experimental component. The experimental component should be further divided into laboratory experiments for condition characterization of in-service girders and field-testing of full-scale girders.

14.2 Future Analytical Modeling

Analytical studies focused on two finite element models: a discrete beam and the full model bridge. These models have helped to identify cracking potential and the significance of some elements on the overall behavior. With the models developed, many additional topics are worthy of further study. The models should be used to improve on current design details so that detrimental mechanisms can be avoided. Details to be considered include the effectiveness of various reinforcement approaches for eliminating end cracking.

Additional cracking at the ends of the I-beam was noted in the field investigation. The analytical model should be used to introduce cracks into the end of members at actual field-noted locations.

While the problem of unknown crack depth extension exists, a conservative approach may be to "insert" a crack the full width of the member. Modeling the influence of all cracks at the same time can provide insight into expected behavior under a cracked state. Unsound, spalled, and delaminated concrete can all be modeled by using a member of reduced cross section. Cross-sectional area reduction should be investigated to determine when a structural capacity reduction occurs. From field investigation notes, 6 to 12-in from the end of the beam in conjunction with an exposed reinforcing cage may be a good starting point. Additional cross-sectional reduction could be used to simulate more aggressive concrete loss, say to behind the reinforcing cage.

Similarly, loss of prestressing strand and mild steel reinforcement in both bond and cross-sectional area can also influence the strength of the member and should be investigated. Corroded bars and strands may or may not be effective in contributing to the flexural, shear, and bearing capacity. Corroded and debonded strands some distance away from the bearing area may accelerate strength loss to an even greater degree.

The I-beams are designed to operate in a simple-supported structural system. Analytical models developed for the full bridge showed that the diaphragms and end beams over abutments result in a structural system that is not really simply supported. The utilization of link-slab as well as the continuous for live load decks also generates end restraints. Design details such as bearing pads and diaphragms can be improved upon by the utilization of a three-dimensional realistic analytical model of a full bridge.

14.3 Future Laboratory Studies

The limited laboratory study included in this research has provided valuable information into the effectiveness of partial depth patching for vertical and overhead repairs in a moderate state of distress. While the three latex-modified polymer repair mortars were specified with corrosion inhibitors, the excessive cracking noted in all three materials (two materials showed wide cracks greater than 6 mils and one material showed significant fine map cracking) warrants them as potentially ineffective in protecting the reinforcing and prestressing strands from further deterioration. Additional materials need to be reviewed for effectiveness in protecting the steel once a repair has been made.

Enhancing the bond of the repair material needs to be addressed. While only a few specimens showed delaminations of the repair material from the concrete substrate, the bond tensile strength results did not meet the performance metric of 400-psi strength. All repairs must adhere to be effective. Additional repair materials as well as bonding agents need to be reviewed for effectiveness in providing adhesion once a repair has been made.

Further investigation into the damage caused to sound concrete by various methods of concrete removal needs to be addressed. While concrete removal using a small rotary hammer is an accepted practice, laboratory results indicate that some damage is done to the sound concrete. Direct bond test results on non-repaired concrete showed higher bond strengths than on repaired specimens that broke in the concrete substrate. Petrographic analysis can be a direct method to determine the concrete removal damage done to the concrete microstructure.

Laboratory and environmental conditions used in this study were relatively mild when compared to actual field conditions. Thermal cycling varied between 32 and 95 degrees Fahrenheit, and no moisture cycles were integrated into this experimental study. Once more suitable repair materials are found to successfully undergo the minimum performance metrics of crack width and adhesion using the above testing methods, the repairs should be subjected to more representative field conditions, including free-thaw cycles and de-icing compound applications.

NOTE: all repaired specimens used in this study will be stored for up to one year (until August 2003) in the event that further study is desired using those specimens.

14.4 Field Testing and Other Studies

Valuable information can be gained from actual field studies. Materials testing and petrographic analysis are ways to evaluate field conditions in a laboratory environment. The use of decommissioned bridges for research can provide information relative to the soundness of the materials used. Testing can include chloride content determination, level of strand and reinforcement deterioration, and linking alkali-silica reactivity (ASR) to end deterioration. While some work has been done by MDOT to correlate elevated chloride levels to deterioration of beams and reduction in strand tensile strength, limiting testing was performed and additional attention to the issue is warranted.

Bridges that are taken out of service can be evaluated for performance in many more ways than just material testing. Evaluation of actual beam structural capacity is needed to truly understand the damage due to deterioration. Full-scale testing results of individual beams in flexure and shear can give insight into the actual strength reduction and can be compared with analytical models. Corresponding models can then be used for future bridge analysis of deteriorated structures to more accurately determine the capacity of the structure. In addition, repaired beams can also be tested for effectiveness in restoring strength.

Additionally, inspection based assessment studies should investigate the performance of Michigan prestressed concrete bridges built with and without corrosion inhibitors. Bridges built during the period of 1989 to 1997 used a corrosion inhibitor that was added to the concrete mixture at the precast plant prior to casting. The corrosion inhibitor additive assists the concrete in providing added protection for the steel by reducing the rate of corrosion. Performance of bridge beams made with the corrosion inhibitors needs to be compared to beams without corrosion inhibitors that experience similar traffic and environmental conditions. This valuable information may show that the use of corrosion inhibitors is the single most important protector to assist beams in achieving long-term performance. Documentation of the condition of these beams will also assist in future decisions regarding the use of corrosion inhibitors in precast concrete bridge beams.

To assist field inspectors and MDOT in selecting appropriate tests to identify the beam-end distress severity, such as noted in Table 7-1, further work is warranted. An optimization technique can be applied to define which test or observation to perform, and based on a test's importance rating, the test results can be used to determine the distress level.

14.5 Future Life-Cycle-Cost-Benefit Optimization Studies

A performance analysis matrix was initialized to aid in selecting appropriate preventative maintenance techniques. I-beam end deterioration appears to be mainly a product of corrosion induced deterioration caused by ineffective transverse deck joints. With over 400 sealers and coatings on the market, as well as hundreds of patching materials and now the use of cathodic protection, the initial cost of such a preventative maintenance technique or repair can be confusing. In addition, the long-term cost associated with preventative maintenance and repair or replacement influences the cost. The process of deciding if one repair is less costly than another is straightforward. Similarly, the process of deciding if a repair performs better than another is somewhat straightforward. However, when these requirements are combined and optimization of both cost and multi-criteria performance is sought, it is not as simple. A decision-making technique similar to Bayesian decision theory needs to be employed to combine the different parameters on which the decision is to be based. Further work is warranted if one is to decide the cost-benefit of the many solutions.

References

- 3M (1998). "3M Zinc-Hydrogel Anode 4727 Technical Data," http://www.3m.com/intl/kr/img/pdf/4727_Zinc-Hydrogel_Anode.pdf (August 21, 2001).
- 3M (2001). "3M (TM) Specialty tapes & products: 3M(TM) Zinc-Hydrogel Anode 4727." http://products.mmm.com/usenglish/mfg_industrial/mfg_industrial_specialty.jhtml?powurl=GSTSMRQS8JbeGSNYTMLW46geGST1T4S9TCgvGSNTN0VJCLgl (August 21, 2001)
- AASHTO (1996). with interims. "Standard Specifications for Highway Bridges, 16th edition". American Association of State Highway and Transportation Officials, Washington, D.C.
- AASHTO (1999). Maintenance Manual: *The Maintenance and Management of Roadways and Bridges*, American Association of State Highway and Transportation Officials, Washington, D.C.
- AASHTO (2000). "Manual for Condition Evaluation of Bridges, 2nd Edition". American Association of State Highway and Transportation Officials, Washington, D.C.
- AASHTO (2001). "2001 Interim Revisions to Manual for Condition Evaluation of Bridges, 2nd Edition." American Association of State Highway and Transportation Officials, Washington, D.C.
- AASHTO (2001). *Pontis (Version 3.4.3). Computer Software*. American Association of State Highway and Transportation Officials, Washington, D.C.
- ABAQUS/Standard Version 5.5 Manual (1998), Hibbitt, Karlson & Sorensen, Inc., Pawtucket, RI.
<http://www.abaqus.com>
- ACI (1956). "ACI 318-56 – Building Code Requirements for Reinforced Concrete", American Concrete Institute, Farmington Hills, Michigan.
- ACI (1963). "ACI 318-63 – Building Code Requirements for Reinforced Concrete", American Concrete Institute, Farmington Hills, Michigan.
- ACI (1971). "ACI 318-71 – Building Code Requirements for Reinforced Concrete", American Concrete Institute, Farmington Hills, Michigan.
- ACI (1980) "ACI 224R-8: – Control of Cracking in Concrete Structures," American Concrete Institute, Farmington Hills, Michigan.
- ACI (1989). "ACI 318-89 – Building Code Requirements for Reinforced Concrete," American Concrete Institute, Farmington Hills, Michigan.

- ACI (1990). "ACI 116R-90 - Cement and Concrete Terminology", American Concrete Institute, Farmington Hills, Michigan.
- ACI (1990b). "ACI 224R-90 – Control of Cracking in Concrete Structures", American Concrete Institute, Farmington Hills, Michigan.
- ACI (1992). "ACI 201.2R-92 - Guide to Durable Concrete", American Concrete Institute, Farmington Hills, Michigan.
- ACI (1994). "ACI 364.1R-94 - Guide for Evaluation of Concrete Structures Prior to Rehabilitation", American Concrete Institute, Farmington Hills, Michigan.
- ACI (1995). "ACI 318-95 - Building Code Requirements for Structural Concrete", American Concrete Institute, Farmington Hills, Michigan.
- ACI (1996). "ACI 222R-96 - Corrosion of Metals in Concrete", American Concrete Institute, Farmington Hills, Michigan.
- ACI (1999). "ACI 318-99 - Building Code Requirements for Structural Concrete and Commentary", American Concrete Institute, Farmington Hills, Michigan.
- ACI, "Building Code Requirements for Structural Concrete", ACI 318-02, MI, 2002
- Ahlborn, T.M, Aktan, H., Kasper, J.M., and Ovanesova, A.V. (2001). "Interim Report: Causes and Cures for Prestressed Concrete I-beam End Deterioration". Michigan Technological University, Houghton, Michigan.
- Al-Qadi, I.L., Prowell, B.D., Weyers, R.E., Dutta, T., Gouru, H., and Berke, N. (1993) "Concrete Bridge Protection and Rehabilitation: Chemical and Physical Techniques, Corrosion Inhibitors and Polymers.", SHRP-S-666, National Research Council, Washington, D.C.
- Andrews-Phaedonos, F., Collins, F. G., Green, W. K., and Peek, A. M. (1997). "Assessment of Protective Coatings for Concrete Bridges in Marine or Saline Environments", *Materials Technology Department Proceedings*, Corrosion Prevention. Paper 010, pp.1-10.
- Arner, R. C., and Panganiban, R. R. (1986). *Cathodic Deck Protection and Latex Modified Concrete Overlay on Steel I-Beam and on Prestressed Concrete Box Beam Bridges*, Research Projects No. 83-09A and B, Pennsylvania Department of Transportation, Harrisburg, Pennsylvania.
- ASCE (2002). "New Polls Show Voters Worried About Aging Infrastructure; Will Affect Candidate Choice." <http://www.asce.org/publicpolicy/vgrelease.cfm> (February 4, 2002).
- ASTM International (2001). *C31/C31M-00e1 Standard Practice for Making and Curing Concrete Test Specimens in the Field*. ASTM International, West Conshohocken, Pennsylvania.
- ASTM International (2001). *C39/C39M-01 Standard Test Method for Compressive Strength of Cylindrical Concrete Specimens*. ASTM International, West Conshohocken, Pennsylvania.
- ASTM International (2000). *C143/C143M-00 Standard Test Method for Slump of Hydraulic Cement Concrete*. ASTM International, West Conshohocken, Pennsylvania.
- ASTM International (1999). *C876-91(1999) Standard Test Method for Half-Cell Potentials of Uncoated Reinforcing Steel in Concrete*. ASTM International, West Conshohocken, Pennsylvania.

- ASTM International (1999). *C109/C109M-99 (1999) Standard Test Method for Compressive Strength of Hydraulic Cement Mortars*. ASTM International, West Conshohocken, Pennsylvania.
- ASTM International (1998). *C511-98 Standard Specification for Moist Cabinets, Moist Rooms, and Water Storage Tanks Used in the Testing of Hydraulic Cements and Concretes*. ASTM International, West Conshohocken, Pennsylvania.
- ASTM International (1997). *C231-97e1 Standard Test Method for Air Content of Freshly Mixed Concrete by the Pressure Method*. ASTM International, West Conshohocken, Pennsylvania.
- Ayyub, B.M. and McCuen, R.H. (1997). *Probability, Statistics, and Reliability for Engineers*. CRC Press, New York, 514 pages.
- Beaudette, M. R. (2001a). "Norcure Chloride Removal Systems", <http://www.norcure.com/index.htm> (August 23, 2001).
- Beaudette, M. R. (2001b). "Galvashield®XP", <http://www.norcure.com/GSdatasheet.htm> (August 23, 2001).
- Beaudette, M. R. (2001c). "Galvashield®CC", <http://www.norcure.com/CCdatasheet.htm> (August 23, 2001).
- Beaudette, M. R. (2001d). "Galvashield®XP Project Reference Lists", <http://www.norcure.com/refer2.htm> (August 23, 2001).
- Beaudette, M.R. (2002a). "Chloride Removal – Technical Papers", <http://www.norcure.com/criteria.htm> (March 6, 2002).
- Beaudette, M.R. (2002b). "Re-Alkalization-Technical Papers", <http://www.norcure.com/criter2.htm> (March 6, 2002).
- Billington, D. P. (1976). "Historical Perspectives on Prestressed Concrete", *PCI Journal*, pp. 48-71.
- Breen, J. E. (1990). "Prestressed Concrete: The State of the Art in North America", *PCI Journal*, pp. 62-67.
- British Standards Institution (1992). *BS 1881:Part 207 - Recommendations for the Assessment of Concrete Strength by Near-to-Surface Tests*, British Standards Institution, London, United Kingdom
- Broomfield, J. P., Davies, K., and Hladky, K. (1999). "Permanent Corrosion Monitoring For New & Existing Reinforced Concrete Structures" Structural Faults + Repair-99, 8th International Conference, London, UK, 13-15 July.
- Bullard, S. J., Covino Jr., B. S., Cramer, S. D., Holcomb, G. R., and McGill, G. E. (1996). "Thermal-Sprayed Zinc Anodes for Cathodic Protection of Steel-Reinforced Concrete Bridges" CORROSION/96, Denver, Colorado, March 24-29.
- Burns, D. (2001). *Telephone Conversation*. Assistant Manager, Vector Corrosion Technologies. June 25.
- Cady, P. D. (1994). "Sealers For Portland Cement Concrete Highway Facilities". NCHRP Synthesis 209 – *A synthesis of Highway Practice*. Transportation Research Board, National Research Council, Washington, DC.

- Cairns, J., and Millard, S. (1999). "Reinforcement Corrosion and Its Effect on Residual Strength of Concrete Structures", "STRUCTURAL FAULTS + REPAIR-99", 8th International Conference London, UK, 13-15 July 1999.
- CFR Title 23—Highways, Chapter I--Federal Highway Administration, Department of Transportation, Part 650--Bridges, Structures, and Hydraulics (1999). http://www.access.gpo.gov/nara/cfr/waisidx_99/23cfr650_99.html (August 21, 2001).
- Clear, K.C. (1989). "Measuring Rate of Corrosion of Steel in Field Concrete Structures", *Transportation Research Record No. 1211*, pp. 28-37.
- Collins, M.P, and Mitchell, D. (1991) "Prestressed Concrete Structures", Prentice-Hall, Englewood Cliffs, New Jersey. (crack discussion on pages 114 and 115).
- Chemrex (2002a). "ThoRoc Product Specifier"
http://www.chemrex.com/thoroc/product_thc.asp (March 19, 2002).
- Chemrex (2002b). "MBT Product Specifier." http://www.chemrex.com/mbt/product_mbt.asp (March 19, 2002).
- Cox, R. (2001). *Telephone Conversation*. Field Operations Section Director, Texas Department of Transportation. August 10.
- Dillard, J.D., Glanville, J.O., Collins, W.D., Weyers, R.E., and Al Qadi, I.L (1993) "Concrete Bridge Protection and Rehabilitation: Chemical and Physical Techniques, Feasibility Studies of New Rehabilitation Techniques.", SHRP-S-665, National Research Council, Washington, D.C.
- Draft Interim Standard Specifications for Construction, (2001). Michigan Department of Transportation, Lansing, Michigan.
- Emmons, P. H. (1994). *Concrete Repair and Maintenance Illustrated*, R.S. Means Company, Inc., Kingston, Massachusetts.
- Emmons, P.H., (1994). *Concrete Repair and Maintenance Illustrated*, R.S. Means Company, Inc., Kingston, Massachusetts.
- Enright, M. P., and Frangopol, D. M. (2000). "Survey and Evaluation of Damaged Concrete Bridges", *Journal of Bridge Engineering*, February, pp. 31-38.
- Ersoy, U., "Reinforced Concrete", METU, Ankara, 1997
- Federal Highway Administration (FHWA) (1997). "Evaluation of Digital Camera Technology For Bridge Inspection", Publication No: FHWA-SA-97-100.
- Funahashi, M., and Daily, S. F. (1996). "New Sacrificial Anode for Cathodic Protection of Reinforced Concrete Structures", *Proceedings of the Materials Engineering Conference (Conference Title: Proceedings of the 1996 4th Materials Engineering Conference. Part 2 (of 2))*, Vol. 2, pp. 1256-1262.
- Ganji, V., Tabrizi, K., and Vittilo, N. (2000). "Project Level Application of Portable Seismic Pavement Analyzer." *Structural Material Technology IV - an NDT Conference, 2000*, S. Alampalli, ed., Technomic, 205-210.
- Gawedzinski, M. (2001). *Telephone Conversation*. Illinois Department of Transportation. August 9.

- Gee, C. K., and Hover, K. C. (1987). "Cathodic Protection for Prestressed Structures", *Concrete International: Design and Construction*, Vol. 9, pp. 26-30.
- Geidl, V. A., and Khafagi, B. K. (1988). "Reliability of Cracked, Prestressed Girders", *Probabilistic Methods in Civil Engineering, Proceedings of the 5th ASCE Specialty Conference*, New York, pp. 309-312.
- Gergely, P., and M.A. Sozen. Design of Anchorage-Zone Reinforcement in Prestressed Concrete Beams. *PCI Journal*, April 1967, pp. 63-75.
- Ghosh, S. K., and Fintel, M. "Development Length of Prestressing Strands, Including Debonded Strands, and Allowable Concrete Stresses in Prestensioned Members", *PCI Journal*, September-October 1986.
- Graybeal, B. A., Rolander, D. D., Phares, B. M., Moore, M. E., and Washer, G. A. (2001). "Highway Bridge Inspection: State-Of-The-Practice Survey", Transportation Research Board, 80th Annual Meeting, Conference Paper, Washington D.C., January 7-11.
- Gucunski, N., Vitillo, N., and Maher, A. (2000). "Bridge Deck Delamination Using Integrated Seismic Devices." *Structural Material Technology IV - an NDT Conference, 2000*, S. Alampalli, ed., Technomic, 329-334.
- Hag-Elsafi, O., and Alampalli, S. (2000). "Strengthening Prestressed Concrete Beams Using Bonded FRP Laminates." *Structural Material Technology IV - an NDT Conference, 2000*, S. Alampalli, ed., Technomic, 287-292.
- Halstead, J. P., O'Connor, J. S., Alampalli, S., and Minser, A. (2000). "Evaluating FRP Wrap with NDT Methods." *Structural Material Technology IV - an NDT Conference, 2000*, S. Alampalli, ed., Technomic, 275-280.
- Hartle, R. A., Amrhein, W. J., Wilson, K. E., Baughman, D. R., and Tkacs, J. J. (1995). *Bridge Inspectors Training Manual 90*, Federal Highway Administration, Washington, D.C.
- Heldt, L. D. (2001). Corrosion workshop at Michigan Technological University. July 11.
- Henderson, M. E., Costley, R. D., and Dion, G. N. (2000). "Acoustic Inspection of Concrete Bridges with the HollowDeck." *Structural Material Technology IV - an NDT Conference, 2000*, S. Alampalli, ed., Technomic, 184-189.
- HyperMesh 2.0 Documentation (1995). Altair Computing, Inc., Troy, Michigan.
<http://www.altairmodel.com>
- HyperMesh 4.0 Documentation (2000). Altair Computing, Inc., Troy, Michigan.
<http://www.altairmodel.com>
- Illinois Department of Transportation (IDOT) (2001). "Final Report, 3M Corporation, Corrosion Abatement System 4727 Zinc-Hydrogel Anode" <ftp://ftp.dot.state.il.us/pub/> (August 15, 2001).
- Iowa State University, "Steel Diaphragms in Prestressed Concrete Girder Bridges TR-424", <http://www.ctre.iastate.edu>, May 2002
- Ishii, K., Seki, H., Fukute, T., and Ikawa, K. (1998). "Cathodic Protection for Prestressed Concrete Structures", *Construction and Building Materials*, Vol. 12, No. 2-3, pp. 125-132.

- Jadun, S. (1990). "Michigan Experience with Prestressed Concrete Bridges," *MATES*, Michigan Department of Transportation, Materials and Technology Division, Issue No. 49, December 1990.
- Jones, D. A. (1992). *Principles and Prevention of Corrosion*, Macmillan Publishing Company, New York, New York.
- Juntunen, D. A. (2000). *Cracks and Deterioration of Prestressed Beams*, Michigan Department of Transportation, Lansing, Michigan.
- Kasper, J. M., (2002). "A Performance Evaluation of Repair Materials for Corrosion Induced Deterioration of Prestressed Concrete Bridges," Master of Science Thesis, Michigan Technological University.
- Keating, P. B., and Fisher, J. W. (1987). "Repair, Rehabilitation, and Strengthening of Highway Bridges in the United States." *Bridge Evaluation Repair and Rehabilitation*, E. Absi, and A. S. Nowak, ed., The University of Michigan, Ann Arbor, Michigan, 185-196.
- Kennedy, R. C. (1991). *Cathodic Deck Protection and Latex Modified Concrete Overlay on Steel I-Beam Bridge*, Pennsylvania Department of Transportation, Montoursville, Pennsylvania.
- Kosaka, Yasuo, Miura, Takashi, Tsukada, and Yukihiro. (1999). "Salt- Damage And Retrofitting Of Prestressed Concrete Bridges At The Japanese Sea Coast In North – Japan", Structural Faults + Repair-99, 8th International Conference, London, UK, 13-15 July 1999
- Kosmatka, S. H., and Panarese, W. C. (1988). *Design and Control of Concrete Mixtures, Thirteenth Edition*, Portland Cement Association, Skokie, Illinois
- Kosmatka, S.H., Kerkhoff, B., and Panarese, W.C., (2002), *Design and Control of Concrete Mixtures, EB001, 14th edition*, Portland Cement Association, Skokie, Illinois, 372 pages.
- Krauss, P. D., and Nmai, C. K. (1996). "Preliminary Corrosion Investigation of Prestressed Concrete Piles in a Marine Environment: Deerfield Beach Fishing Pier", *ASTM Special Technical Publication (Conference Title: Proceedings of the 1994 Symposium on Techniques to Assess the Corrosion Activity of Steel Reinforced Concrete)*, Vol. 1276, pp.161-172.
- Lanyi, R. S. (1994). "Field prestressing repairs to precast concrete bridge girders" SP-151 American Concrete Institute, Farmington Hills, Michigan
- Legat, A., Kuhar, V., Bevc, L., and Vehovar, L. (1996). "Some Considerations of Potential-Mapping as a Method for the Detection of Corrosion in Reinforced and Prestressed Concrete Structures", *13th International Corrosion Congress Proceedings*, Paper 186, pp.1-6.
- Lenschow, R.J., and M.A. Sozen. Practical Analysis of the Anchorage Zone Problem in Prestressed Beams. *Journal of the American Concrete Institute*, November 1965, pp. 1421-1439.
- Leonhardt, F. (1964). *Prestressed Concrete Design and Construction*, Wilhelm Ernst & Sohn, Berlin.
- Lin, T. Y., and Burns, N. H. (1981). "Design of Prestressed Concrete Structures", Third Edition, John Wiley & Sons

- Liu, W., Hunsperger, R., and Kunz, E. (2001). "Nondestructive Corrosion Monitoring of Prestressed HPC Bridge Beams Using Time Domain Reflectometry", Transportation Research Board, Conference Paper, Washington D. C, January 7- 11.
- MacGregor, J.G. (1992). "Reinforced Concrete Mechanics and Design, Second Edition." Prentice-Hall, Englewood Cliffs, New Jersey. p. 46.
- Mari, R. A., and Valdes, M. (2000). "Long-Term Behavior of Continuous Precast Concrete Girder Bridge Model", Journal of Bridge Engineering, pp. 22-30.
- McDonald, J.E., Vaysburd, A.S., Emmons, P.H., Poston, R.W., and Kesner, K. (2002). "Selecting Durable Repair Materials: Performance Criteria – Summary". Concrete International, American Concrete Institute, January, pp 37-44.
- MDOT (1984a). *MDOT Design Division Informational Memorandum 320-B*, Michigan Department of Transportation, Lansing, Michigan.
- MDOT (1984b). *MDOT Design Division Informational Memorandum 332-B*, Michigan Department of Transportation, Lansing, Michigan.
- MDOT (1989). *MDOT Design Division Informational Memorandum 411-B*, Michigan Department of Transportation, Lansing, Michigan.
- MDOT (1991). *MDOT Design Division Informational Memorandum 402-B*, Michigan Department of Transportation, Lansing, Michigan.
- MDOT (1992). *MDOT Design Division Informational Memorandum 447-B*, Michigan Department of Transportation, Lansing, Michigan.
- MDOT (1996). *Standard Specifications for Construction*, Michigan Department of Transportation, Lansing, Michigan.
- MDOT (1997a). *MDOT Design Division Informational Memorandum 484-B*, Michigan Department of Transportation, Lansing, Michigan.
- MDOT (1997b). *Michigan Structure Inventory and Appraisal Coding Guide*. Michigan Department of Transportation, Lansing, Michigan.
- MDOT (1999). *Michigan Pontis Bridge Inspection Manual*. Michigan Department of Transportation, Lansing, Michigan.
- MDOT (2000). *Special Provision for Vertical and Overhead Structure Repairs*. Michigan Department of Transportation, Lansing, Michigan.
- MDOT (2001a). *Bridge Design Manual*. Michigan Department of Transportation, Lansing, Michigan.
- MDOT (2001b). *Bridge Design Guides*. Michigan Department of Transportation, Lansing, Michigan.
- MDOT (2001c). *MDOT - 2001 Materials Source Guide –Index*.
<http://www.mdot.state.mi.us/mappub/materialsguide/> (March 9, 2002).
- Mindess, S. and Young, J.F. (1981). *Concrete*. Prentice-Hall, Englewood Cliffs, New Jersey.
- Monterio, P. J. M., Frank, M., and Frangos, W. (1998). "Nondestructive Measurement of Corrosion State of Reinforcing Steel in Concrete", *ACI Material*, Vol. 95, No. 6, pp.704-709.

- Moore, D. G., Klodt, D. T., and Hensen, R. J. (1970). "Protection of Steel in Prestressed Concrete Bridges" *NCHRP Report No. 90*. National Research Council, Washington, D.C.
- Narasimhan, E. S., and Wallbank, E. J. (1999). "Bridge Inspections - Current Thinking And Regimes" *Structural Faults + Repair-99*, 8th International Conference, London, UK, 13-15 July.
- National Association of Corrosion Engineers (1970). "*NACE Basic Corrosion Course*", NACE, Houston, Texas.
- Nawy, E.G. (2000) *Prestressed Concrete – A Fundamental Approach*, Third Edition, Prentice Hall, Upper Saddle River, New Jersey, p. 49.
- Needham, D. (1999). *Prestressed Concrete Beam End Repair (Interim Report)*, Research Report R-1373, Michigan Department of Transportation, Lansing, Michigan.
- Needham, D. (2000). *Prestressed Concrete Beam End Repair*, Research Report RR-1380, Michigan Department of Transportation, Lansing, Michigan.
- Needham, D. (2001). "Development and Evaluation of Passive Cathodic Protection Systems Used on PCI-Beam Ends", *Transportation Research Record No. 00795442*, Transportation Research Board, Washington, D.C.
- Needham, D., and Juntunen, D. A. (1997). *Investigation of Condition of Prestressed Concrete Bridges in Michigan*, Research Report R-1348, Michigan Department of Transportation, Lansing, Michigan.
- Nogueira, C. L. (1999). "Bridge Evaluation Using Nondestructive Testing In Bridge Inspections As A Tool For Bridge Management Systems", *Structural Faults + Repair-99*, 8th International Conference, London, UK, 13-15 July.
- Ohio Department of Transportation (OhDOT) (2001). <http://www-ltap.eng.ohio-state.edu/bms/beams/pcibeams.htm> (September 25, 2001).
- Ohyama, H., Fujiwara, T., Kawakami, M., Shoyin, M., and Kosaka, Y. (1999). "Investigation & Retrofitting of Prestressed Concrete Bridges In Northeastern District of Japan", *Structural Faults + Repair-99*, 8th International Conference, London, UK, 13-15 July.
- Ota, M., Numata, A., and Kondo, S. (1985). "Life Time Test of Prestressed Concrete", *Ocean Space Utilization '85, Proceedings of the International Symposium*, Tokyo, pp. 463.
- Park, R., Paulay, T., "Reinforced Concrete Structures", 1975
- Pascale, G., Bonfiglioli, B., Carli, R., and Arduini, M. (1999). "Bridge RC Beams: Repair & Monitoring", *Structural Faults + Repair-99*, 8th International Conference, London, UK, 13-15 July.
- PCI Design Handbook, Fifth Edition, (1999). Raths, Raths, & Johnson, Inc., editor, Prestressed Concrete Institute, Chicago, Illinois
- Pedferri, P. (1996). "Cathodic Protection and Cathodic Prevention", *Construction and Building Materials*, Vol. 10, No. 5, pp. 391-402.
- Perenchio, W. F., Fraczek, J., and Preiffer, D. W. (1989). "Corrosion Protection of Prestressing Systems in Concrete Bridges" *NCHRP Report No. 313*, National Research Council, Washington D.C.

- Petrangeli, M. P., and Sarno, R. (1999). "NDT Of Prestressing Cables By Impact-Echo Method" Structural Faults + Repair-99, 8th International Conference, London, UK, 13-15 July.
- Portland Cement Association (PCA) (2001). "Concrete Information: Effects of Substances on Concrete and Guide to Protective Treatments." IS001, Portland Cement Association, Skokie, Illinois.
- Preston, H. K., Osborn, A. E. N., and Roach, C. E. (1987). *Restoration of Strength in Adjacent Prestressed Concrete Box Beams*, Wiss, Janey, Elstner Associates, Inc., Princeton Junction, New Jersey.
- Puzey, C. (2001). *Telephone Conversation*. Bridge Investigations and Repair Plans Unit Chief, Illinois Department of Transportation. August 9.
- Rabbat, B.G. and Aswad, A. (2002) "Design of Precast Prestressed Girders Made Continuous" www.portcement.org/br/design_for_continuity.pdf (May 6, 2002).
- Rabbat, B. G., and Russell, H. G. (1982). "Optimized Sections for Precast Prestressed Bridge Girders", PCI Journal, pp. 88-104.
- Rengaswamy, N. S., and Rajagopalan, K. S. (1977). "Corrosion of High-Strength Steel in Prestressed Concrete: 1- Electrochemical Studies," *Indian Concrete Journal*, Vol. 51, No. 10, October, pp. 301-304.
- Russell, B. W. "Measurements of Transfer Lengths on Pretensioned Concrete Elements", *Journal of Structural Engineering*, May 1997
- S-B Power Tool Company (2002). "Product List" http://www.boschtools.com/Tools+and+Accessories/Tools/product_list.htm?link=product&hierarchy_id=59141 (March 19, 2002).
- Sealants and Coatings.com (2001). <http://www.sealantsandcoatings.com/frameset.cfm?sheetLink=http%3A%2F%2Fwww%2Edelamtools%2Ecom%2Fpages%2Fdel2000%2Ehtml> (August 22, 2001).
- Settipani, A. (1987). "Inspection of Reinforced and Prestressed Concrete by means of Gammagraphy." *Bridge Evaluation Repair and Rehabilitation*, E. Absi, and A. S. Nowak, ed., The University of Michigan, Ann Arbor, Michigan, 498-505.
- Shanafelt, G. O., and Horn, W. B. (1985). "Guidelines for Evaluation and Repair of Prestressed Concrete Bridge Members." *NCHRP Report No. 280*, Transportation Research Board, Washington D.C.
- Shanafelt, G. O., and Horn, W. B. (1980). "Damage Evaluation and Repair of Prestressed Concrete Bridge Members." *NCHRP Report No. 226*, Transportation Research Board, Washington D.C.
- Sika USA (2002). "Welcome to Sika USA." <http://www.sikausa.com/> (March 19, 2002).
- Smith, J. L., and Virmani, Y. P. (2000). "Materials and Methods for Corrosion Control of Reinforced and Prestressed Concrete Structures in New Construction", Report Submitted to Federal Highway Agency, Report No. FHWA-RD-00-081.
- Staton, J. (2001). *Re: Approval process for vertical and overhead concrete repair materials*. E-mail to James Kasper. November 27, 2001.

- Sterritt, G., and Chryssanthopoulos, M. K. (1999). "Deterioration Prediction & Updating As A Means Of Structure Specific Bridge Management", Structural Faults + Repair-99, 8th International Conference, London, UK, 13-15 July.
- Texas Transportation Institute (TTI) (1998). "Innovative Highway Technologies," <http://leadstates.tamu.edu/All/information.stm> (August 30, 2001).
- Till, R. D. (2001a). *PC I-Beam End Project*. E-mail to Project Team with Attachments. March 16, 2001.
- Till, R. D. (2001b). *Re: Q1 report comments*. E-mail to Project Team with Attachment. July 18, 2001.
- Till, R.D. (2001c). *Re: mix design for lab tests*. Facsimile to Project Team. December 18.
- Tilly, G. P. (1987). "Performance and serviceability of concrete bridges." *Bridge Evaluation Repair and Rehabilitation*, E. Absi, and A. S. Nowak, ed., The University of Michigan, Ann Arbor, Michigan, 119-134.
- Titman, D. J. (1999). "Applications Of Thermography In NDT Of Structures", Structural Faults + Repair-99, 8th International Conference, London, UK, 13-15 July.
- Tortorete, J (2001) "Bridge Deck Resurfacing" Presentation at the 2001 Michigan Bridge Conference, Mount Pleasant, Michigan, May 30.
- TxDOT (1993). <ftp://ftp.dot.state.tx.us/pub/txdot-info/cmd/cserve/specs/1993/spec/es4302.pdf> (September 25, 2001).
- USACE (1992). "CRD-C 164-92 Standard Test Method for Direct Tensile Strength of Cylindrical Concrete or Mortar Specimens," *Handbook for Concrete and Cement*, U.S. Army Corps of Engineers Waterways Experiment Station, Vicksburg, Mississippi.
- Vaysburd, A.M. and McDonald, J.E. (1999). "An Evaluation of Equipment and Procedures for Tensile Bond Testing of Concrete". Technical Report REMR-CS-61, U.S. Army Corps of Engineers, Washington D.C.
- Vector Corrosion Technologies (2001). "Galvashield® CC Project History – City of Winnipeg, Prestressed Girder Rehabilitation", Vector Corrosion Technologies, Winnipeg, Manitoba, Canada.
- Virmani, Y.P and Clemena, G.G (1998). "Corrosion Protection – Concrete Bridges", *FHWA-RD-98-088*, Federal Highway Administration, McLean, Virginia.
- Weyers, R. E., Prowell, B. D., Sprinkel, M. M., and Vorster, M. (1993). "Concrete Bridge Protection, Repair, and Rehabilitation relative to Reinforcement Corrosion: A Methods Application Manual," *SHRP-S-360*, National Research Council, Washington, D.C.
- Whiting, D. A., Stejskal, B. G., and Nagi, M. A. (1993). "Conditions of prestressed concrete bridge components: Technology review and field surveys." *FHWA-RD-93-037*, Federal Highway Administration, Washington, D.C.
- Whiting, D. A., Stejskal, B. G., and Nagi, M. A. (1998). "Rehabilitation of Prestressed Concrete Bridge Components By Non-Electrical (Conventional) Methods." *FHWA-RD-98-189*, Federal Highway Administration, Washington, D.C.

- Whiting, D. A., Ost, B., Nagi, M., and Cady, P. D. (1992). "Condition Evaluation of Concrete Bridges Relative to Reinforcement Corrosion, Volume 5: Methods for Evaluating the Effectiveness of Penetrating Sealers." SHRP-S /FR-92-107, Strategic Highway Research Program, Washington, D.C.
- Xanthakos, P. P. (1996). *Bridge Strengthening and Rehabilitation*, Prentice-Hall PTR, New Jersey
- Yazdani N., Eddy S., Cai C.S., "Effect of Bearing Pads on Precast Concrete Bridges". *Journal of Bridge Engineering*. Vol. 5, August 2000, pp. 224-232
- Zemajtis, J., and Weyers, R. E. (1998). "Corrosion Protection Service Life of Low Permeable Concretes and Low Permeable Concrete with a Corrosion Inhibitor", Transportation Research Board 77th Annual Meeting, Conference Paper, Washington, D.C., January 11-15.
- Zhang, J., Monterio, P. J. M., and Morrison, F. H. (2001). "Non Invasive Surface Measurement of the Corrosion Impedance of Rebar in Concrete Part I", *ACI Material Journal*, pp.116-126.

Additional Documents

The interested reader may also refer to the following documents for information on the inspection, assessment, preventive maintenance, and repair of prestressed concrete I-beams.

"ACI 201.1R-92 - Guide for Making a Condition Survey of Concrete in Service." (1992). American Concrete Institute, Farmington Hills, Michigan.

"ACI 222.2R-01: Corrosion of Prestressing Steels." (2001). American Concrete Institute, Farmington Hills, Michigan.

"ACI 224.1R-93 - Causes, Evaluation, and Repair of Cracks in Concrete Structures." (1993). American Concrete Institute, Farmington Hills, Michigan.

"ACI 228.2R-98 - Nondestructive Test Methods for Evaluation of Concrete in Structures." (1998). American Concrete Institute, Farmington Hills, Michigan.

"ACI 364.1R-94 - Guide for Evaluation of Concrete Structures Prior to Rehabilitation." (1994). American Concrete Institute, Farmington Hills, Michigan.

"ACI 546.1R-80: Guide for Repair of Concrete Bridge Superstructures" (1980). American Concrete Institute, Farmington Hills, Michigan.

"ACI 546R-96 - Concrete Repair Guide." (1996). American Concrete Institute, Farmington Hills, Michigan.

"Condition Evaluation of Prestressed Strands in Bridges." NCHRP Project 10-53

"FHWA-SHRP Showcase - Assessment of Physical Condition of Concrete Bridge Components." (1996) CONCORR Inc., Ashburn, Virginia

"ICRI Guideline No. 03730 - Guide for Surface Preparation for the Repair of Deteriorated Concrete Resulting from Reinforcing Steel Corrosion." International Concrete Repair Institute

"ICRI Guideline No. 03733 - Guide for Selecting and Specifying Materials for Repair of Concrete Surfaces." International Concrete Repair Institute

"ICRI Guideline No. 03734 - Guide for Verifying Field Performance of Epoxy Injection of Concrete Cracks." International Concrete Repair Institute

"Management of Highway Structures" ed. P.C. Das, Thomas Telford Publishing, London, 1999.

"Safety of Bridges", ed. P.C. Das, Thomas Telford Publishing, London, 1997.

Chase, S. B. and Washer, G., "Nondestructive Evaluation for Bridge Management in the Next Century", Turner-Fairbank Highway Research Center, July 1997

- Ciolko, A. T. and Tabatabai, H., "Nondestructive Methods for Condition Evaluation of Prestressing Steel Strands in Concrete Bridges", National Cooperative Highway Research Program, Transportation Research Board, and National Research Council, NCHRP Project 10-53, March 1999
- Das, P. C., Frangopol, D. M. and Nowak, A. S., ed., "Bridge Design, Construction and Maintenance", International Conference in Singapore, Thomas Telford, London, October 1999.
- Das, P. C., Frangopol, D. M. and Nowak, A. S., ed., "Bridge Design, Construction and Maintenance", International Conference in Singapore, Thomas Telford, London, October 1999.
- Fam, A.Z., Rizkala, S.H., and Tadros, G. (1997). "Behavior of CFRP for Prestressing and Shear Reinforcements of Concrete Highway Bridges." ACI Structural Journal (1/97), American Concrete Institute, Farmington Hills, Michigan.
- Federal Highway Administration, (1981). "Detection of Flaws in Reinforcing Steel in Prestressed Concrete Bridge Members", Contract No: DOT-FH-11-8999
- Federal Highway Administration, (1989). "Salt Penetration and Corrosion in Prestressed Concrete Members", Publication No: FHWA-SA-97-100.
- Federal Highway Administration, (1997). "Evaluation of Digital Camera Technology For Bridge Inspection", Publication No: FHWA-PD-91-015
- Federal Highway Administration, (2000). "Materials and Methods for Corrosion Control of Reinforced and Prestressed Concrete Structures in New Construction", Publication No: FHWA-RD-00-081. On microfiche in JRVP: TD 2.30:00-081
- Feldman, L.R., Jirsa, J.O., and Kowal, E.S. (1998). "Repair of Bridge Impact Damage." Concrete International (2/98), American Concrete Institute, Farmington Hills, Michigan.
- Fiorato, A. E., "Inspection Guide for Reinforced Concrete Vessels", USDOT, US Coast Guard, Contract No: DOT-CG-832171-A, October, 1981
- Freitag, S. A., Bruce, S. M., and Hickman, W. E., "Reinforcement Corrosion in New Zealand Concrete", Advances in Concrete Technology, ACI SP-171, 1997
- Hachem, Y., Zografos, K., and Soltani, M., "Bridge Inspection Strategies", Journal of Performance of Constructed Facilities, Vol. 5, No.1, February, 1991
- Kim, S., Nowak, A.S., and Saraf, V., "Field Evaluation of Existing Bridges", US-Canada-Europe Workshop on Bridge Engineering, Zurich, Switzerland, July 1997.
- Konig, G. and Nowak, A.S., ed., "Bridge Rehabilitation", Ernst & Sohn, Berlin, Germany, 1992.
- Lamberson, E.A. (1983). "Post-tensioning Concepts for Strengthening and Rehabilitation of Bridges." ASCE Structures Congress, Preprint SC-10, Houston.
- Management of Highway Structures, ed. P.C. Das, Thomas Telford Publishing, London, 1999.
- Medlock, R. D., and Laffrey, D. C., ed., "Structural Materials Technology III: An NDT Conference." Texas Dept. of Transportation, Austin, Texas, 1998.

- Naaman, A.E. (1985). "Partially Prestressed Concrete Review and Recommendations." PCI Journal, Vol. 30, No. 6.
- Nawy, E.G. (1996). Prestressed Concrete. A Fundamental Approach.
- Novokshchenov, V., "Prestressed Bridges and Marine Environment", Journal of Structural Engineering, Vol. 116, No. 11, November, 1990
- Nowak, A.S. and Kim, S. , "Development of a Guide for Evaluation of Existing Bridges, Part I", UMCEE 98-12, Final Report submitted to MDOT, June 1998.
- Nowak, A.S., ed., "Bridge Evaluation, Repair and Rehabilitation," NATO ASI Series E, Vol. 187, Kluwer Academic Publishers, Dordrecht, Netherlands, 1990.
- Nowak, A.S., Sanli, A., Kim, S. Eom, J., and Eamon C., "Development of a Guide for Evaluation of Existing Bridges, Part II", UMCEE 98-13, Final Report submitted to MDOT, June 1998.
- Nowak, A.S., Saraf, V. and Kim, S., "Evaluation of Bridges using Field Testing", International Conference on Rehabilitation and Development of Civil Eng. Infrastructure Systems, Beirut, Lebanon, June 1997, Vol. I, pp. 391-402.
- Safety of Bridges, ed. P.C. Das, Thomas Telford Publishing, London, 1997.
- Saraf, V., Nowak, A.S. and Kim, S., "Nondestructive Testing of Bridges", Fourth National Workshop on Bridge Research in Progress, Buffalo, NY, June 1996, pp. 45-50.
- Shubinsky, G., "Visual & Infrared Imaging for Bridge Inspection", Northwestern University BIRL Basic Industrial Research Laboratory, June 1994
- Tabsh, S. W., "Sensitivity Analysis of Damaged Concrete Bridge Girders", Designing Concrete Structures for Serviceability and Safety, ACI SP-133, 1992
- Van Begin, C., "Durability of Concrete Bridges in Belgium—Balance of the Systematic Inspection", Concrete Durability, ACI SP-100, Vol. 1, 1987
- Veshosky, D., Beidleman, C. R., Buetow, G. W., and Demir, M., "Comparative Analysis of Bridge Superstructure Deterioration", Journal of Structural Engineering, Vol. 120, No. 7, July, 1994
- Workshop on Optimal Maintenance of Structures, Delft, The Netherlands, October 2000